SRESA's International Journal of

LIFE CYCLE RELIABILITY AND SAFETY ENGINEERING

Vol.2 **Issue No.1** **Jan – March 2013** **ISSN – 2250 0820**

Special Issue :

On

" Hybrid Uncertainty Modelling"

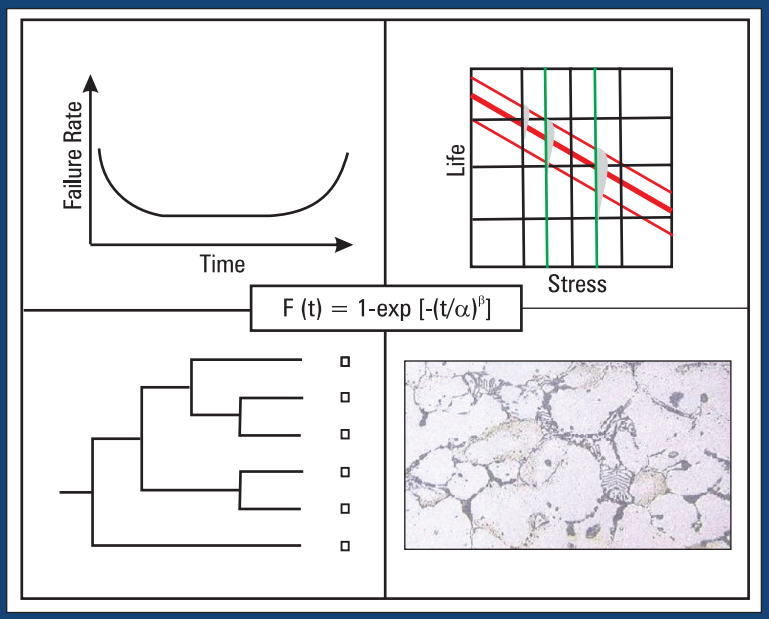

Guest-Editors
K. Balaji Rao
Chandra S. Putcha

Chief-Editors
P.V. Varde
A.K. Verma
Michael G. Pecht

Society for Reliability and Safety

website : http://www.sresa.org.in

SRESA Journal of Life Cycle Reliability and Safety Engineering

Extensive work is being performed world over on assessment of Reliability and Safety for engineering systems in support of decisions. The increasing number of risk-based / risk-informed applications being developed world over is a testimony to the growth of this field. Here, along with probabilistic methods, deterministic methods including Physics-of-Failure based approach is playing an important role. The International Journal of Life Cycle Reliability and Safety Engineering provides a unique medium for researchers and academicians to contribute articles based on their R&D work, applied work and review work, in the area of Reliability, Safety and related fields. Articles based on technology development will also be published as Technical Notes. Review articles on Books published in the subject area of the journal will also form part of the publication.

Society for Reliability and Safety has been actively working for developing means and methods for improving system reliability. Publications of quarterly News Letters and this journal are some of the areas the society is vigorously pursuing for societal benefits. Manuscript in the subject areas can be communicated to the Chief Editors. Manuscript will be reviewed by the experts in the respective area of the work and comments will be communicated to the corresponding author. The reviewed final manuscript will be published and the author will be communicated the publication details. Instruction for preparing the manuscript has been given on inside page of the end cover page of each issue. The rights of publication rest with the Chief-Editors.

SCOPE OF JOURNAL

System Reliability analysis	**Structural Reliability**	**Risk-based applications**
Statistical tools and methods	Remaining life prediction	Technical specification optimization
Probabilistic Safety Assessment	Reliability based design	Risk-informed approach
Quantitative methods	Physics-of-Failure methods	Risk-based ISI
Human factor modeling	Probabilistic Fracture Mechanics	Risk-based maintenance
Common Cause Failure analysis	Passive system reliability	Risk-monitor
Life testing methods	Precursor event analysis	Prognostics & health management
Software reliability	Bayesian modeling	Severe accident management
Uncertainty modeling	Artificial intelligence in risk and reliability modeling	Risk-based Operator support systems
Dynamic reliability models	Design of Experiments	Role of risk-based approach in Regulatory reviews
Sensitivity analysis	Fuzzy approach in risk analysis	Advanced electronic systems reliability modeling
Decision support systems	Cognitive framework	Risk-informed asset management

SRESA AND ITS OBJECTIVES

a) To promote and develop the science of reliability and safety.

b) To encourage research in the area of reliability and safety engineering technology & allied fields.

c) To hold meetings for presentation and discussion of scientific and technical issues related to safety and reliability.

d) To evolve a unified standard code of practice in safety and reliability engineering for assurance of quality based professional engineering services.

e) To publish journals, books, reports and other information, alone or in collaboration with other organizations, and to disseminate information, knowledge and practice of ensuring quality services in the field of Reliability and Safety.

f) To organize reliability and safety engineering courses and / or services for any kind of energy systems like nuclear and thermal power plants, research reactors, other nuclear and radiation facilities, conventional process and chemical industries.

g) To co-operate with government agencies, educational institutions and research oganisations

SRESA's International Journal of

LIFE CYCLE RELIABILITY AND SAFETY ENGINEERING

Vol.2 Issue No.1 Jan–March 2013 ISSN – 2250 0820

Special Issue :
On
" Hybrid Uncertainty Modelling"

Guest-Editors

K. Balaji Rao
Chandra S. Putcha

Chief-Editors

P.V. Varde
A.K. Verma
Michael G. Pecht

SOCIETY FOR RELIABILITY AND SAFETY

Copyright 2013 SRESA. All rights reserved

Photocopying

Single photocopies of single article may be made for personnel use as allowed by national copyright laws. Permission of the publisher and payment of fee is required for all other photocopying, including multiple or systematic photocopying for advertising or promotional purpose, resale, and all forms of document delivery.

Derivative Works

Subscribers may reproduce table of contents or prepare list of articles including abstracts for internal circulation within their institutions. Permission of publishers is required for required for resale or distribution outside the institution.

Electronic Storage

Except as mentioned above, no part of this publication may be reproduced, stored in a retrieval system or transmitted in form or by any means electronic, mechanical, photocopying, recording or otherwise without prior permission of the publisher.

Notice

No responsibility is assumed by the publisher for any injury and /or damage, to persons or property as a matter of products liability, negligence or otherwise, or from any use or operation of any methods, products, instructions or ideas contained in the material herein.

Although all advertising material is expected to ethical (medical) standards, inclusion in this publication does not constitute a guarantee or endorsement of the quality or value of such product or of the claim made of it by its manufacturer.

Typeset & Printed

EBENEZER PRINTING HOUSE
Unit No. 5 & 11, 2nd Floor, Hind Services Industries,
Veer Savarkar Marg,
Dadar (west), Mumbai -28
Tel.: 2446 2632/ 3872
E-mail: outwork@gmail.com

© 2013 SRESA All rights reserved

CHIEF-EDITORS

P.V. Varde,
Professor, Homi Bhabha National Institute &
Head, SE&MTD Section, RRSD
Bhabha Atomic Research Centre, Mumbai 400 085
Email: Varde@barc.gov.in

A.K. Verma
Professor, Department of Electrical Engineering
Indian Institute of Technology, Bombay, Powai, Mumbai 400 076
Email: akvmanas@gmail.com

Michael G. Pecht
Director, CALCE Electronic Products and Systems
George Dieter Chair Professor of Mechanical Engineering
Professor of Applied Mathematics (Prognostics for Electronics)
University of Maryland, College Park, Maryland 20742, USA
(Email: pecht@calce.umd.edu)

Advisory Board

Prof. M. Modarres, University of Maryland, USA	Prof. V.N.A. Naikan, IIT, Kharagpur
Prof A. Srividya, IIT, Bombay, Mumbai	Prof. B.K. Dutta, Homi Bhabha National Institute, Mumbai
Prof. Achintya Haldar, University of Arizona, USA	Prof. J. Knezevic, MIRCE Akademy, UK
Prof. Hoang Pham, Rutger University, USA	Dr. S.K. Gupta, AERB, Mumbai
Prof. Min Xie, University of Hongkong, Hongkong	Prof. P.S.V. Natraj, IIT Bombay, Mumbai
Prof. P.K. Kapur, University of Delhi, Delhi	Prof. Uday Kumar, Lulea University, Sweden
Prof. P.K. Kalra, IIT Jaipur	Prof. G. Ramy Reddy, HBNI, Mumbai
Prof. Manohar, IISc Bangalore	Prof. Kannan Iyer, IIT, Bombay
Prof. Carol Smidts, Ohio State University, USA	Prof. C. Putcha, California State University, Fullerton, USA
Prof. A. Dasgupta, University of Maryland, USA.	Prof. G. Chattopadhyay CQ University, Australia
Prof. Joseph Mathew, Australia	Prof. D.N.P. Murthy, Australia
Prof. D. Roy, IISc, Bangalore	Prof. S. Osaki Japan

Editorial Board

Dr. V.V.S Sanyasi Rao, BARC, Mumbai	Dr. Gopika Vinod, HBNI, Mumbai
Dr. N.K. Goyal, IIT Kharagpur	Dr. Senthil Kumar, SRI, Kalpakkam
Dr. A.K. Nayak, HBNI, Mumbai	Dr. Jorge Baron, Argentina
Dr. Diganta Das, University of Maryland, USA	Dr. Ompal Singh, IIT Kanpur, India
Dr. D. Damodaran, Center For Reliability, Chennai, India	Dr. Manoj Kumar, BARC, Mumbai
Dr. K. Durga Rao, PSI, Sweden	Dr. Alok Mishra, Westinghouse, India
Dr. Anita Topkar, BARC, Mumbai	Dr. D.Y. Lee, KAERI, South Korea
Dr. Oliver Straeter, Germany	Dr. Hur Seop, KAERI, South Korea
Dr. J.Y. Kim, KAERI, South Korea	Prof. P.S.V. Natraj, IIT Bombay, Mumbai
Prof. S.V. Sabnis, IIT Bombay	Dr. Tarapada Pyne, JSW- Ispat, Mumbai

Managing Editors

N.S. Joshi, BARC, Mumbai
Dr. Gopika Vinod, BARC, Mumbai
D. Mathur, BARC, Mumbai
Dr. Manoj Kumar, BARC, Mumbai

© 2013 SRESA All rights reserved

Editorial

It is established that the engineering decisions have to be taken in the face of uncertainties. The type of uncertainty to be handled by the engineer varies depending on its source. In such cases decisions should take into account the presence of a single or multiple types of uncertainties. This special issue, being brought out in two parts, is dedicated to basically handling of hybrid uncertainties. However, two papers, one dealing with the fuzzy and the other with probabilistic uncertainties are included since they are insightful.

The first paper of this issue is by Padhy et al, on 'Simplified fuzzy-random seismic fragility of open ground storey buildings'. The topic of this paper is important since open storey buildings are being constructed and the ground storey is used as parking lots. During the Bhuj earthquake, in 2001, this type of buildings suffered extensive damage and in some instances collapsed. Thus, seismic fragility analysis of open storey buildings is a topic of current research interest. The authors carry out detailed nonlinear time history analysis of the RC frames for estimating capacity and also evaluate the seismic demand. While the seismic demand and capacity have been considered, in the displacement space, to follow lognormal distributions, the limit state has been fuzzified. The analysis of fragility curves for different values of fuzziness parameter showed that the fragility curves are sensitive to limit state thresholds when fuzziness is high. The coupling effect of structural irregularity with the fuzziness is found to be insignificant.

The second paper is by Balu and Rao on 'Bounds on reliability of structures with multiple design points using MHDMR'. The authors propose two approaches to determine the bounds on reliability of structures namely, (i) coupled MHDMR−FFT based reliability analysis, and (ii) coupled MHDMR−MCS based reliability analysis. Both the methods are able to handle the random and fuzzy variables and nonlinear limit state function with multiple design points. The efficacy of the proposed methodologies has been demonstrated for three example problems. The proposed approaches are elucidated in the form of flow charts and the examples clearly show how the proposed approaches are computationally efficient compared to the simple Monte Carlo techniques. These approaches show promise especially when the dimensionality of the problem increases.

The next paper in this issue is on 'Expert elicitations: A tool for decision making in risk management issue', by Gopika Vinod and Sanyasi Rao, deals with an important aspect of engineering decision making namely, expert elicitation. The authors have presented briefly, but effectively, different commonly used approaches with respect to structured expert judgment and also highlighted their advantages and disadvantages appropriately. The authors provide two very insightful examples namely, a typical example of finding failure probability of a component taking into account the results of risk based inspection, and, forecasting research areas and their importance ranking using Delphi technique.

The paper by Anoop et al on 'Remaining life estimation of corrosion-affected RC bridge girders using online monitoring data – a fuzzy-random approach' presents a new approach for remaining life estimation of corrosion-affected reinforced concrete (RC) flexural members in the presence of fuzzy and random uncertainties. The proposed approach takes into consideration the delay in detection of corrosion initiation using the online monitoring data. Using the proposed approach, bounds for characteristic value of failure probability for a RC T-beam bridge girder has been determined. The approach will be useful for making decisions regarding scheduling of in-service inspections.

'Sensitivity studies on fatigue crack growth parameters in concrete', by Fathima and Chandra Kishen, deals with the explanation of fatigue crack growth in concrete members within the framework of thermodynamics. The authors have made use of concepts of dimensional analysis and self-similarity to determine the parameters in the crack propagation law. The authors carry out both deterministic and probabilistic sensitivity analyses to identify important parameters affecting the fatigue crack propagation in concrete. In their study they consider the test results reported by Bazant and Xu on three notched beams. The authors also indicate that there is a need to carry out further investigations by considering the crack length as a fuzzy variable.

Rama Rao et al present in their paper 'Fuzzy analysis of the moment of resistance of a doubly reinforced concrete beam with uncertain structural parameters' the static stress analysis of doubly reinforced concrete flexural members subject to parametric uncertainty. The two variables considered as fuzzy are area of steel and the Young's modulus of steel and the same are represented as number of α - sublevels. The interval analysis is performed using three different approaches. A direct interval computation, and two response surface based approximate approaches. The authors find that, with respect to the problem considered, all three approaches perform satisfactorily in determining the fuzzy set for moment of resistance.

One of the guest editors, Dr K. Balaji Rao, is very thankful to his colleague Dr M. B. Anoop, of Risk and Reliability of Structures Group of CSIR-SERC, for helping in reviewing some of the papers and also in helping in discussions regarding the papers. The guest editors are very thankful to the chief-editors in general and, Dr Varde and Dr Gopika Vinod in particular. We are very thankful to all the authors who have responded to our invitation and the publishers who have done a good job of bringing out this special issue.

K. Balaji Rao
Chandra S. Putcha

© 2013 SRESA All rights reserved

Dr K. Balaji Rao, completed his M.E and Ph D from Indian Institute of Science, Bangalore, in the years 1984 and 1990 respectively. After a very brief stint at Tata Consulting Engineers, Bengaluru, he joined CSIR-Structural Engineering Research Centre, Taramani, Chennai in the year 1990. Currently he is a chief scientist at CSIR-SERC and is a faculty of AcSIR. His research interests include stochastic mechanics, stochastic modelling of natural hazards, Markov chain modelling of engineering systems at different scales, vulnerability analysis of built environment and risk-consistent design of engineering structures. He has led a number of in-house and sponsored R&D projects. Important among the sponsored projects are: (i) A methodology for risk informed in-service inspection for safety related systems, (ii) Seismic vulnerability analysis of brick masonry buildings, (iii) Development of probabilistic seismic hazard map of India. He has published a number of refereed journal and conference papers apart from number of R&D reports. He was deputed by CSIR-SERC to Rice University and University of Notre Dame in 1994 under SERC-UNDP fellowship. He did collaborative work with Prof. R. Rackwitz. Universität der Bundeswehr München, Germany, in 1999, when he visited CSIR-SERC under CSIR-DAAD exchange programme. He was a visiting scientist at Electronic Enterprises Laboratory, Department of Computer Science and Automation, IISc, Bangalore, in 2006. He has guided two Ph D candidates and a number of B.Tech/M.E students. He is a member of Editorial board of the following journals: Journal of Structural Engineering, CSIR-SERC, International Journal of Engineering under uncertainty: hazards, assessment and mitigation, Open Journal of Safety Science and Technology, Journal of Chemical Engineering and Materials Science. He has been identified as a mentor at CSIR-SERC and is currently working in the area of stochastic multi-scale modelling and sustainability-based design.

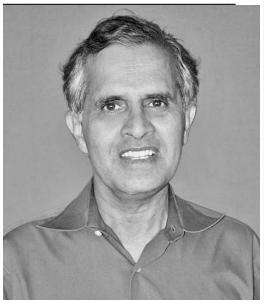

Dr. Chandrasekhar Putcha is a Professor in the Department of Civil and Environmental Engineering at California State University, Fullerton. He has been at this place since 1981. Before that he was on the research faculty at West Virginia University, Morgantown, WV and a post-doctoral fellow at University of Sherbrooke in Canada. His research areas of interest are –Reliability, Risk Analysis, Optimization and Mathematical Modeling. Because of his interdisciplinary areas of research, Dr. Putcha has published more than 135 research papers in various disciplines such as Engineering, Medicine, Kinesiology, Political Science and Sociology. He has done consulting work for several leading companies and received research grants from companies such as Boeing, Northrop Grumman Corporation (NGC) and from federal agencies such as – NASA, Navy, Air Force, US Army Corps of Engineers.

Dr. Putcha did his Ph.D.and M.S. in Civil Engineering from Indian Institute of Technology, Kanpur in 1975 and 1971 respectively and B.S. from IIIT/BHU in 1969. He was the Head of Civil and Environmental Engineering Department at California State University, Fullerton (CSUF) from 1996-2002.

Key Awards

1. CSUF Outstanding Professor (2006-07)
   (First time recipient from the college of Engineering in 44 years Since this award was instituted in 1963)
2. College of Engineering and Computer Science outstanding Professor award (May 1994)
3. "Prestigious Engineering Educator" Award from Orange County Engineering Council (OCEC), Feb. 26, 2005.
4. "Distinguished Engineering Educator" Award from Orange County Engineering Council (OCEC), Feb. 24, 2001.

© 2013 SRESA All rights reserved

Life Cycle Reliability and Safety Engineering
Vol.2 Issue 1 (2013) 01-12

Remaining Life Estimation of Corrosion-Affected RC Bridge Girders using Online Monitoring Data – a Fuzzy-Random Approach

M.B. Anoop[*], K. Balaji Rao[*] and B.K. Raghuprasad[**]
** - Scientist, CSIR-Structural Engineering Research Centre, CSIR Campus, Taramani, Chennai, INDIA*
*** - Professor, Department of Civil Engineering, Indian Institute of Science, Bangalore, INDIA*
email: anoop@serc.res.in

Abstract

A new approach for remaining life estimation of corrosion-affected reinforced concrete (RC) flexural members in the presence of fuzzy and random uncertainties presented in this paper. The proposed approach takes into consideration the delay in detection of corrosion initiation using the online monitoring data. The approach combines the vertex method of fuzzy set theory with Monte Carlo simulation technique for fuzzy-random modelling of the evolution of deterioration of moment of resistance of a corrosion-affected RC structural member. The fuzzy sets of failure probability against the limit state of collapse in flexure at different instants of time are constructed. It is also shown how to determine the bounds for characteristic value of failure probability from the resulting fuzzy set with minimal computational effort. Using the proposed approach, bounds for characteristic value of failure probability for a RC T-beam bridge girder has been determined. The fuzzy-random approach presented will be useful for remaining life estimation and for making decisions regarding scheduling of in-service inspections.

Keywords: ***Reinforced Concrete; Chloride-Induced Corrosion; Online Monitoring; Change Point Detection; Hybrid Uncertainties; Remaining Life Estimation;***

1 Introduction

With the emphasis being placed on development of new infrastructure and life extension programs for existing structures to meet the challenges of sustainable structures, online health monitoring has become a practical requirement. In particular, this is required in the case of bridge stocks consisting of large number of bridges which are to be monitored simultaneously. The advances made in sensing technologies, data acquisition and data communication has made possible the long-term continuous monitoring of major structures using permanent monitoring systems [1]. A major shortcoming of permanent monitoring systems is the extensive lengths of cables required for transfer of sensor measurements, leading to higher costs. The costs can be reduced by eliminating the cables through integration of wireless radio with sensor [2]. Most of the power in the wireless sensing units is used by the wireless radios, which can be reduced by transmitting only the significant data. This can be achieved by examining the data in the wireless sensing unit itself using integrated sophisticated microcontroller, and then transmitting only the required indicators [3]. For instance, damage detection algorithms could be used to determine if damage is present and wireless radio is used for transmitting the information only if damage was sensed [4].

In civil structures, the detection of damage before critical failure is of extreme importance. Most of the damage detection problems involve detection of one or several changes in some characteristic properties of the considered system [5]. The time instant at which the change occurs is called the change point [6]. With the development of more comprehensive strategies for online monitoring and the developments in smart sensor technology and digital data acquisition [7], there is a need to develop change point detection algorithms which can be used online for automated damage detection.

One of the major degradation mechanisms for reinforced concrete (RC) structures located in marine environment is the chloride-induced corrosion of reinforcement embedded in concrete. For these structures, detection of corrosion of reinforcement in its early stages will be useful for undertaking suitable measures for mitigating the corrosion damage. This will help in optimal allocation of resources. From

© 2013 SRESA All rights reserved

laboratory experimental investigations [8-12], it is noted that electrochemical noise can indicate the current level of corrosion activity of steel in concrete, especially transition from passive state to active corrosion state. Electrochemical noise technique is an emerging technique for monitoring corrosion of reinforcement in concrete [13-14]. There is a need to develop automated procedures to identify the corrosion initiation from the online monitored electrochemical noise data. Towards this, in the present study, the identification of time of corrosion initiation is modeled as a problem of detection of change point in online monitored electrochemical current noise data. For change point detection, an algorithm based on Bayesian approach is proposed [15]. A new approach for remaining life estimation of corrosion-affected RC flexural members in the presence of fuzzy- and random- uncertainties, taking into consideration the delay in detection of corrosion initiation using the online monitoring algorithm, is presented in this paper. The fuzzy-random approach presented will be useful for making decisions regarding scheduling of in-service inspections.

2. Detection of Corrosion Initiation using Online Monitoring Data

The localized corrosion processes, such as that associated with chloride-induced corrosion of reinforcement in concrete, give rise to electrochemical noise as already indicated. The coefficient of variation of corrosion current noise ranges from 10^{-3} for general corrosion to 1.0 for localized corrosion [13]. Before initiation of corrosion, the reinforcement in concrete is in the passive state (corrosion currents are negligible, i.e., < 1 mA/m^2) and hence the mean corrosion current can be considered as zero. When depassivation of steel occurs, there is a shift in the mean corrosion current, which indicates initiation of active corrosion. The initiation of corrosion can be identified by detecting this shift in the mean corrosion current. In this study, identification of time of corrosion initiation (t_i) is posed as a problem of detection of single change point in online monitored electrochemical current noise data. This information is further used for the remaining life estimation of the RC structural element.

2.1 Change point detection for identifying time of corrosion initiation

Consider a RC structural element, having two identical, electronically isolated, rebar probes embedded in concrete coupled through a zero resistance ammeter (ZRA) to monitor the corrosion currents. At t_i (when depassivation of steel occurs), there is a shift in mean value of corrosion current, indicating initiation of active corrosion. The actual shift in mean value of corrosion current depends on different factors (viz. humidity content in concrete, temperature, etc.). Andrade *et al.* [16] presented typical ranges for corrosion current for different exposure conditions, based on measurements made on laboratory specimens and on real structures. These ranges of values of corrosion current for different exposures can be further subdivided [17], using typical trend of variation of rate of corrosion with water-cement ratio [18]. Thus, knowing the exposure condition and water-cement ratio used, the range of values of corrosion current that can be expected in the girder during active state of corrosion can be determined, which will give an idea about amplitude of shift in mean corrosion current. The identification of t_i can be viewed as a problem of identifying the time of shift in mean of the monitored corrosion current data, i.e., a change point detection problem.

2.2 Algorithm based on Bayesian approach for identification of time of corrosion initiation

Bayesian approach is based on the assumption that a priori information about the probability distribution of the time of change (time of corrosion initiation in the present study) is available. It is assumed that the monitored corrosion current data can be represented using a Gaussian white noise (GWN) process. Balaji Rao *et al.* [19] proposed an algorithm for detecting time of shift in mean amplitude of online monitoring data modeled as a GWN process. This algorithm is modified and used for identification of time to corrosion initiation in reinforced concrete structures using electrochemical noise data obtained using ZRA technique [15]. The salient features of proposed algorithm are as follows.

It is assumed that the observed continuous time random process $\{Y(t), t \geq 0\}$ has the form:

$$Y(t) = A.U(t-\lambda) + \xi(t) \qquad t \geq 0 \tag{1}$$

where $\{\xi(t), t \geq 0\}$ is a standard GWN process with zero mean and Dirac delta function correlation function. ξ(t) represents the randomness in the system performance with time. A is the shift in the mean of the observed process. $U(t-\lambda)$ is the unit step function; $U(t-\lambda) = 0$ for $t < \lambda$ and $U(t-\lambda) = 1$ for $t \geq \lambda$.

© 2013 SRESA All rights reserved

λ is the time instant at which a step shift in the mean level of the observed process occurs. It is assumed that λ is a random variable with known distribution function $F_\lambda(t) = P\{\lambda \le t\}$.

The optimal (Bayesian) least squares estimate of the shift time is the conditional mean [20]

$$\hat{\lambda} = \left\langle \lambda \middle| y_0^t \right\rangle \tag{2}$$

where y_0^t is the observed time history of the process, $\{Y(s), 0 \le s \le t\}$. It has been shown by Fishman [20] that, for all $t \ge 0$, the optimal estimate has the form

$$\hat{\lambda}(t) = \frac{\zeta(t)}{\Lambda(t)} \tag{3}$$

where $\zeta(t)$ and $\Lambda(t)$ are statistics defined by a system of stochastic differential equations

$$d\zeta(t) = \frac{A}{I}\left[\zeta(t) - \int_t^\infty x.dF_\lambda(x)\right] y(t)dt \tag{4}$$

$$d\Lambda(t) = \frac{A}{I}[\Lambda(t) + F_\lambda(t) - 1] y(t)dt \tag{5}$$

satisfying the initial conditions

$\Lambda(0) = 1$, and $\zeta(0) = \int_{-\infty}^{\infty} x.dF_\lambda(x)dx$,

and I is the intensity of the GWN process. Thus, the initial estimate of $\zeta(t)$ is the mean value of the random variable λ itself, and since $\Lambda(0) = 1$, $\hat{\lambda}(0)$ is also equal to the mean value of λ, i.e., the initial estimate of time of shift is the mean of λ, since that is the best information available at time $t = 0$. It is noted from Eq. 3 that Λ(t) is the likelihood ratio in the problem of testing two hypotheses:

$H_0 : y(t) = \xi(t)$ (no change has occurred);

$H_1 : y(t) = A.U(t - \lambda) + \xi(t)$ (change has occurred).

$F_\lambda(\lambda)$ is the known distribution function, decided based on engineering judgment, for the time of shift.

The estimate of the shift time (Eq. 3) given by Fishman [20] is based on the condition that $y(t)$ is a random process. However if $y(t)$ is available (or is continuously observable in real time), Eqs. 4 and 5 become ordinary differential equations, and can be solved using numerical methods such as Runge-Kutta methods. From the simulation studies carried out at CSIR-SERC, it is noted that there is a need to apply a modification to $\hat{\lambda}(t)$ (Eq. 3), when $y(t)$ is assumed to be continuously observable in real time. The following decision function is proposed:

$$\lambda(t) = \frac{\left| \int_0^t \hat{\lambda}(x)dx - \hat{\lambda}(t) \cdot t \right|}{\left| \hat{\lambda}(0) - \hat{\lambda}(t) \right|} \tag{6}$$

The time of shift is the value to which $\lambda(t)$ converges (or when the successive values of $\lambda(t)$ do not differ by more than a specified tolerance). Since the entire observed time history of the process need not be considered for determining $\hat{\lambda}(t)$, a sliding window of width W containing specified sample size S is considered. The assumption made when a sliding window is considered is that the change point can be detected within S time steps after it has occurred. The algorithm is suitable for online detection of change point, since data points in the time series are progressively included and analyzed.

The modified algorithm can be applied to identify the time of corrosion initiation in a reinforced concrete structure using electrochemical noise data. The delay in detection (t_d) is given by:

$$t_d = t_a - t_o \text{ ; for } t_a > t_o \tag{7}$$

where t_a is the time of shift detected using the proposed algorithm and t_o is the actual time of shift in the time series. In the present investigation, only the case of $t_a > t_o$ is considered, since this case is detrimental to the engineering decision making scenario.

3. Remaining Life Estimation

A rational estimation of remaining life of reinforced concrete structural elements subject to corrosion of reinforcement is required for making engineering decisions regarding the inspection/maintenance activities of these elements. Internationally, efforts are being made to develop methodologies for service life design and remaining life estimation of reinforced concrete structural elements [17, 21-31]. In almost all these investigations, the variables involved in service life design and/or remaining life estimation, such as diffusion coefficient governing the diffusion of chlorides into cover concrete, surface chloride content, critical chloride content are considered as stochastic variables.

As is known, amongst other factors, service life of a structural element with respect to corrosion of reinforcement depends upon the exposure condition

© 2013 SRESA All rights reserved

and the type and quality of concrete used. In most of the codes of practice, exposure conditions are classified in a general and qualitative manner using linguistic terms (eg., mild, moderate, severe, very severe, extreme). Also, the quality of construction is often specified using linguistic terms (eg., excellent, good, average, poor, very poor). While there are several techniques for handling uncertainties arising from randomness, imprecision, vagueness, ambiguity etc., fuzzy sets are commonly used for handling uncertainties arising due to the use of linguistic terms [32]. Therefore, a more rational approach for remaining life estimation should take into consideration the fuzzy and random uncertainties together. Different methods have been proposed by various researchers for handling of fuzzy and random uncertainties together (for instance, [33-38]). One of the methods is to determine equivalent probability distributions for the fuzzy sets (or vice versa), and carry out the analysis in the framework of probability theory (or fuzzy set theory) [33, 34, 36, 38]. But, a major draw back of these approaches is that according to possibility theory, if the membership function of the fuzzy set is the only available information, there is a class of probability measures which are equally valid [39]. Therefore, it is not always possible to obtain a unique equivalent probability distribution for a fuzzy set. Thus, there is a need to develop methods which can handle fuzzy and random uncertainties as they are in the service life estimation. Anoop *et al.* [37] proposed a methodology for service life estimation of corrosion-affected reinforced concrete flexural elements in the presence of fuzzy and random uncertainties, by combining the vertex method of fuzzy set theory with Monte Carlo simulation (MCS) technique. This methodology is used in the present study for modeling the fuzzy-random evolution of resistance deterioration in RC members.

3.1 Modeling resistance deterioration

In this study, the interest is on the estimation of remaining life after the detection of corrosion initiation, and hence the time is reckoned from the time of detection of corrosion initiation. Also, there can be a time delay (t_d) in the detection of corrosion initiation using the online monitoring data. The diameter of the reinforcing bar at any time t_p, after corrosion initiation, is given by,

$$\phi(t_p) = \phi(0) - 0.0116\ \alpha\ I_{corr}\ (t_p + t_d) \qquad (8)$$

where $\phi(0)$ and $\phi(t_p)$ are diameters of bar before corrosion initiation and at time 't', respectively; α is a parameter varying in the range 4 to 8 for pitting type of corrosion; I_{corr} is the corrosion current density; t_p is the time elapsed after detection of corrosion initiation, and t_d is the delay in detection of the algorithm used. Rule-bases, in the form of simple *if-then* rules, are developed for determining the values of I_{corr} and α based on the exposure conditions and water-cement ratios defined/specified in codes of practice [31]. Additive fuzzy system is used for combining the output fuzzy set for I_{corr}. The rule-bases are given in Fig. 1. Knowing the diameter of the reinforcing bars, cross-sectional dimensions of reinforced concrete member, strengths of steel and concrete, it is possible to estimate the resistance of the member in flexure/shear/torsion at any given time. In the present study, the ultimate moment of resistance at any time ($M_u(t_p)$) is computed using

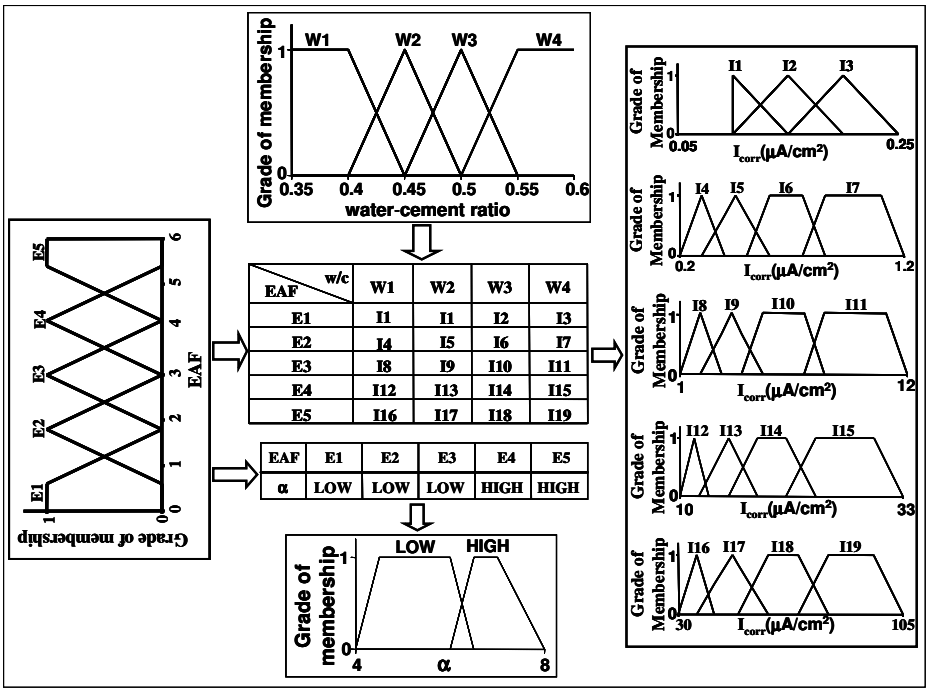

Figure. 1 Rule-bases for determining I_{corr} and α

© 2013 SRESA All rights reserved

the relations given in IS 456-2000 [40] without the partial safety factors.

3.2 Estimation of failure probability

In the present study, remaining life estimation of RC structural elements is carried out considering the limit state of collapse in flexure, given by

$$g(t_p) = M_u(t_p) - M_{SL} \quad (9)$$

where $M_u(t_p)$ is the ultimate moment of resistance at any time t (capacity) and M_{SL} is the moment due to service loads (demand).

In the remaining life estimation, the strengths of materials (namely, compressive strength of concrete and yield strength of steel), the dimensions of the cross-section (namely, breadth and depth) and the time to corrosion initiation are considered as random variables, while the corrosion current I_{corr} and the pitting factor a are considered as fuzzy variables. Therefore, $M_u(t_p)$ is a fuzzy-random variable, and hence the failure probability, $P_F(t_p)$, against the limit state considered will be a fuzzy set. In the present study, the fuzzy set of $P_F(t_p)$ is determined using a hybrid method involving a combination of vertex method with MCS technique. A brief explanation of the vertex method is given below.

Vertex method, introduced by Dong and Shah [41], is an approach for computing functions of fuzzy variables, based on λ-cut concept and standard interval analysis. Vertex method provides a computationally efficient solution technique for calculation of functions of fuzzy variables. Suppose I_λ is the λ-cut interval, i.e., $I_\lambda = [a, b]$, of fuzzy set A. If fuzzy set B is image of A given by the mapping $B = f(A)$, then interval representing B at a particular value of λ, say B_λ, can be obtained by

$$B_\lambda = f(I_\lambda) = [\min(f(a), f(b)), \max(f(a), f(b))] \quad (10)$$

When the mapping is for n input variables, i.e., $y = f(x_1, x_2, \ldots, x_n)$, and each input variable is described by an interval, say $I_{i\lambda}$ at a specific λ-cut, where $I_{i\lambda} = [a_i, b_i]$, $i = 1, 2, \ldots, n$, then values of interval function representing output fuzzy set B at a particular value of λ, is given by

$$B_\lambda = f(I_{1\lambda}, I_{2\lambda}, \ldots, I_{n\lambda}) = [\min_j(f(c_j)), \max_j(f(c_j))], \quad j = 1,2,\ldots,m \quad (11)$$

where $m = 2^n$, and c_j represents all possible combinations of input interval variables, i.e., they are vertices of input space in the n-dimensional Cartesian region.

The vertex method is applicable only if the function is continuous and monotonic on $I_{i\lambda} = [\alpha_i, b_i]$, $i = 1, 2, \ldots, n$. In the present study, I_{corr} and α are considered as the fuzzy variables. As noted from Eq. 8, the remaining diameter of the reinforcing bar ($\phi(t)$), at any time t, decreases with increase in either I_{corr} or α, indicating that $\phi(t)$ is a monotonic function of I_{corr} and α. The form of the Eq. 8 also suggests that $\phi(t)$ is a continuous function of I_{corr} and α. The moment of resistance at any time t, $M_u(t)$, increases (decreases) with increase (decrease) in $\phi(t)$, indicating that $M_u(t)$ can be considered as a continuous and monotonic function of $\phi(t)$. Since the failure probability at any time t increases (decreases) with decreases (increase) in $M_u(t)$, the vertex method is applicable in the present investigation for estimating the fuzzy set for failure probability.

In the present study, λ-cut levels are taken as 0+, 0.2, 0.4, 0.6, 0.8 and 1.0. For each λ-cut level, possible combinations of the fuzzy variables are considered. Since there are two fuzzy variables (namely, *Icorr* and α), four combinations are possible for each λ-cut level. For each combination of I_{corr} and α, $P_F(t)$ is determined for different values of t using Monte Carlo simulation with importance sampling technique [42], by considering width of beam, effective depth of beam, yield strength of steel, compressive strength of concrete and time to corrosion initiation as random variables. The target coefficient of variation of failure probability is kept as 0.05 while carrying out the simulation. From four values of $P_F(t)$ (each value corresponding to one combination of I_{corr} and α) for a specific λ-cut level, interval of fuzzy set of $P_F(t)$ is determined. In this way, fuzzy set of $P_F(t)$ at any specific time against the limit state of collapse in flexure is determined.

3.3 Determination of bounds for characteristic value of failure probability using possibility theory

While the fuzzy set of $P_F(t)$ can be determined using the procedure given in section 3.2, specification of characteristic value of $P_F(t)$ will be more useful for engineering decision making. In this section, the procedure for determination of bounds for characteristic value of $P_F(t)$ using possibility theory is presented [39].

Possibility theory, introduced by Zadeh [43], is an uncertainty theory devoted to the handling of incomplete information. Similar to probability

© 2013 SRESA All rights reserved

theory, possibility theory is also based on set functions. But it differs from probability theory by the use of a pair of dual set-functions (possibility and necessity measures) instead of only one (probability measure). Thus, the theory of possibility is based on two measures of confidence, namely, possibility measure ($\prod$) and necessity measure (N). A confidence measure is a number $0 \le g(A) \le 1$, which represents the confidence one has on the occurrence of event A [44]. A basic notion in possibility theory is the possibility distribution. A possibility distribution is a mapping from a set of states of affairs to a totally ordered scale such as the unit interval [0,1]. The possibility distribution is a representation of the state of knowledge, i.e., a description of the way we think the state of affairs is [44]. The possibility distribution π_X can be viewed as the membership function of fuzzy set of possible values of a quantity X. Knowing the possibility distribution, the likelihood of events can be described by means of possibility and necessity measures. If interest is on the occurrence of an event A, with membership function for fuzzy set X as available information, possibility and necessity measures are defined as:

$$\Pi(A) = \sup_{\omega \in A} \pi_X(\omega) \tag{12}$$

$$\begin{aligned} \mathrm{N}(A) &= \inf_{\omega \in \overline{A}} (1 - \pi_X(\omega)) \\ &= 1 - \Pi(\overline{A}) \end{aligned} \tag{13}$$

by considering membership function of X as possibility distribution π_X. $\overline{A}$ denotes complement of event A. The possibility $\Pi(A)$ defines to what extent at least one element in A is consistent with the available information π_X. The necessity $\mathrm{N}(A)$ defines to what extent no element outside A is possible, i.e., to what extent π_X implies A [44]. It has been shown that possibility and necessity are limit cases of an equivalence class of probability distributions compatible with available data [33]. This is in line with the consistency principle proposed by Zadeh [43] which can be translated as: "the degree of possibility of an event is greater than or equal to its degree of probability, which must be itself greater than or equal to its degree of necessity" [45]. Thus, an equivalence class P_c of probability measures P compatible with available data can be defined as:

$$\mathrm{P}_C = \{P | \forall A, \mathrm{N}(A) \le P(A) \le \Pi(A)\} \tag{14}$$

Without any additional information, all probability measures defined by Eq. 14 are equally valid [39].

A procedure has been proposed by Savoia [39] to estimate bounds for characteristic values corresponding to fractiles of probability distributions compatible with available information. This procedure is used in present study to determine bounds for characteristic values of $P_F(t)$ at any time using fuzzy set of $P_F(t)$, determined using the procedure outlined.

Consider a fuzzy set Q with membership function $\mu_Q(x)$. Considering an event A as $A = (-\infty, x]$, based on the necessity and possibility of A, the following CDFs can be defined:

$$\begin{aligned} F_*(x) &= \mathrm{N}((-\infty, x]) \\ F^*(x) &= \Pi((-\infty, x]) \end{aligned} \tag{15}$$

These CDFs represent lower- and upper- bound for all probability measures P belonging to class P, compatible with available data. That is,

$$F_*(x) \le F(x) \le F^*(x)$$

where $F(x) = P((-\infty, x])$ (16)

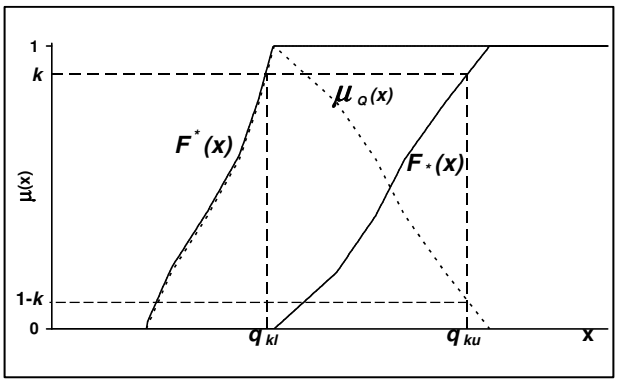

Figure. 2 Bounds for characteristic value corresponding to a specified fractile k

Since $F_*(x)$ and $F^*(x)$ are the necessity and possibility, $F_*(x)$ and $F^*(x)$ can be rewritten in terms of possibility distribution (which can be considered as membership function of fuzzy set Q) using Eqs. 11 and 12, as:

$$\begin{aligned} F_*(x) &= \inf\{1 - \mu_Q(\omega) | \omega > x\} \\ F^*(x) &= \sup\{\mu_Q(\omega) | \omega \le x\} \end{aligned} \tag{17}$$

© 2013 SRESA All rights reserved

where ω denotes a particular value of X. Since the aim is to determine a conservative estimate of P_F, bounds for a characteristic value corresponding to a high fractile, k (say, 0.95), need to be defined. It has been shown by Savoia [39] that lower bound for characteristic value is given by lower limit of the interval corresponding to λ-cut of fuzzy set Q at k (q_{kl}) and upper bound is given by upper limit of interval corresponding to λ-cut of fuzzy set Q at 1-k (q_{ku}) as shown in Fig. 2. The fractile k (say, 0.95) is shown in Fig. 2 as a particular value of membership function. Accordingly, from fuzzy sets of P_F at different times,

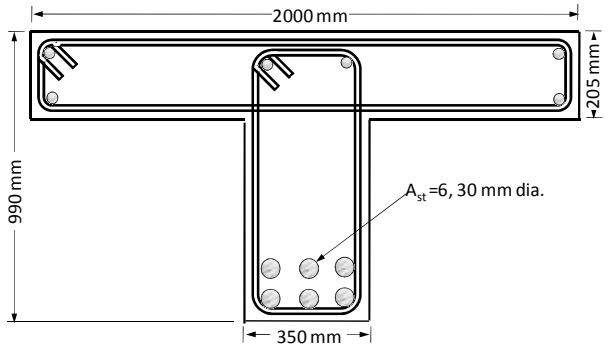

Fig. 3 Cross-sectional details of reinforced concrete bridge girder

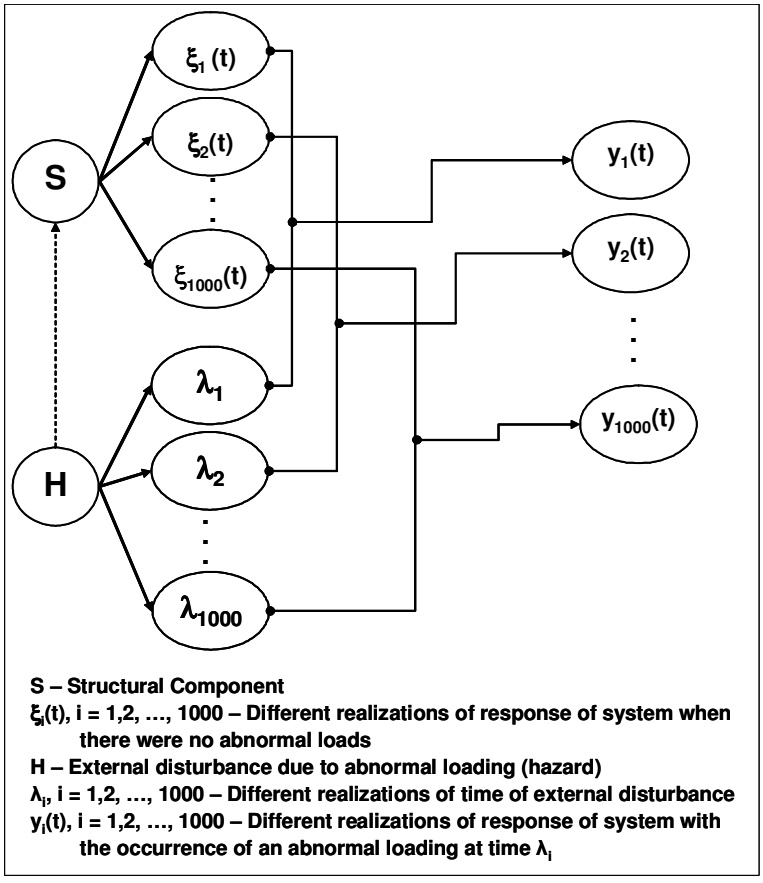

Figure. 4 Schematic representation of problem considered

Table 1 Values of mean and standard deviation (SD) for the random variables considered for determination of time for corrosion initiation

variable	mean	SD	Remarks
d (mm)	45	2.25	Assumed cov of 0.05
D (cm^2/s)	5 x 10^{-8}	1 x 10^{-8}	cov = 0.20 [48]
c_s (% by weight of concrete)	0.25	0.05	cov = 0.20 [48]
c_{cr} (% by weight of concrete)	0.125	0.025	Assumed cov of 0.20

it is possible to determine bounds for characteristic values corresponding to any fractile k (taken as 0.95 in this study since a conservative estimate of P_F is required). The upper bound of the characteristic value is recommended for decision-making purposes.

The upper bound for characteristic value of $P_F(t)$ can be used in the service life estimation. The usefulness of the proposed algorithm for identification of corrosion initiation and remaining life estimation is illustrated through an application.

4. Application

A reinforced concrete bridge girder, located in a severe environment (as per the definitions of exposure conditions in IS 456-2000 [40]) with cross-sectional details as shown in Fig. 3 is considered. The specified water-cement ratio is 0.45. For studying the efficiency of the proposed algorithms for change point detection, an ensemble of $y(t)$ is generated which is assumed to represent the electrochemical current noise data obtained from online monitoring and stochasticity in time of occurrence of change point event (initiation of chloride-induced corrosion) is taken into consideration. The entire problem has been formulated within the framework of Monte Carlo simulation, and is depicted schematically in Fig. 4.

Assuming ingress of chlorides into cover concrete as a diffusion process, time to corrosion initiation (t_i) can be determined from Fick's second law of diffusion as

$$t_i = \frac{d^2}{4D}\left[erf^{-1}\left(\frac{c_s - c_{cr}}{c_s}\right)\right]^{-2} \qquad (18)$$

© 2013 SRESA All rights reserved

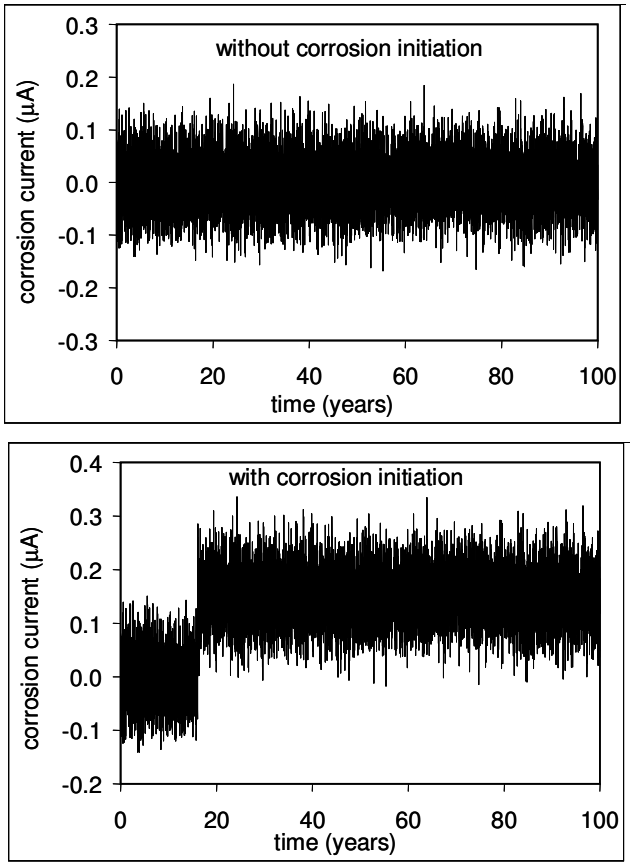

Figure 5 Typical realizations of the observed process (simulated in the present study) without- and with- shift (time of corrosion initiation = 16.1 years)

where d is the clear cover to reinforcement, D is the diffusion coefficient for chlorides in concrete, c_s is the surface chloride concentration and c_{cr} is the critical chloride concentration. To account for variations in workmanship and exposure conditions, d, D, c_s and c_{cr} are treated as random variables. The values of mean and standard deviation of these random variables are given in Table 1. All the random variables are assumed to be statistically uncorrelated with each other. The mean and standard deviation of time to corrosion initiation are determined using first order approximation as 14.11 years and 9.42 years, respectively. It is assumed that t_i follows a lognormal distribution [46], i.e., $F_\Lambda(\lambda)$ in Eqs. 4 and 5 is lognormal.

The amplitude of shift in mean corrosion current is taken as 0.15 μA/cm^2, which is consistent with exposure condition for the girder. The cov of current noise indicates type of corrosion, ranging from 10^{-3} for general corrosion to 1.0 for localized corrosion [13]. A value of 0.33 is assumed as the cov of corrosion current in this study. In the present study, simulated electrochemical noise data, representing the monitored corrosion currents, is used. Cottis *et al.* [47] used a shot noise model to simulate electrochemical noise data. It is assumed that monitored electrochemical noise data can be represented by a GWN process. One thousand realizations of GWN process are generated representing the possible realizations of monitored electrochemical noise for a period of 100 years at an interval of 0.01 years (for each realization). One thousand lognormal random variables, representing time-to-corrosion initiation, one for each realization of the observed process, are generated. Typical realizations of the observed process (electrochemical noise) without and with shift (corrosion initiation) are shown in Fig. 5.

Figure 5 Typical realizations of the observed process (simulated in the present study) without- and with- shift (time of corrosion initiation = 16.1 years)

For the change point detection algorithm, width of sliding window is taken as 5 years (i.e., S = 500). The window width should be chosen long enough so that detection of change point is possible, but short enough for computational efficiency. Thus, the selection of window width is a pareto-optimal problem; however, this aspect is not considered in this study. Fourth-order Runge-Kutta method is used for solving the ordinary differential equations (Eqs. 4 and 5), and the time of shift (t_a) is determined using Eq. 6 for each realization of the process. The values of delay in detection (t_d) are determined for the cases $t_a > t_o$ using Eq. 7, and the statistical properties (namely, mean and standard deviation) of t_d are computed. The delay in detection is assumed to follow a lognormal distribution. The information on delay in detection of the change point detection algorithm is used further in the remaining life estimation of the RC bridge girder considered.

The moment due to service loads (M_{SL}) is considered to be deterministic, and is equal to 711.0 kN-m (17). In the present study, the ultimate moment of resistance at any time ($M_u(t)$) is computed using the relations given in IS 456-2000 [40] without the partial safety factors. The breadth of flange, effective depth, compressive strength of concrete, yield strength of steel and delay in detection are considered as random variables. The statistical properties of these random variables are given in Table 2.

© 2013 SRESA All rights reserved

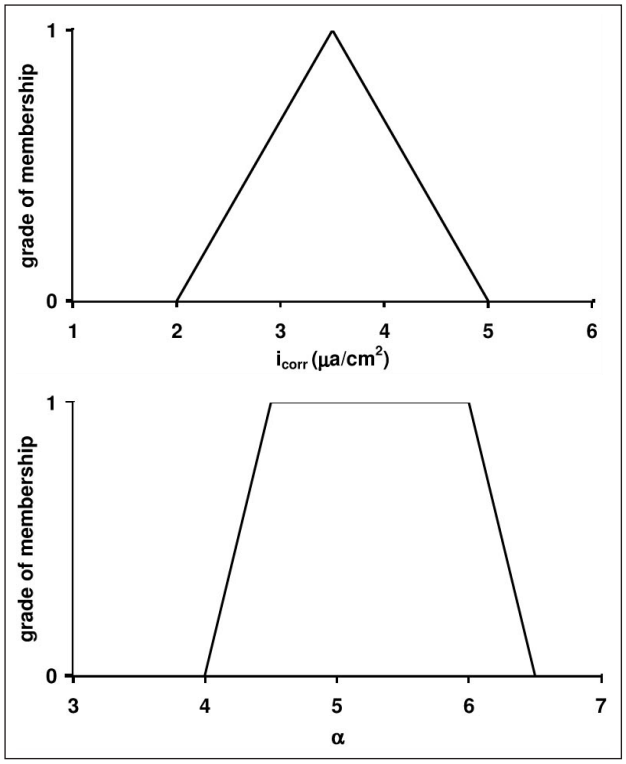

Figure. 6 Fuzzy sets for corrosion current density and a for the example considered

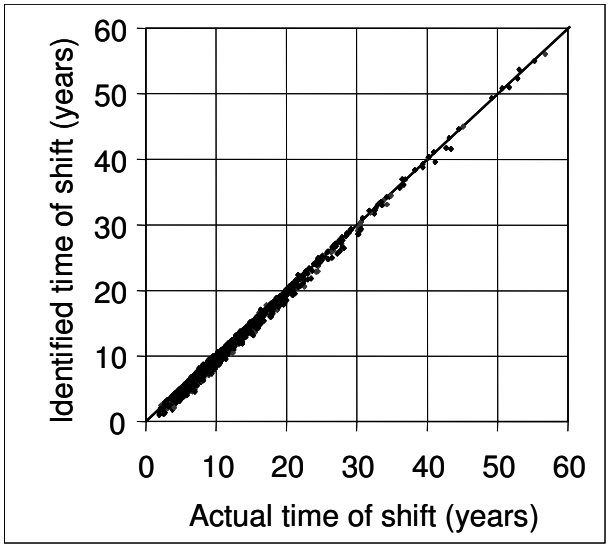

Figure. 7 Comparison of actual and predicted times of shift

The fuzzy sets for I_{corr} and a are selected from Figure 1 based on the exposure condition and water-cement ratio used, and are shown in Fig. 6. Fuzzy sets for failure probability at different times are computed according to section 3.2. Four combinations of I_{corr} and a are considered for each of the λ-cut levels of 0^+, 0.2, 0.4, 0.6 and 0.8, and two combinations of I_{corr} and α are considered for the λ-cut level of 1.0, giving a total

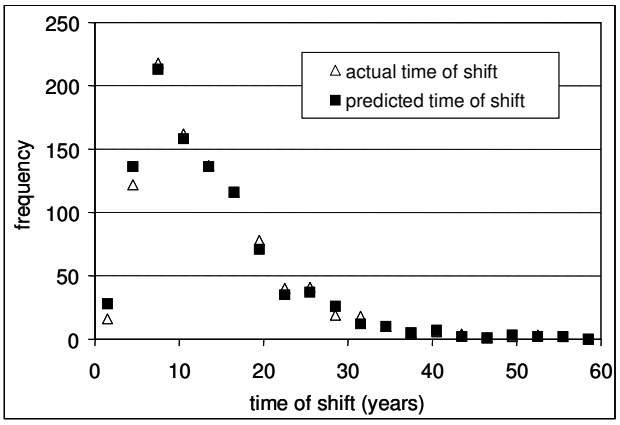

Figure. 8 Frequencies of actual and predicted times of shift

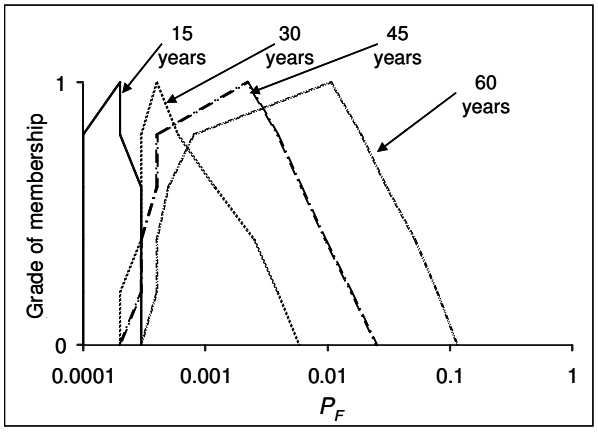

Figure. 9 Fuzzy sets for failure probability at different times after detection of corrosion initiation (Failure criterion: $M_u(t) < M_{SL}$)

Table 2 Random variables considered for remaining life estimation problem

Variable	Mean	COV	Distribution	Reference
Breadth of flange (mm)	2000	0.03	Normal	[49]
Effective depth (mm)	891	0.03	Normal	[49]
Compressive strength of concrete (N/mm^2)	30	0.176	Lognormal	[49]
Yield strength of steel (N/mm^2)	415	0.12	Lognormal	[49]
Delay in detection of corrosion initiation (years)	0.139	0.105	Lognormal	Based on simulation

© 2013 SRESA All rights reserved

Figure. 10 Variation in defuzzified values of failure probability with time (Failure criterion: $M_u(t) < M_{SL}$)

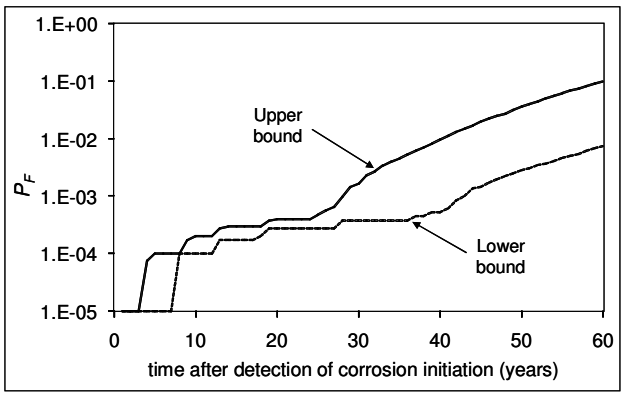

Figure. 11 Bounds for characteristic value of P_F corresponding to 0.95 fractile (Failure criterion: $M_u(t) < M_{SL}$)

of 22 combinations of I_{corr} and α. For each combination, the failure probability against limit state of flexure (Eq. 9) is computed using the importance sampling technique. Thus, the fuzzy sets of P_F at different times after detection of corrosion initiation are constructed, and the defuzzified values of P_F are determined using defuzzification. The bounds for characteristic values of failure probability (corresponding to 0.95 fractile) are determined from fuzzy sets of failure probability at different times using the approach given in section 3.3.

5 Results and Discussion

5.1 Change point detection using proposed algorithm

The comparison between the actual and predicted times of shift for the one thousand realizations considered are shown in Fig. 7, and the frequency distributions of actual and predicted times of shift are shown in Fig. 8. From these figures, it is noted that the predicted times of shift are in good agreement with the actual times of shift. The mean and standard deviation for delay in detection are obtained as 0.139 and 0.105 years, respectively. The small values of delay in detection indicate the usefulness of the proposed algorithm. The delay in detection is assumed to be lognormally distributed. The information of delay in detection is used in the remaining life estimation of the RC bridge girder.

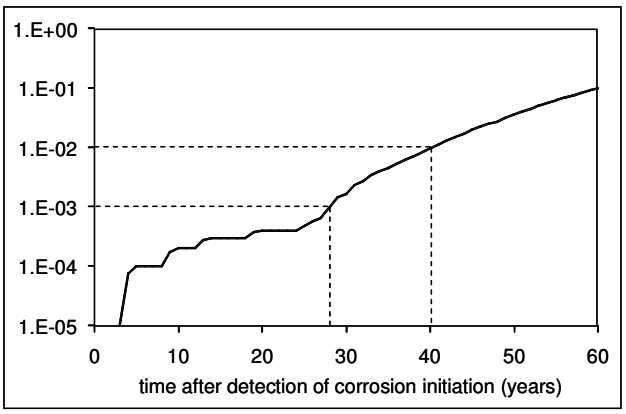

Figure. 12 Upper bound for characteristic value of P_F corresponding to 0.95 fractile (Failure criterion: $M_u(t) < M_{SL}$)

5.2 Remaining life estimation

The fuzzy sets of P_F at 15, 30, 45 and 60 years after detection of corrosion initiation are shown in Fig. 9. From this figure, it is noted that interval lengths of fuzzy sets of P_F at a given λ-cut level increase with age, resulting in the increase in uncertainty about P_F with age. The increase in uncertainty about P_F with age can be attributed to increase in uncertainty about remaining diameter of the reinforcement with increase in time.

The defuzzified values of P_F (determined using centroidal defuzzification method) obtained from fuzzy-random analysis are shown in Fig. 10. The P_F values obtained from fuzzy-random analysis are more rational since appropriate representations of uncertainty are used for the different variables. Also, by carrying out a probabilistic analysis, while it is possible to obtain bounds on P_F, it may be computationally expensive to obtain probability distribution for P_F. But from the resulting fuzzy set of P_F obtained using the proposed procedure, one can obtain not only the possibility distribution of P_F, but also the bounds for characteristic values of P_F corresponding to a specified fractile, with minimal computational effort. The bounds for characteristic values of P_F corresponding to 0.95 fractile obtained from fuzzy sets of P_F at different times, are shown in Fig. 11. The upper bound for characteristic value of P_F

© 2013 SRESA All rights reserved

(shown separately in Fig. 12) can be used for remaining life estimation (by comparing with the allowable value of P_F). For instance if the allowable value of probability of failure is 10^{-3}, then the remaining life of the structure after detection of corrosion initiation is about 28.3 years, while if the allowable value of probability of failure is 10^{-2}, then the remaining life of the structure after detection of corrosion initiation is about 40 years. This type of information will be useful for decision-making regarding in-service inspections.

6 Summary

An algorithm, based on the Bayesian approach, is proposed for identifying time of corrosion initiation in reinforced concrete structures affected by chloride-induced corrosion of reinforcement. The usefulness of the algorithm is studied by using an example problem of identification of time of corrosion initiation in a reinforced concrete bridge girder, using simulated corrosion current data. The small values of delay in detection indicate the usefulness of the proposed algorithm for online change point detection. The statistical properties of the delay in detection of the proposed change point detection algorithm are determined. A methodology for remaining life estimation of corrosion-affected reinforced concrete flexural members, in the presence of fuzzy and random uncertainties, taking into consideration the delay in detection of corrosion initiation using the online monitoring algorithm, is presented. The usefulness of the approach is demonstrated through an example problem of remaining life estimation of a reinforced concrete bridge girder. It is also illustrated that one can determine the bounds for characteristic value of failure probability from the resulting fuzzy set for failure probability with minimal computational effort.

Acknowledgement

The paper is being published with the kind permission of Director, CSIR-Structural Engineering Research Centre, CSIR Campus, Taramani, Chennai, INDIA.

References

1. Aktan, A.E., Catbas, F.N., Grimmelsman, K.A. and Pervizpour, M. (2002). *Development of a model health monitoring guide for major bridges*, Report submitted to Federal Highway Administration Research and Development, CONTRACT/ORDER NO. DTFH61-01-P-00347.
2. Straser, E.G. and Kiremidjian, A.S. (1998). *A modular wireless damage monitoring system for structures*, Report No. 128, John A. Blume Earthquake Engineering Center, Department of Civil and Environmental Engineering, Stanford University, Stanford, CA.
3. Lynch, J.P. (2002). *Decentralisation of wireless monitoring and control technologies for smart civil structures*, Report No. 140, John A. Blume Earthquake Engineering Center, Department of Civil and Environmental Engineering, Stanford University, Stanford, CA.
4. Lynch, J.P. (2004). Overview of wireless sensors for real-time health monitoring of civil structures. Proceedings of the 4th International Workshop on Structural Control and Monitoring, New York City, NY, USA, June 10-11, 2004.
5. Bornn, L., Farrar C.R., Park, G. (2010). Damage Detection in Initially Nonlinear Systems, *International Journal of Engineering Science*, 48(10), 909-920.
6. Basseville, M. and Nikiforov, I.V. (1993). *Detection of abrupt changes: theory and applications*. Prentice-Hall, Englewood Cliffs, NJ.
7. Pines, D. and Aktan, A.E. (2002). Status of structural health monitoring of long-span bridges in the United States. Progress in Structural Engineering and Materials, 4:372-380.
8. Hardon, R.G., Lambert, P. and Page, C.L. (1988). Relationship between electrochemical noise and corrosion rate of steel in salt contaminated concrete. British Corrosion Journal, 23:225-228.
9. Katwan, M.J., Hodgkiess, T. and Arthur, P.D. (1996). Electrochemical noise technique for the prediction of corrosion rate of steel in concrete. Materials and Structures, 29(189):286-294.
10. Mariaca, L., Bautista, L., Rodriguez, P. and Gonzalez, J.A. (1997). Use of electrochemical noise for studying the rate of corrosion of reinforcement embedded in concrete. *Materials and Structures*, 30(204):613-617.
11. Smulko, J.M., Darowicki, K. and Zieliński, A. (2006). Evaluation of reinforcement corrosion rate in concrete structures by electrochemical noise measurements. Russian Journal of Electrochemistry, 42: 546-550.
12. Cottis, R.A. and Llewellyn, A. (2007). Electrochemistry for corrosion. http://www.cp. umist.ac.uk/lecturenotes/Echem/Noisefile.html (last accessed on 06.06.2007).
13. Gowers, K.R. and Millard, S.G. (1999). Electrochemical techniques for corrosion assessment of reinforced concrete structures. Proceedings of Institution of Civil Engineers, Structures & Buildings, 134:129-137.
14. Legat, A., Leban, M. and Bajt, Ž. (2004). Corrosion processes of steel in concrete characterized by means of electrochemical noise. *Electrochimica Acta*, 49:2741-2751.
15. Anoop, M.B., Balaji Rao, K. and Lakshmanan, N. (2008). An algorithm for detection of change point in on-line monitoring data. Journal of Infrastructure Systems, ASCE. 14(1):33-41.
16. Andrade, C., Alonso, M.C. and Gonzalez, J.A. (1990). An initial effort to use the corrosion rate measurements for estimating rebar durability. in Berke, N.S., Chaker, V. and Whiting, D., Ed., *Corrosion rates of steel in concrete*, ASTM STP 1065, American Society for Testing and Materials, Philadelphia, pp. 29-37.
17. Anoop, M.B., Balaji Rao, K. and Appa Rao, T.V.S.R. (2003). A methodology for durability-based service life design of reinforced concrete flexural members. *Magazine of Concrete Research*, 55(3), 289-303.
18. Baweja, D., Roper, H. and Sirivivatnanon, V. (1999), Chloride-induced steel corrosion in concrete: Part 2 - gravimetric and electrochemical comparisons. *ACI Materials Journal*, 96(3), 306-313.

© 2013 SRESA All rights reserved

19. Balaji Rao, K., Anoop, M.B. and Lakshmanan, N. (2006), *An algorithm for detection of change point in on-line monitoring data*, SERC Project Report No. SS-OLP11641/COR12-RR-2006-4, Structural Engineering research Centre, Chennai, November 2006.
20. Fishman, M. (1986). Bayesian mean square estimation of the instant of one-step shift of the mean level of white gaussian noise. In: L. Telksnys, ed. *Detection of changes in random processes*, Optimization Software Inc. Publication Division, New York.
21. BRITE/EURAM (1995), *The Residual Life of Reinforced Concrete Structures*. Final Technical Report, Report No. BRUE-CT92-0591.
22. Lay, S. and Schieβl, P. (2003), *LIFECON deliverable 3.2: service life models*. cbm-Technische Universität München.
23. *fib*. (2006). *Model Code for Service Life Design*. *Fib* Bulletine 34, International Federation for Structural Concrete, Lausanne.
24. ISO. (2008), *General Principles in the Design of Structures for Durability*, ISO/WD 13823 International Standards Organization, Switzerland.
25. Siemes T., Polder R. and de Vries H. (1998), Design of concrete structures for durability - Example: chloride penetration in the lining of a bored tunnel, HERON, 43(4): 227-244.
26. Sarja, A., Bamforth, P.B., Caccavelli, D., Chevalier, J.-L. and Durucan, S. (2005), *European Guide for Life Time Design and Management of Civil Infrastructures and Buildings*. VTT Building and Transport, Finland.
27. Raupach, M., Warkus, J. and Gulikers, J. (2006). Damage process due to corrosion of reinforcement bars – current and future activities. Materials and Corrosion, 57(8):648-653.
28. Ying, L. and Vrouwenvelder, T. (2007), Service life prediction and repair of concrete structures with spatial variability. *HERON*, 52(4), 251-268.
29. Vu, K.A.T. and Stewart, M.G. (2000). Structural reliability of concrete bridges including improved chloride-induced corrosion models. *Structural Safety*, 22, 313-333.
30. Val, D.V. and Stewart, M.G. (2003), Life-cycle cost analysis of reinforced concrete structures in marine environments. *Structural Safety*, 25, 343-362.
31. Anoop, M.B., Balaji Rao, K. and Appa Rao, T.V.S.R. (2002). Application of fuzzy sets for estimating the service life of reinforced concrete structural members in corrosive environments. *Engineering Structures*, 24(9), 1229-1242.
32. Ross, T. J. (1985), Fuzzy Logic with Engineering Applications. McGraw-Hill, CA.
33. Dubois, D., Prade H. and Sandri, S. (1993), On possibility/probability transformations, In: Lowen R, Roubens M, (Ed.). *Fuzzy Logic*. Dordrecht, Kluwer.
34. Klir, G.J. and Parviz, B. (1992), Probability-possibility transformations: a comparison. *International Journal of General Systems*, 21, 291-310.
35. Möller, B., Graf, W. and Beer, M. (2003). Safety assessment of structures in view of fuzzy randomness, *Computers and Structures* 81, 1567–1582.
36. Anoop, M.B., Balaji Rao, K. and Gopalakrishnan, S. (2006). Conversion of probabilistic information into fuzzy sets for engineering decision analysis. *Computers & Structures*, 84, 141-155.
37. Anoop, M.B., Raghuprasad, B.K. and Balaji Rao, K. (2012), A refined methodology for durability-based service life estimation of reinforced concrete structural elements considering fuzzy and random uncertainties, Computer-Aided Civil and Infrastructure Engineering, 27(3), 170-186.
38. Chakraborty, S. and Sam, P.C. (2007), Probabilistic safety analysis of structures under hybrid uncertainty, *International Journal for Numerical Methods in Engineering*. 70(4), 405-422.
39. Savoia M. (2002), Structural reliability analysis through fuzzy number approach, with application to stability. *Computers and Structures*, 80, 1087-1102.
40. BIS (2000), Indian standard code of practice for plain and reinforced concrete: IS 456-2000. Bureau of Indian Standards, New Delhi.
41. Dong, W. and Shah, H. (1987), Vertex method for computing functions of fuzzy variables. *Fuzzy Sets and Systems*, 24, 65-78.
42. Haukaas, T. (2001), *FERUM (Finite Element Reliability Using MATLAB) User's Guide*, available at http://www.ce.berkeley.edu/projects/ferum/User_s_Guide/user_s_guide.html
43. Zadeh, L. (1978). Fuzzy sets as a basis for a theory of possibility. *Fuzzy Sets and Systems*, 1(1), 3-28.
44. Dubois, D., Prade, H. and Yager, R. (1999). Merging fuzzy information, in Bezdek, J.C., Dubois, D., Prade, H. Eds., *Fuzzy sets in Approximate Reasoning and Information Systems*. Kluwer Academic Publishers, Dordrecht, 335-401.
45. Dubois, D., and Prade, H. (1980). *Fuzzy Sets and Systems: Theory and Applications*. Academic Press Inc., San Diego.
46. Balaji Rao K., Anoop M. B. and Appa Rao T. V. S. R. (2001). A methodology for reliability-based design of concrete cover thickness with reference to chloride induced corrosion of reinforcement. Proceedings of International Conference on Civil Engineering, ICCE - 2001, Department of Civil Engineering, Indian Institute of Science, Bangalore, 2001, pp. 215-221.
47. Cottis, R.A., Al-Awadhi, M.A.A., Al-Mazeedi, H. and Turgoose, S. (2001). Measures for the detection of localized corrosion with electrochemical noise. Electrochimica Acta. 46:3665-3674.
48. Balaji Rao, K., Anoop, M. B., Gopalakrishnan, S., Manjuprasad, M. and Lakshmanan, N. (2004), *Seismic vulnerability analysis of corrosion-affected reinforced concrete structures*, SERC Project Report SS-OLP09441-RR-2004-3, Structural Engineering research Centre, Chennai, May 2004.
49. Prakash Desayi and Balaji Rao, K. (1987), Probabilistic analysis of the cracking of RC beams. Materials and Structures, 20(120):408-417.

© 2013 SRESA All rights reserved

Life Cycle Reliability and Safety Engineering
Vol.2 Issue 1 (2013) 13-20

Simplified Fuzzy-Random Seismic Fragility of Open Ground Storey Buildings

Tushar K Padhy, Devdas Menon and A Meher Prasad
Department of Civil Engineering, Indian Institute of Technology Madras,Chennai
e-mail : dmenon@iitm.ac.in

Abstract

Open ground storey buildings are very common in urban areas in countries like India. They are also the most vulnerable type of vertically irregular buildings in the event of earthquake. In this study, the coupled effect of vertical irregularity with the fuzziness of limit states, on the seismic fragility of buildings, is studied. Seismic fragility of typical open ground storey buildings designed as per IS 1893 (2002) are evaluated for various damage states. The predominant failure mode for the open ground storey building is a soft-storey mechanism in the ground storey, and hence inter-storey drift at ground storey has been considered as the demand parameter. A simplified power–law model is then utilised to construct the probabilistic demand as proposed by Cornell et al. Fuzziness in the limit states is then introduced through a recently proposed membership function. It is found that fuzziness information has a significant role on the seismic fragility at ultimate limit states for open ground storey frames, as well as for regular frames.

Keywords: seismic fragility, soft storey, fuzzy–random, membership function

1. Introduction

Performance in the past earthquakes indicates that the buildings with open ground storey or the 'pilotis-storey' are susceptible to extensive damage [1]. Despite their vulnerability to earthquakes, they are still preferred, especially in the urban areas for providing parking space in apartments and multi-functional spaces in hotels and commercial establishments. The absence of non-structural walls in the ground storey of such buildings creates considerable vertical irregularity in both stiffness and strength, resulting in very large inter-storey drift compared to the storeys above. This has prompted a concerted research effort to evaluate such buildings with and without the retrofitting measures [2- 5].

There are various sources of uncertainty to be considered. Firstly, there is the inherent randomness in the ground shaking; secondly, there is some uncertainty in the estimated material properties of the structure; thirdly, the threshold limits for the damage states are also not precisely defined. In this study, the first two sources of uncertainty are accounted for in the probabilistic formulation, and the third is accounted for in terms of fuzziness in the definition of the limit states, by means of a membership function.

2. Seismic Fragility Analysis

Seismic fragility is defined as the probability of reaching or exceeding a limit state or performance level as a function of specific ground motion intensity measure. In other words, it is the conditional probability of demand exceeding the capacity for a given seismic intensity. Assuming the capacity and demand to be log-normal and independent of each other, it can be expressed in closed-form as [7]:

$$P\left(C-D\le 0|IM\right)=\Phi\left(\frac{\ln {S_d}/{S_c}}{\sqrt{\beta_{d|IM}^2+\beta_c^2}}\right) \qquad (1)$$

Where C is the drift capacity, D is the demand, S_d is the median of the structural demand and S_c is the median structural capacity of the chosen limit state (LS). $\beta_{d|IM}$ and β_c are the logarithmic standard deviations or dispersion measures in the demand and capacities respectively.

The seismic demand on the structure is determined through the nonlinear time history analyses that are performed using an ensemble of ground motions. The demand can be related to the seismic intensity using a simplified probabilistic seismic demand model, as suggested by Cornell et al [6]:

© 2013 SRESA All rights reserved

$$D = a\,(IM)^b\,\varepsilon \tag{2}$$

where ε is a log-normal random variable with median 1.0 and dispersion $\beta_{d|IM}$. This dispersion represents the uncertainty due to record-to-record variability. *a* and *b* are the linear regression parameters (using least squares) found from the 'cloud' analysis. Here, 'cloud' analysis refers to a wide range of intensity measures unlike the 'stripe' analysis wherein the analysis is done for a particular value of intensity measure [7]. In this study, the structural demand measure is selected to be the absolute maximum inter-storey drift of the ground storey, which occurs as the dynamic response during the earthquake excitation. This choice of demand measure presumes the failure mechanism to be a storey-mechanism at the ground floor as observed in several earthquake reconnaissance surveys. The seismic intensity measure is taken to be the peak ground acceleration (PGA) of the ground motion. The analysis involved nonlinear time history analyses of thirty statistically equivalent analytical models to obtain a set of thirty inter-storey drifts (δ) for the corresponding PGAs. Simulation has been carried out using Latin Hypercube Sampling in which the ground motion and the system parameters (viz. characteristic compressive strength of concrete and yield strength of steel) are considered as random. The parameters *a* and *b* are determined for the set of thirty values through the 'cloud analysis' [8] and the values are presented in Table 1.

Table 1 Regression Parameters

Frame	a	b
OGS	52.746	1.233
Fully-infilled	52.300	1.653
Bare	114.434	1.111

The structural capacities are defined as the allowable maximum inter-storey drift (which occurs at the ground storey) corresponding to three widely used performance levels: (a) *immediate occupancy* (IO) at which the structure can be occupied safely without significant repair (b) *life safety* (LS) a limit state signifying considerable damage but with a safe margin against incipient collapse and (c) *collapse prevention* (CP), defined as the point of incipient collapse. Since these limits are hard to quantify in terms of inter-storey drift, fuzziness has been introduced in this study with 'most probable' drift limits as suggested by Ghobarah [9]. The dispersion in capacity, β_c, is dependent on the building type and construction quality. Wen et al [10] have suggested a value of 0.3 whereas ATC 58-75% draft [11] suggests 0.10, 0.25 and 0.40 depending on the quality of construction. In this study, a uniform value of 0.25 has been assumed for the dispersion of the median capacity (Table 2).

Table 2 Limit State Definitions

Limit states	c (%) with infill	c (%) without infill	β_c
IO	0.2	0.4	0.25
LS	0.4	1.0	0.25
CP	0.8	3.0	0.25

3. Fuzzy Random Method

The failure probability according to classical reliability theory can be expressed as follows [19]:

$$P(R<S) = \iint_{R<S} f_{RS}\,dr\,ds = \int_0^\infty \left[\int_0^s f_R(r)\,dr\right] f_S(s)\,ds$$

$$= \int_0^\infty \left[\int_r^\infty f_S(s)\,ds\right] f_R(r)\,dr \tag{3}$$

where *R* and *S* are the resistance and response of the structural system at a certain performance level, respectively. Both *R* and *S* are assumed to be independent random variables with some probability distribution. In the following text, these notations are substituted by *C* and *D*, denoting capacity and demand, in lieu of *R* and *S*, respectively.

It is important to consider fuzziness in the thresholds of capacity for defining various damage states. There is the presence of subjective judgment while specifying the level of damages, using linguistic terms ('few', 'moderate',' extensive'). Giovinazzi and Lagomarsino [12] used a weighted approach to overlapping membership functions to arrive at the vulnerability index. Möller et al [13] introduced the concept of 'fuzzy FORM' to deal with fuzzy limit state surface, wherein the fuzzy reliability index is computed by α-level optimization. Gu and Lu [14] suggested two fuzzy-random membership function to define occurrence of a limit state and exceedance of a limit state, respectively. The fuzzy interval was based on the drift values associated with non-structural and structural limit states. This definition of membership function has been utilised and a simpler membership function is proposed in a recent work [15].

The probability of a fuzzy-random event, *A*, is defined as the expectation of its membership function $m_A(x)$ [16] as

$$P(A) = E\left[m_A(x)\right] = \int m_A(x)\,f_X(x)\,dx \tag{4}$$

© 2013 SRESA All rights reserved

where $f_X(x)$ is the probability density function of X.

Reaching or exceeding a damage state is considered here as a fuzzy event whose occurrence is uncertain. A recently proposed membership function [15], which simplifies the formulation while satisfying the restriction on boundedness and convexity, has been adopted. It is defined by a two-piece second-degree polynomial, $m(x)$, as

$$m(x)=\begin{cases}0 & ;\ x\le(1-\gamma)c\\ \frac{1}{2}\left[\frac{x-(1-\gamma)c}{\gamma c}\right]^2 & ;(1-\gamma)c\le x\le c\\ 1-\frac{1}{2}\left[\frac{(1+\gamma)c-x}{\gamma c}\right]^2 & ;c\le x\le(1+\gamma)c\\ 1 & ;(1+\gamma)c\le x\end{cases} \quad (5)$$

where x here denotes the demand D. In the absence of any fuzziness with regard to the damage state, failure occurs when x exceeds a 'crisp' threshold of capacity $C = c$. The fuzziness in the threshold is represented by the 'fuzzy parameter', γ, which can take any value between 0 and unity, and distributes the fuzziness equally on both sides of c. Typical extreme values of γ are 0.10 and 0.95, the former corresponding to low fuzziness and the latter to high fuzziness. The variation of the membership function for these two extreme values of γ are depicted in Fig. 1, for a typical value of c = 0.40. The value of c will depend on the damage state under consideration (IO, LS or CP).

When the capacity and demand are assumed to be log-normal and independent of each other, the failure probability, in the presence of fuzziness in capacity, can be expressed as [15]

$$P_f = 1+\frac{1}{\gamma^2}\sum_{h=1}^{9}\alpha_h\,\Phi(\beta_h) \quad (6)$$

4. Numerical Example

The OGS building frames considered for numerical analysis in the present study are located in Indian seismic zone IV with medium soil conditions [17]. These frames are designed as per prevailing practice in India, ignoring the soft-storey effect. Seismic loads are estimated as per IS: 1893 (2002) [17] and the design of the RC elements is carried out as per IS: 456 (2000) [18]. The characteristic strength of concrete and steel were taken as 25MPa and 415MPa. The buildings are assumed to be symmetric in plan, and hence a single plane frame may be considered to be representative of the building along one direction. Typical bay width and column height in this study are selected as 3.2m and 3.0m respectively, as observed from the study of typical existing OGS residential buildings (Table 3). Concrete compressive strength, f_{ck} and steel yield strength, f_y are taken as normal random variables whose distribution parameters are assumed as per Ranganathan [19]. The OGS frame 4s5band a building frame with infill walls extended to the ground storey (4s5b-full) considered for the present study are shown in Fig. 2. The dead load of the slab (3 m x 3 m panel), including floor finishes, is taken as 2.5 kN/m^2 and live load as 3 kN/m^2. The non-structural brick masonry infill is 230 mm thick. The unit weight of infill is taken

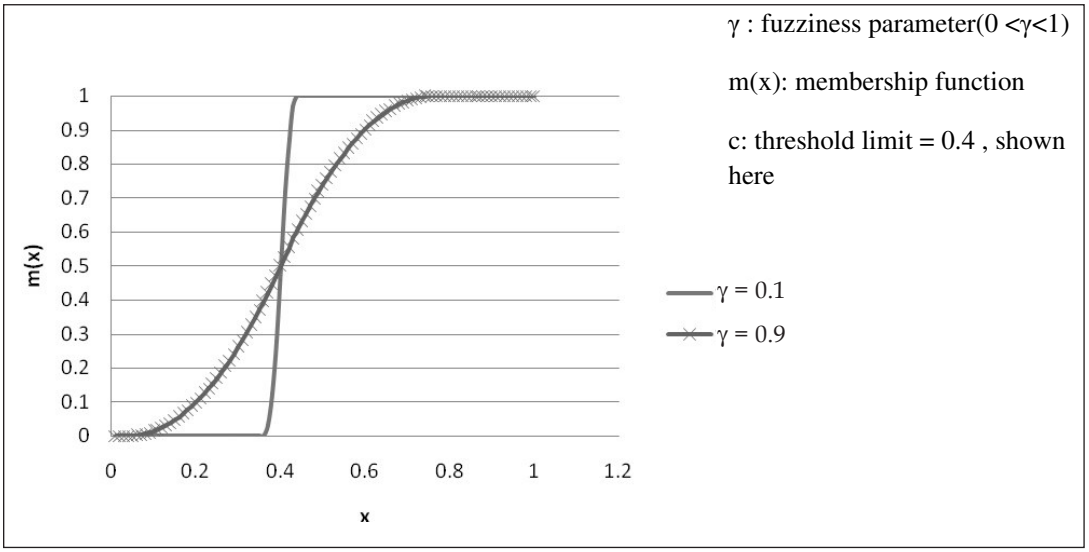

Figure 1 Membership Function

© 2013 SRESA All rights reserved

as 18 kN/m^3, maximum allowable shear strength is 0.45 MPa, initial elastic modulus is 5000 MPa and the masonry prism strength is 9.09 MPa.

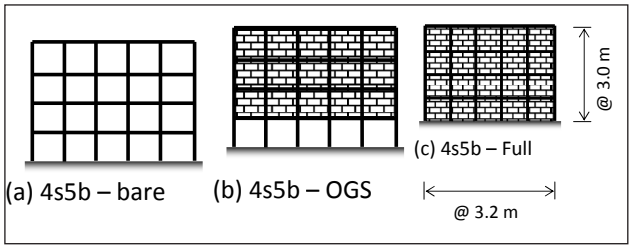

Figure 2 Example Buildings

The design base shear (V_B) is calculated as per IS: 1893 (2002) as

$$V_B = \left(\frac{ZI}{2R} \frac{S_a}{g} \right) W \quad (7)$$

where seismic zone factor, Z = 0.24, Importance factor I = 1.0, Response reduction factor R = 3.0.

'Seismostruct' has been used throughout the study for developing nonlinear analytical models. In 'Seismostruct', fibre approach is made use of to represent the cross-sectional behaviour, where each fibre is associated with a uniaxial stress-strain relationship; the sectional stress-strain state of beam-column elements is then obtained through the integration of the nonlinear stress-strain response of individual fibres with which the section has been discretised [20]. Both force-based (infrmFB) and displacement-based (infrmDB) analysis options are available in the program to simulate inelastic behaviour of the beam-column elements. Here, the displacement-based option has been chosen for the analyses of all the elements. Each element is assigned five integration points along its length where the nonlinear axial-flexural behaviour of the cross-section is monitored. The fibres in each cross-section are assigned material properties to represent unconfined concrete, confined concrete and the steel reinforcement. Here, Mander's nonlinear model [21] has been chosen to represent both confined and unconfined concrete. For reinforcement steel, Menegotto and Pinto stress-strain relationship with Filippou's isotropic hardening rule is used [22]. The main advantages of the fibre model include the ability to capture axial-flexural interaction and the effects of concrete tensile strength and tension stiffening along with user friendly inputs without extensive calibration. However, it does not take into account the bond-slip and reinforcing bar buckling which may contribute to larger degradation in the case of direct simulation of collapse. Skyline solver method and Hilber-Hughes-Taylor integration scheme has been used for non-linear time history analysis. Seismostruct uses Crisafulli's model [23] to represent nonlinear response of infill masonry panels.

For nonlinear time history analyses, a set of ground motion records are required, consistent with the prevailing earthquake scenario. Also, there are very few natural records available for the current scenario. So, there is a need to generate artificial ground motion or to select and modify the natural ground motion records. The latter is preferred as it preserves the natural spectral shape [24]. But presently, there are no guidelines available to select ground motions. The number of ground motions required for an unbiased estimate of the structural response is 7 as per ASCE 7-05 [25]. However, ATC 58 75% draft [11] recommends a suite of 11 pairs of ground motions for a reliable estimate of the response quantities. ASCE/SEI 41 [26] suggests 30 recorded ground motions to meet the spectral matching criteria for nuclear infrastructures. A set of 30 naturally recorded ground motions are with consistent magnitudes and distances required for this study and are modified in the frequency-domain using wavelets [27].

To consider the effect of the fuzziness parameter γ, two extreme values of γ are taken corresponding to low (γ = 0.10) and high (γ = 0.95) fuzziness, respectively. It is seen that the fragility curve for γ = 0.10coincides with that of the crisp limit state (γ = 0), across the limit states as expected, whereas for γ = 0.95, the fuzziness effect is quite significant, especially in case of CP limit state (Figure 3). The fragility curves, with and without fuzziness, intersect each other at a probability of failure of around 0.5. This can be attributed to the shape of the chosen membership function, which is symmetrical about the median capacity. As the fragility curves become flatter towards LS and CP limit states, the effect of fuzziness is observed to be significant. It can be seen that the probability of failure gets under-estimated up to 7% for PGA beyond the intersection

Table 3 OGS Frame Building Details

Frame	Bay width(m)	Storey height(m)	Ground storey column size (mm^2)	% of reinforcement	Fundamental period(sec.)
4s5b	3.2	3.0	300 x 300	2.79	0.44

© 2013 SRESA All rights reserved

point and over-estimated up to 15% for lower PGA values (Figure 3), and this corroborates the results of the previous study [15]. Similar trend has been also observed in the case of fully-infilled frames. This trend can be seen in all the limit states. In the case of frames without any infill (i.e. bare frames), the fragility curves are flatter compared to those pertaining to OGS frames at CP limit state and hence, the effect of fuzziness is more prominently observed here (Figure 4). Further, the sensitivity of fragility curves to threshold values of median capacity, *c* and dispersion, β_c is investigated for CP limit state (Figure 5 and 6). For low values of fuzzy parameter, γ, the fragility curve is neither sensitive to changes in limit state threshold value nor the variance (Figure 5). For higher values of γ, with limiting capacity varying between 0.75c and 1.25c, there is significant over-estimation of probability of failure with increase in median threshold capacity for PGA values that lie before the intersection point (Figure 6(b)). Similarly, there is an over-estimation of failure probability up to 17% when the dispersion, β_c is decreased by 25%, whereas the fuzzy-random fragility curve closes in with the fragility curve without the fuzziness effect for higher values of dispersion ($1.25\beta_c$). In order to understand the effect of fuzziness on structural irregularity, the fragility curves of OGS and a fully-infilled frame are compared. The coupling effect of structural irregularity with the fuzziness is found to be insignificant i.e. structural irregularity does not change the trend of effect of fuzziness on the fragility curve (Figure 7).

5. Summary and Conclusion

A study has been undertaken to incorporate the fuzziness information in limit state function in the computation of seismic fragility. This is achieved through a membership function which represents the fuzziness effect using a fuzziness parameter γ. It is found that when the value of γ is high, the fuzziness effect can be significant, especially at higher level limit states (collapse prevention) whereas its effect on serviceability limit states is marginal. Also, at higher limit states, the fuzzy-random fragility curve

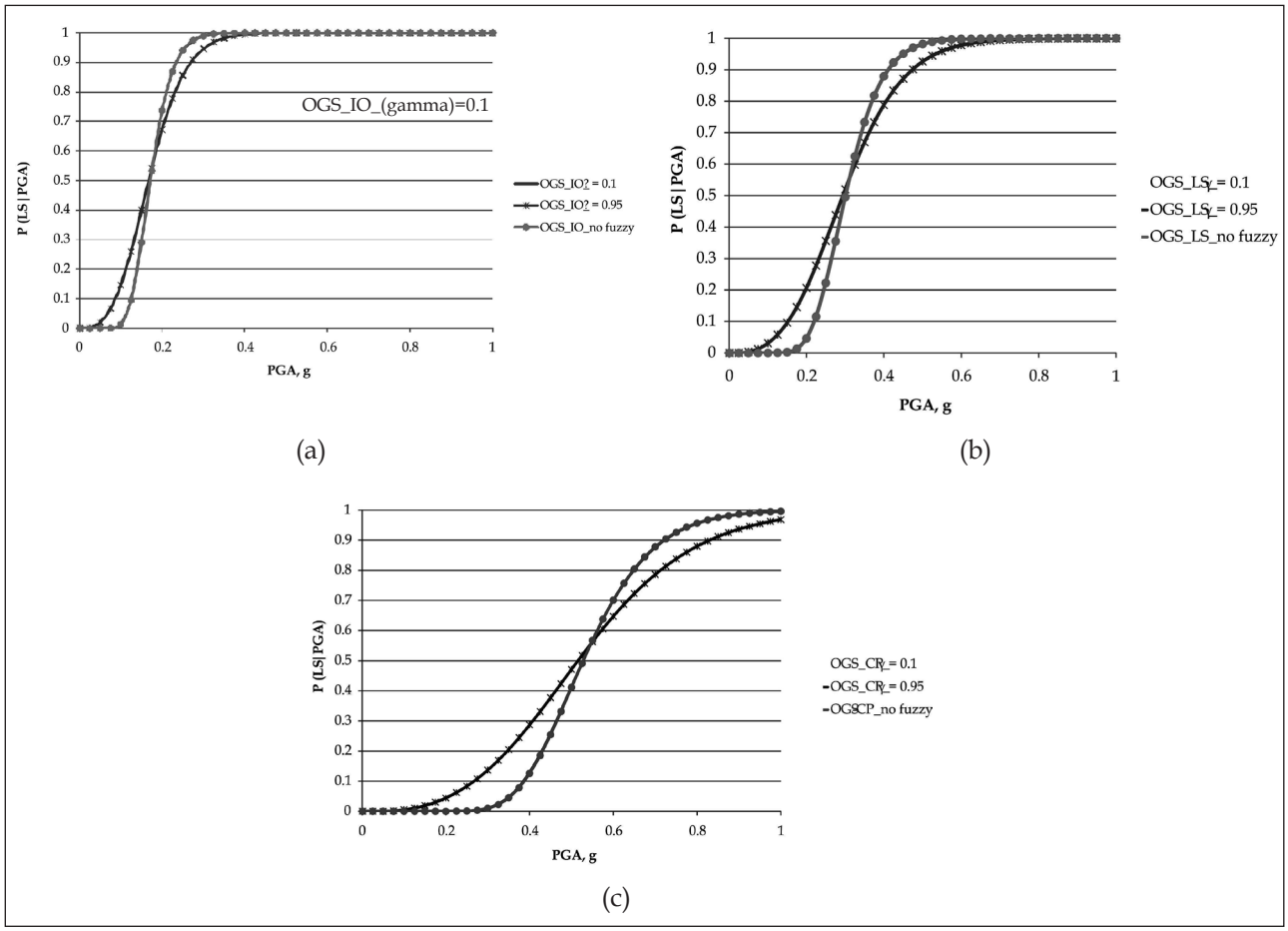

Figure 3 Fragility curves for OGS buildings

© 2013 SRESA All rights reserved

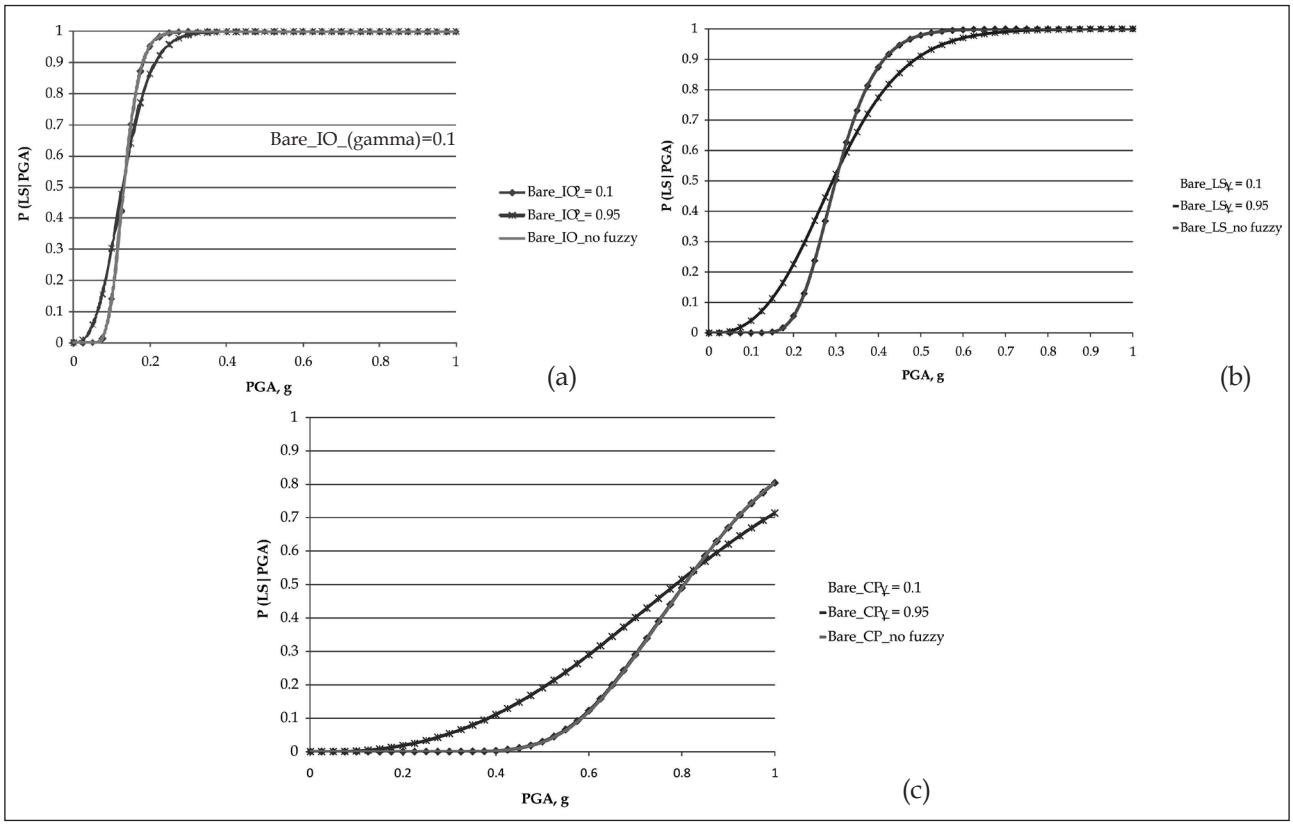

Figure 4 Fragility curves for Bare Frames

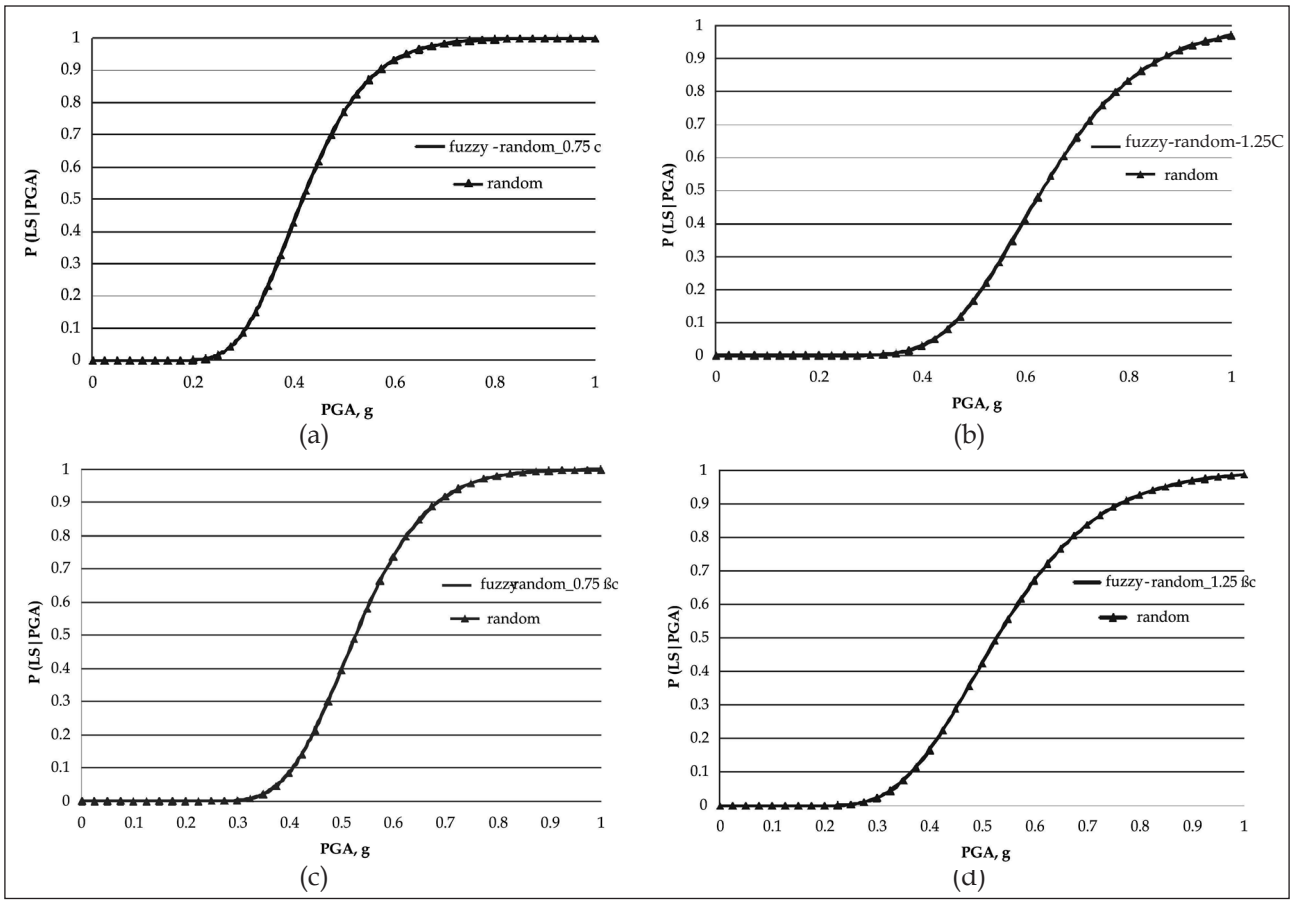

Figure 5 Sensitivity of Limit state function at low fuzziness

© 2013 SRESA All rights reserved

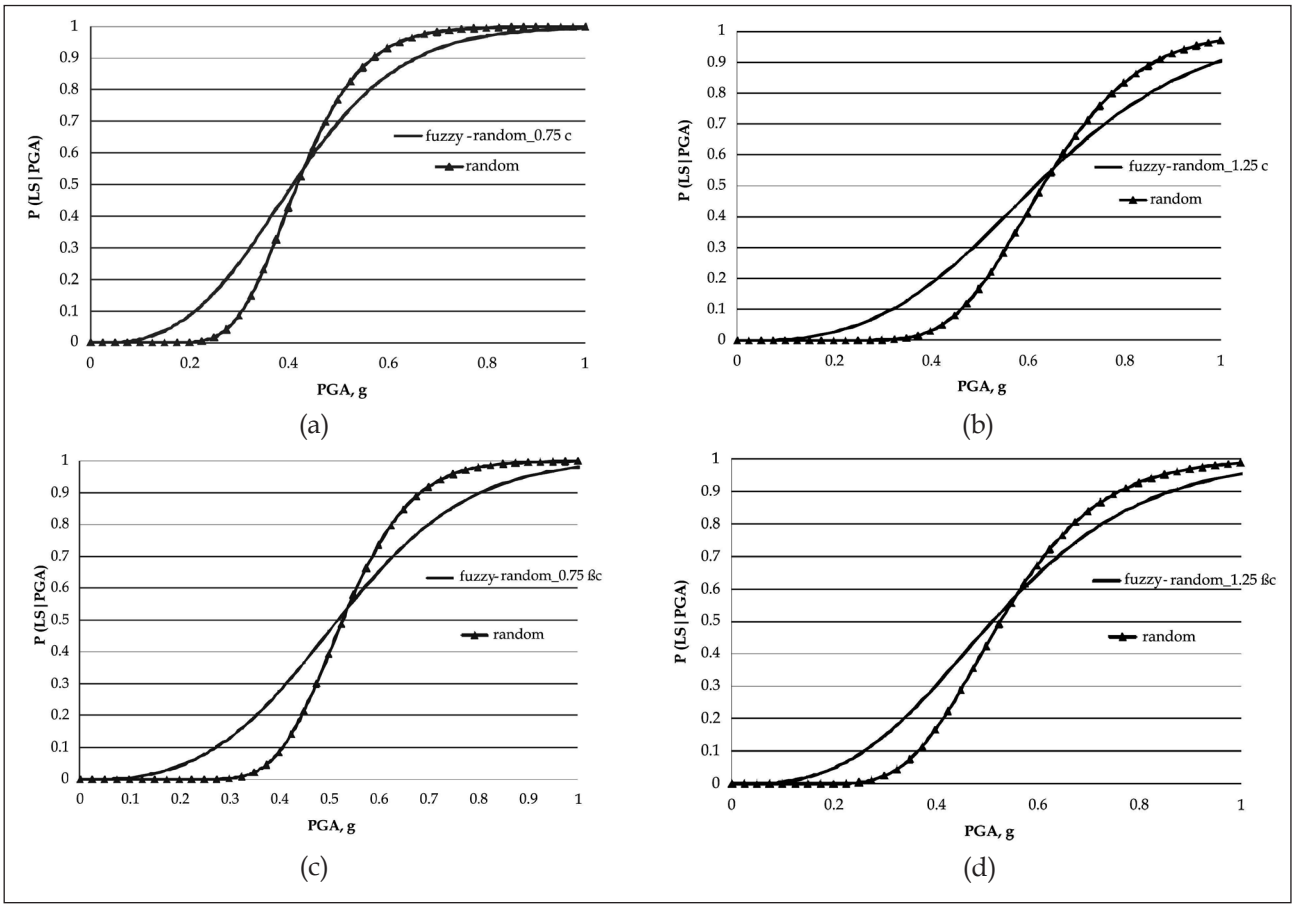

Figure 6 Sensitivity of Limit state function at high fuzziness

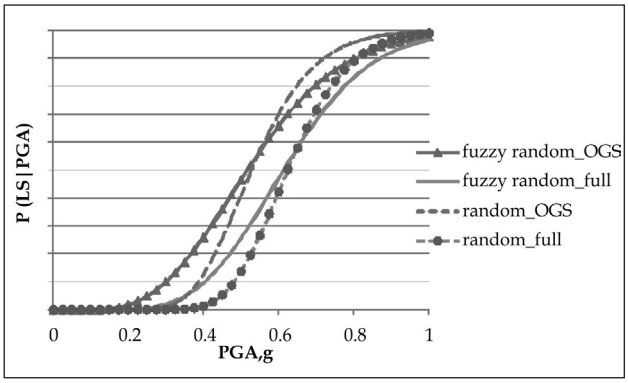

Figure 7 Comparison of effect of irregularity on fuzziness

underestimates failure in the low intensity of seismic excitation whereas it overestimates in the higher excitation range. The fragility curves are sensitive to limit state thresholds when the presence of fuzziness is high. The coupling effect of structural irregularity with the fuzziness is found to be insignificant.

Appendix

When the capacity and demand are assumed to be log-normal and independent of each other, the failure probability, with γ as a fuzziness parameter, can be expressed as [15]

$$P_f = 1 + \frac{1}{\gamma^2}\sum_{h=1}^{9}\alpha_h\,\Phi(\beta_h)$$

$\Phi(.) =$ *standard normal cumulative distribution function*

$$\alpha_1 = 1$$

$$\alpha_2 = -(1-\gamma)^2/2$$

$$\alpha_3 = -(1+\gamma)^2/2$$

$$\text{where } \alpha_4 = -2\exp(-\mu_{\ln Z} + \sigma^2_{\ln Z}/2)$$

$$\alpha_5 = -\alpha_4(1-\gamma)/2$$

$$\alpha_6 = -\alpha_4(1+\gamma)/2$$

$$\alpha_7 = \exp\left\{2(-\mu_{\ln Z} + \sigma^2_{\ln Z})\right\}$$

$$\alpha_8 = \alpha_9 = -\alpha_7/2$$

The other parameters are defined as

$$\mu_{\ln Z} = \mu_{\ln R} - \mu_{\ln S}$$

$$\sigma_{\ln Z} = \sqrt{\sigma^2_{\ln R} + \sigma^2_{\ln S}}$$

© 2013 SRESA All rights reserved

$$\beta_1 = \mu_{\ln Z} / \sigma_{\ln Z}$$
$$\beta_2 = \beta_1 + \ln(1-\gamma) / \sigma_{\ln Z}$$
$$\beta_3 = \beta_1 + \ln(1+\gamma) / \sigma_{\ln Z}$$
$$\beta_h = \beta_{h-3} - \sigma_{\ln Z} \qquad h = 4, 5..., 9$$

References

1. Jain S.K., Murty C.V.R., Dayal U, Arlekar J.N., and Chaubey S.K. "Preliminary Observations on the Origin and Effects of the January 26, 2001 Bhuj (Gujarat, India) Earthquake," EERI Special Earthquake Report, EERI Newsletter, Vol. 35, No. 4.,2001
2. Kampanya, N. and Bracci J.M., "Performance based Seismic Evaluation of RC Frames Prone to Soft Story First Failure", Technical Report CBDC–01–01, Texas A&M University,2001
3. Nagae, T., K. Suita and M. Nakashima, "Performance Assessment for RC Buildings with Soft First Stories", Annuals of Disaster Prevention Research Institute,49 C, Kyoto University,2006
4. Lagaros N.D. "Probabilistic Fragility Analysis: A Tool for Assessing the Design Rules for RC Buildings", Earthquake engineering and Engineering Vibration 7(1), 45–56,2008
5. Davis, R. "Earthquake Resistant Design of Open Ground Storey RC Framed Buildings", Ph.D. Thesis, Indian Institute of Technology Madras,2009
6. Cornell, C. A., F. Jalayer, R.O. Hamburger and D.A. Foutch, "The Probabilistic Basis for the 2000 SAC/FEMA Steel Moment Frame Guidelines", Journal of Structural Engineering 128(4), 526–533,2002
7. Jalayer F. "Direct Probabilistic Seismic Analysis: Implementing Non-linear dynamic assessments", Ph.D. Thesis, Stanford University, 2003
8. Davis R., Padhy T.K., Menon D. and Prasad A.M. " Seismic Fragility of Open Ground Storey Buildings in India", 9th US and 10th Canadian conference on Earthquake Engineering, Toronto, Paper No. 926,2010
9. Ghobarah A. Performance-based Design in Earthquake Engineering: State of Development, Engineering Structures 23, 878–884,2001
10. Wen Y.K., Ellingwood R and Bracci J. "Vulnerability function framework for consequence-based engineering", MAE Center Project DS–4 report,Illinois,2004
11. ATC 58 75% Draft "Guidelines for Seismic Performance Assessment of Buildings", Applied Technology Council, Redwood City, CA, 2011
12. Giovinazzi S. and Lagomarsino S. "A macroseismic method for vulnerability assessment of buildings", Proc. 13th World Conference on Earthquake Engineering.Vancouver,2004
13. Möller B., Graf W., Beer M. and Sickert J. "Fuzzy probabilistic method and its application for the safety assessment of structures", European Conference on Computational Mechanics, Cracow, Poland, 2001
14. Gu X. and Lu Y. "A fuzzy-random analysis model for seismic performance of framed structures incorporating structural and non-structural damage", Earthquake Engineering and Structural Dynamics, Vol 34, pp 1305–1321,2005
15. Colangelo F. "A simplified model to include fuzziness in the seismic fragility curve and relevant effect compared with randomness", Earthquake Engineering and Structural Dynamics, Vol 41, pp 969–986,2012
16. Zadeh L.A. "Probability measures of fuzzy events", Journal mathematical Analysis and Applications, Vol 23,No 2,pp 421–427,1968
17. IS 1893 (Part 1) Indian Standard Criteria for Earthquake Resistant Design of Structures. Bureau of Indian Standards. New Delhi. 2002
18. IS 456 Indian Standard for Plain and Reinforced Concrete - Code of Practice, Bureau of Indian Standards, New Delhi, 2000
19. Ranganathan, R. (1999) Structural Reliability Analysis and Design, Jaico Publishing House, Mumbai.
20. Seismostruct (2012) SeismoStruct - A Computer Program for Static and Dynamic Nonlinear Analysis of Framed Structures [online]. < http://www.seismosoft.com/ > (last accessed on Aug. 30, 2012).
21. Mander J.B., Priestley M.J.N. and Park R. "Theoretical stress-strain model for confined concrete", Journal of Structural Engineering (ASCE), Vol 114, No 8, pp 1804–1826, 1988
22. Yassin M.H.M. "Nonlinear analysis of prestressed concrete structures under monotonic and cyclic loads", Ph.D. Thesis, University of California, Berkeley, 1994
23. Smyrou E., Blandon C., Antoniou S., Pinho R. and Crisafulli F. "Implementation and verification of masonry panel model for nonlinear dynamic analysis of infilled RC frames", Bulletin of Earthquake Engineering, Vol 9, No. 5,pp 1519–1534, 2011
24. Carballo J.E. "Probabilistic Seismic Demand Analysis: Spectrum Matching and Design", Ph.D. Thesis, Stanford University, 2000
25. ASCE 7-05 "Minimum Design Loads for Buildings and Other Structures", American Society of Civil Engineers, Reston, Virginia, 2005
26. ASCE/SEI 41 "Seismic Rehabilitation of Existing Buildings", American Society of Civil Engineers, Reston, Virginia, 2007
27. Mukherjee, S and V.K. Gupta "Wavelet-based Generation of Spectrum Compatible Time-histories", Soil dynamics and Earthquake engineering 22, 799–804.2002.

© 2013 SRESA All rights reserved

Life Cycle Reliability and Safety Engineering
Vol.2 Issue 1 (2013) 21-32

Expert Elicitations: A Tool for Decision Making in Risk Management Issues

Gopika Vinod and V.V.S. Sanyasi Rao
Reactor Safety Division, Bhabha Atomic Research Centre, Mumbai – 400 085
e-mail: vgopika@barc.gov.in

Abstract

Expert elicitation is one of the powerful technique to combine subjective information and experimental observations. However, traditional approach followed in eliciting expert's opinion has its own limitations. There are concerns regarding the usability of results considering the scatter of information collected from such exercise. This has resulted in formulating a structured expert judgment uncertainty quantification model, which was developed at the Delft University of Technology over the last 17 years. This model has succesfully demonstrated techniques to enable performance-based weighted combination of experts' distributions and analytical tools for opinion aggregation. This paper explains the classical model for structured expert judgment and the performance measures, and demonstrates with suitable case studies.

Keywords: structured expert judgement, seed variable, expert calibration, aggregation.

1. Background

Quality of the information is the key basis for determining the efficiency of decision making in Risk management issues [1]. Various techniques are utilized to enhance the quality content of information, be it to improve the quality of existing qualitative information or to exploit the information content in existing (quality assured) information in a more efficient way to assure decisions that are more robust. There are mainly four classes of information that are used as a basis for decision making ranging from quantitative statistics to qualitative subjective judgment. Figure 1 shows the relation between the information classes to assessment techniques.

In the context of this paper, techniques and tools will be explored for carrying out expert judgment in a structured manner.

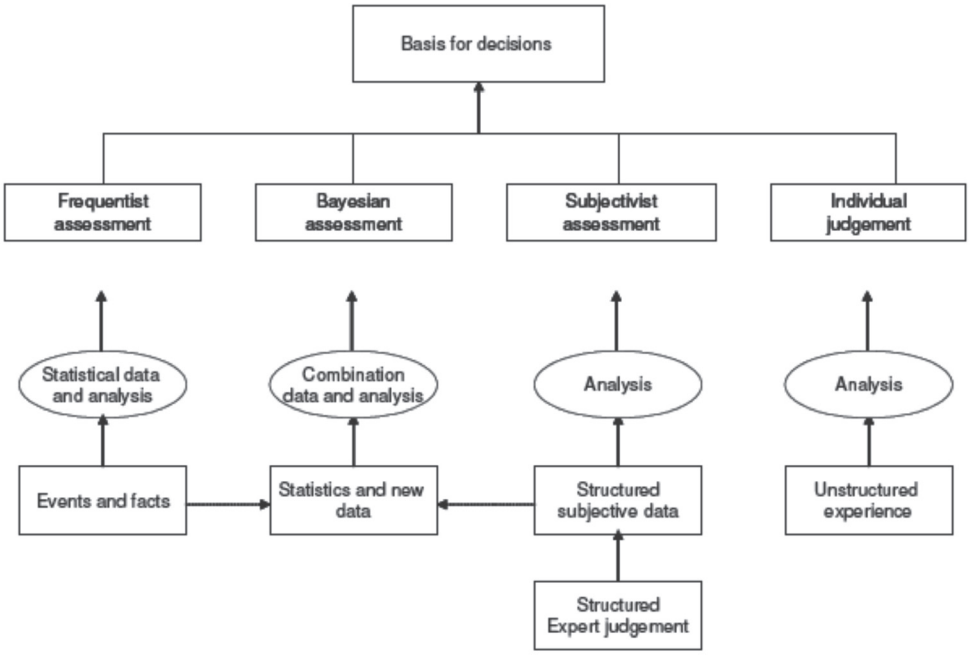

Figure 1 : Relation between the information classes to assessment techniques

© 2013 SRESA All rights reserved

2. Introduction to Expert Judgment

Expert judgments can provide useful information for forecasting, making decisions, and assessing risks. Such judgments have been increasingly used as an informal approach from earlier days. Recent advances in expert elicitation techniques have introduced formal and structured methods for conducting these studies in a systematic and efficient manner [2]. However, it has to be kept in mind that the application areas can become diverse ranging from engineering problems, to social, cultural and economic policy issues. This has resulted in providing judgments of different kinds such as forecasting, estimates, or probabilistic assessment. In this paper, the application of expert judgment to forecasting and quantitative assessment has been explored.

In the world of engineering, technical expertise is generally separated from value judgements. Engineering judgement is often applied to bridge the gap between hard technical evidence and mathematical rules on the one hand, and, unknown characteristics of a technical system on the other hand. Suitable numerical data have to be derived for the practical problem at hand. Engineers are quite able to provide these data which are essentially subjective in nature and are driven by engineering models and experience. The same is true for expert judgements. Engineering models and experience largely drive the subjective experts' assessments.

When expert opinions are being used as data, some trends can be observed such as [3].

1. Expert opinion estimates typically exhibit a large scatter.
2. Estimates, given by the experts, are not always independent. For example: if an expert judges negative of one aspect within a study, then he could also have a tendency to be negative of other aspects within the study, too.
3. In general, if the same expert opinion method is applied several times on the same problem, it doesn't produce similar results.
4. Mostly, the subjective probabilities don't agree with observed frequencies.

The above trends were attributed to the fact that expert opinion is unstructured; without the use of formal processes/methodologies. This emphasizes the use of structured expert judgement. In order to ensure the structured nature, the following steps should be taken during the expert elicitation process.

1. Preparation of the expert elicitation process
2. Identification of variables
3. Identification and selection of experts
4. Elicitation of expert opinions
5. Handling the results of the elicitation session

The fundamental goal of science is to build rational consensus and, therefore, the process of collecting expert assessments must be subjected to the following five basic principles (the first and second principles are later combined as a scrutability/accountability principle [3]:

1. Reproducibility: All results must be reproducible, with calculation models and data being clearly specified and made available.
2. Accountability: The source of data (name and institution) must be identified, and data must correspond to the exact source from which the data are elicited.
3. Empirical Control: Experts' assessments must be, in principle, physically observable.
4. Neutrality: The elicitation process must ensure that the actual beliefs of experts be collected (e.g. no punishment or rewards through a self-rating system, where the experts rate their opinions themselves).
5. Fairness: All experts must be regarded equally before the aggregation process.

3. Structured Expert Judgment Methods

As explained in the previous section, for carrying out expert elicitation in a structured manner, five steps mentioned above have to be meticulously followed. The techniques and tools involved in adopting these steps are explained in the sub sections below:

3.1. Preparation of the expert elicitation process

One of the key stages in the expert elicitation process is the definition of the problem or issue to be judged. Here, we should analyse the subject of interest and how we are going to tackle the issue. For example, *are we looking for a quantitative probability assessment of an issue or interest in forecast of policy planned to be implemented? or do we need an estimate of the variables for our problem in hand?*

- Definition of the case structure document: This document contains the description of the field of interest, what is expected from the experts, and in what way the experts will be queried about the problem.

© 2013 SRESA All rights reserved

- Deciding the type of questionnaires according to the problem on hand.

The case structure document contains the framework for the panel of experts, specifying all issues to be taken into account, while conducting the expert elicitation process. Depending on the nature of issue, there are following types of quantities of interest.

1. Point values: experts are asked to guess the values of unknown quantities as single point estimates. This type of assessment is not popular, due to some of its disadvantages like difficulty in combining scores for variables measured on different scales, no indication of uncertainty, difficulty in combining judgements, etc.
2. Paired comparisons: In the paired comparison method, experts are asked to rank alternatives pair wise according to some criterion like preference, feasibility, etc. If 20 items are involved in total, 190 comparisons must be made; each item is compared with the 19 others. Since each item is compared with all the other items, there is a great deal of possible redundancy in the judgement data. Various processing methods are proposed for distilling a rank order from the pair wise comparison data.
3. Discrete event probabilities: Experts are asked to assess the probability of occurrence of uncertain events. The assessment takes the form of a single point value in the [0,1] interval, for each uncertain event. The assessment of discrete event probabilities must be distinguished from the assessment of limit relative frequencies of occurrence in a potentially infinite class of experiments (the so-called reference class).
4. Distributions of continuous uncertain quantities: For applications in uncertainty analysis, we are mostly concerned with random variables taking values in some continuous range, described by a subjective probability distribution. Typically, only the 5%, 50% and 95% quantiles are requested, and distributions are fitted based on the elicited quantiles.

In some typical issues, for example related to policies, surveys are used, which is another form of expert elicitation for measuring attitude. Typically in ranking using "Likerts scale", subjects are asked to express agreement or disagreement on a five-point scale. Each degree of agreement is given a numerical value, for example from one to five. Thus, a total numerical value can be calculated from all the responses. This ranking method is popular method used for relative ranking of issues and is an excellent tool for qualitative decision making.

3.2. Identification of variables

Not all experts perform equally well with respect to a given assessment case. Assessments of 'better' experts should get a higher weight (score) in the overall linear combination [3]. There are two types of questions. S*eed,* or *calibration* questions allow to measure how good the experts are in quantifying their uncertainty. Second, there are questions of *interest variables*, i.e. questions on uncertain quantities being assessed. Seed questions must be chosen from the expert's research field, related to the questions of interest. Answers to them are known or will become known in the time after the project. A score measuring 'goodness' of an expert is calculated based on the answers to seed variables as a product of two values, namely, a *calibration score* and an *information score*. The calibration score says how statistically well the expert performs. The information score measures the expert's uncertainty about the requested matter. The second type of questions concerns assessing the quantities we are interested in called *interest or target or query variables.*

- Identification of the **seed variables**: Variables whose true values are unknown to experts when giving their opinion, but whose values are known to the evaluators.
- **Target variables**: Which variables are to be quantified by the experts
  - √ Identification of the **query variables**: These are the variables to be assessed by the experts. The target variables may not be appropriate for direct elicitation. Then it is needed to find derived variables for these.

Information score and calibration score: Let us assume that we have one seed question with realization r and N experts.

Each of them give *(5%,50%,95%)* quantiles for this seed variable

$(q_5(e), q_{50}(e), q_{95}(e)), e = 1,..., N$

<u>*Information score:*</u> In order to compute information

© 2013 SRESA All rights reserved

score, intrinsic range is to be defined. I*ntrinsic range* is the interval *(l,h),* such that

$$l = \min_{e=1\ldots N} \{q_5(e), r\} \quad , \quad h = \max_{e=1\ldots N} \{q_{95}(e), r\} \qquad (1)$$

i.e. it is the minimum interval containing all experts' assessments and the realization of the chosen seed variable. Intrinsic range should contain the whole distribution. For this reason, *k%* overshoot is often included in range *(l,h)*. The sensitivity to the choice of *k* must be checked.

$$q_l = l - k(h-l) \quad q_h = h + k(h-l) \qquad (2)$$

The information score defines the- degree to which the experts' assessments are concentrated relative to user-defined *background measure.* This measure is assigned to each variable for each expert. For the uniform and for the lognormal distributions, for example, the background measure is respectively:

$$F(x) = \frac{x-l}{h-l} \quad , \quad x \in (l,h) \qquad (3)$$

$$F(x) = \frac{\ln x - \ln l}{\ln h - \ln l} \quad , \quad x \in (l,h) \qquad (4)$$

If the background measure distribution is uniform, then the expert's distribution for seed variables is uniform between quantiles 0 and 5%, 5% and 50%, 50% and 95%, and, 95% and 100%. *The information score* of an expert for one seed question is then defined as

$$I(e,i) = \sum_{i=1}^{4} p_i \ln \frac{p_i}{r_i} \ , \ p = (0.05,0.45,0.45,0.05) \qquad (5)$$

where r_i is a background measure for interval *i,* that is

$$\begin{aligned} r_1 &= F(q_5(e)) - F(q_l(e)) \\ r_3 &= F(q_{95}(e)) - F(q_{50}(e)) \\ r_2 &= F(q_{50}(e)) - F(q_5(e)) \\ r_4 &= F(q_h(e)) - F(q_{95}(e)) \end{aligned} \qquad (6)$$

Let us have *M* seed questions. The *information score* of an expert is defined as the average of information scores for each of the seed variables:

$$I(e) = \frac{1}{M} \sum_{i=1}^{M} I(e,i) \qquad (7)$$

The information score shows how confident the expert is in estimations, i.e. how concentrated is the distribution. The value of the information score depends on the choice of background measure and intrinsic range, but usually this dependence is negligible.

Calibration score: Let us consider one expert and *M* seed questions. We would like to estimate the ability of the expert to predict realizations. If we ask him/her to give (5%,50%,95%) quantiles, then 5% of the realizations should fall in the interval (<5%), 45% in the interval (5%-50%), 45% in the interval (50%-95%) and 5% in the interval (>95%). Let us denote these realizations as (s_1(e), s_2(e), s_3(e), s_4(e)).

i.e.

s1(e) = #{ i | xi ≤ 5% quantile}/N
s2(e) = #{ i | 5% quantile < xi ≤ 50% quantile}/N
s3(e) = #{ i | 50% quantile < xi ≤ 95% quantile}/N
s4(e) = #{ i | 95% quantile < xi }/N

where, N is the total number of experts participating in the elicitation process, x_i is the value given by the expert for the i^{th} seed question

If the expert e is well calibrated we should expect that approximately 5% of the true values fall beneath 5% quantile, 45% should fall between 5% and 50% quantiles, etc. To evaluate how close the empirical density of the expert (s_1, s_2, s_3, s_4) is to the hypothetical one (p_1, p_2, p_3, p_4) = (5%,45%,45%,5%), so-called *relative information* is used:

$$I(s,p) = \sum_{i=1}^{4} s_i \, \mathrm{h} \, \frac{s_i}{p_i} \qquad (8)$$

Its minimum value zero is achieved if and only if *s=p*. *Calibration score* is based on *I* (*s, p*). It is the likelihood of statistical hypothesis which is defined for each expert as [3]:

The realizations may be regarded as independent samples from a distribution corresponding to the expert's quantile assessments.

We would like to test the degree to which the realizations for seed variables support this hypothesis, i.e. to check if discrepancies between the realizations and the expert's assessments have appeared by chance. It is well-known that [4].

$$P(2M * I(s,p) \le x) \approx \chi_3^2(x) \qquad (9)$$

© 2013 SRESA All rights reserved

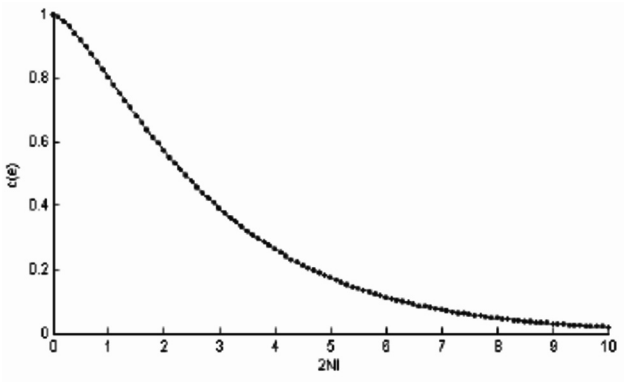

The *calibration score* for expert is defined as the probability to get the relative information score worse than obtained, under assumption that his/her true distribution is(p_1, p_2, p_3, p_4). The score is expressed as

$$c(e) = 1 - P(\chi_3^2 \langle 2M\ (s,p) \quad = 1 - \chi_3^2\ (2M\ (s,p) \tag{10}$$

The best case is when $c(e)$ =1, where the expert's empirical distribution is just the same as the hypothetical one. Low calibration score (say less then 0.05) means that the expert's probabilities are not supported by seed variables. We choose experts with higher information score between those with approximately equal calibration scores. Identification and selection of experts

This step involves choosing experts, and selecting from the initial list of experts the final group for the elicitation process, on the basis of a few selection criteria: reputation in the field of interest, diversity in background, familiarity with uncertainty concepts. Sometimes, it is required to train/prepare experts in making probabilistic assessments, if they are not familiar with these concepts.

3.3 Elicitation of expert opinions

In the *elicitation*, either the expert is interviewed alone or the questionnaire in a web based environment is designed and experts are notified through email for their participation. Instructions of how the questionnaire must be filled-in will be described and an example will be presented in order to clarify the use of quantiles. Experts are encouraged to provide answers to all the queries. In addition, some background information of the subject of interest is also provided to assit experts in giving the clear picture of issue on hand.

3.4. Handling the results of elicitation session

Combining and aggregating the results of elicitation session is the most critical step of the whole structured expert judgment process and needs detailed description of various methods used. It involves (i) Scoring the expert, and, (ii) Combining the result. Since it is still an evolving area, some of the classical methods are described in this paper.

3.4.1. Scoring the experts

The first step in this process is to score the experts. Three schemes are used for computing the weights of experts. Before going to estimate the weights for the experts, it is assumed that information score and calibration score has been computed according to equation (7) and (8) respectively.

1. Global weights – w_e equals the product of the calibration and information score (each score normalised).

   $W_e = I(e)\ x\ c(e)$ (11)

2. Equal weights, $w_e = \frac{1}{N}$ where N is the number of the total experts (12)

3. Item weights – uses individual scores for each of the experts and items,and the same calibration score for any of the items within each of the experts.

$$w_e = \frac{c(e) \times I(e)}{\sum_{e=1}^{N} c(e) \times I(e)} \tag{13}$$

Another simple, qualitative combination approach is to use the Saaty's analytic hierarchy process [7]. This involves pairwise comparisons concerning information about the experts' qualifications. A numeric value is assigned to the ratio of the qualifications between the two experts. The weights for each experts are just the normalized eigen vector corresponding to the maximum eigen value of the pairwise comparison matrix. This procedure is demonstrated by considering the following pairwise comparisons:

1 vs 2: Better	2 vs 3: Worse	3 vs 4: Same	4 vs 5: Same	5 vs 6: Same	6 vs 7: Worse
1 vs 3: Same	2 vs 4: Worse	3 vs 5 : Better	4 vs 6: Better	5 vs 7: Worse	
1 vs 4 : Same	2 vs 5: Worse	3 vs 6: Better	4 vs 7: Same		
1 vs 5 : Better	2 vs 6: Worse	3 vs 7: Same			
1 vs 6 : Better	2 vs 7: Worse				
1 vs 7: Better					

© 2013 SRESA All rights reserved

A scale of 1 to 9 is often used, depending on the magnitude of the relative importance between the two experts. For this simple case, we let Better = 2.72, Worse = 1/ Better = 0.37, and same =1. In principle, any appropriate based on judgment can be assigned to these variables. Our comparison matrix is then

$$W = \begin{bmatrix} 1 & 2.72 & 1 & 1 & 2.72 & 2.72 & 2.72 \\ .37 & 1 & .37 & .37 & .37 & .37 & .37 \\ 1 & 2.72 & 1 & 1 & 2.72 & 2.72 & 1 \\ 1 & 2.72 & 1 & 1 & 1 & 2.72 & 1 \\ .37 & 2.72 & .37 & .37 & 1 & 1 & .37 \\ .37 & 2.72 & .37 & .37 & 1 & 1 & .37 \\ .37 & 2.72 & 1 & 1 & 2.72 & 2.72 & 1 \end{bmatrix}$$

The maximum eigen value is $\lambda_{MAX} = 7.324$ and the corresponding normalized eigen vector is (0.23, 0.06, 0.19, 0.17, 0.1, 0.08, 0.17). These would be the weights given to each expert. The disadvantage of this method is that it can only be used to combine single values, like a median. We cannot calculate the uncertainty of the estimates.

3.4.2.Combining / Aggregation of expert opinions

Combination, or aggregation [4], procedures are often dichotomized into mathematical and behavioral approaches, although in practice aggregation might involve some aspects of each. Mathematical aggregation methods range from simple summary measures such as arithmetic or geometric means of probabilities assessed by experts to procedures based on axiomatic approaches or on various models of information-aggregation process requiring inputs regarding characteristics such as the quality of and dependence among the experts' probabilities. In contrast, behavioral aggregation approaches attempt to generate agreement among the experts by having them interact in some way. This interaction may be face-to-face or may involve exchanges of information without direct contact. Behavioral approaches consider the quality of individual expert judgments and dependence among such judgments implicitly rather than explicitly.

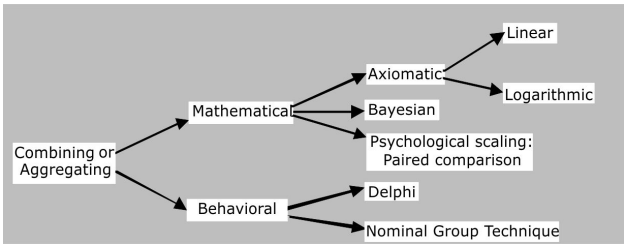

Figure 2: Relation between different approaches for combining or aggregarting expert opinions

3.4.2.1. Mathematical approaches

Let $p(e) = (p_5(e), p_{50}(e), p_{95}(e))$, e 1,...,N be the assessment of N experts of the variable of interest. We need to combine these distributions to get the distribution of the variable of interest. An appealing approach to the aggregation of probability distributions is the **linear opinion pool**,

$$p(\theta) = \sum_{e=1}^{N} w_e p_e(\theta) \quad (14)$$

where N is the number of experts, $p_e(\theta)$ represents expert e's probability distribution for variable of interest, θ, p(θ) represents the combined probability distribution, and the weights w_e are non-negative and sum to one.

Another typical combination approach uses multiplicative averaging and is sometimes called a **logarithmic opinion pool**. In this case, the combined probability distribution is of the form

$$p(\theta) = k\prod_{e=1}^{N} p_e(\theta)^{w_e} \quad (15)$$

where k is a normalizing constant and the weights w_e satisfy some restrictions to assure that p(θ) is a probability distribution. Typically, the weights are restricted to sum to one.

Perhaps the most robust technique in combining expert opinion is the **Bayesian method**. In this method, the decision maker uses experts' probability assessments as data to update his own prior belief about the distribution of an unknown quantity of interest, according to Bayes' Theorem [5]. Let P(x) be the decision-maker's prior probability distribution for some unknown quantity x, and P(D|x) be the likelihood of some observational data D given x. Then the decision-maker's posterior distribution is P(x|D) = [P(D|x)*P(x)] / P(D) via Bayesian update.

The **psychological scaling models** assume that every expert has some internal value associated with a variable of interest and he/she can only provide his or her qualitative input (no numerical estimates). The decision-maker asks experts to state their preference or views on **pairwise comparisons**. This approach originated from the study of estimating intensities of physical stimuli, which later developed into the study of estimating relative intensities of psychological

© 2013 SRESA All rights reserved

stimuli among experts. Using simulation, experts' assessments lead to a consensus with confidence bounds. Their inputs are measured for their consistency and concordance. Suppose there are N experts, and each expert is asked to express his/her preference for one of two events. Let A(1), …, A(t) be events to be compared, V(1), …, V(t) be the true probabilities of events. Let V(i, e) denote the internal value of expert e for event i. If expert e prefers event A(i) to event A(j), (i.e. A(i) > A(j)), then A(i) is judged more probable than A(j) by e, and V(i, e) >V(j, e). The paired comparison models are appealing in that experts are not required to be familiar with numerical assessments and the overall elicitation process is relatively simple. They have, however, disadvantages such as requiring a large number of experts and forcing stringent assumptions about experts' underlying assessment mechanisms.

3.4.2.2. Behavioural approaches

Behavioral combination approaches require experts to interact in some fashion [6]. Some possibilities include face-to-face group meetings, interaction by computer, or sharing of information in other ways. The group may assess probabilities or forecasts, or simply discuss relevant issues and ideas with only informal judgmental assessment. Emphasis is sometimes placed on attempting to reach agreement, or consensus, within the group of experts; at other times, it is simply placed on sharing of information and having the experts learn from each other. The degree to which the risk- assessment team is involved in structuring and facilitating the expert interaction can vary. Specific procedures (e.g., Delphi, Nominal Group Technique) can be used, or the risk- assessment team can design the interaction process to suit a particular application. The simplest behavioral approach is to assemble the experts and assign them the task of generating a ''group'' probability distribution. Discussion and debate can be wide-ranging, presumably resulting in a thorough sharing of individual information.

One of the most well known behavioral approaches is the Delphi technique, which was developed in the 1950s. In this method, experts are asked to anonymously judge the assessments made by other experts in a panel. Each of the experts is then given a chance to reassess his/her initial judgment based on the others' review. Typically, the process is repeated several rounds until a smaller spread of experts' opinions is achieved. The Delphi method later incorporated a self-rating mechanism, allowing experts to rate their expertise. The Nominal Group method is another well-known behavioral method, in which experts are allowed to discuss their estimates directly with one another in a controlled environment.

The expert panel typically faces one of the following three generic types of choice problems

1. to agree or disagree or determine the extent of its disagreement with one or more policy propositions
2. to develop a preference ranking over a set of items
3. or to produce quantitative estimates of one or more parameters for use in subsequent calculations that contribute to a policy recommendation

Regarding (3) it may be that suitable empirical information for estimating the parameters by a more conventional data driven approach is simply not available or else is deemed to be of insufficient quality to merit use without "expert judgment" interpretation or augmentation.

Delphi

Delphi involves an iterative survey of experts. A dialectical process, Delphi was designed to provide the benefits of a pooling and exchange of opinions so that respondents can learn from each other's views, without the sort of undue influence likely in conventional face-to-face settings (which are typically dominated by the people who talk the loudest or have most prestige). Each participant completes a questionnaire and then is given feedback on the whole set of responses. With this information in hand, (s)

Figure 3 depicts the flow of information envisaged between different DELPHI rounds.

ROUND 1	ROUND 2	ROUND 3
CURVE PROJECTIONS HISTORICAL TRENDLINE	RE-PROJECTION 50% BOUNDARIES	50% BOUNDARIES RE-PROJECTION
ASSUMTIONS UNCERTAINTIES	ASSUMPTIONS VALIDITY JUDGMENTS PROJECTION	AGREEMENT AVERAGED DISAGREEMENTS RE-EVALUATED
FLOW OF CHART	KEY DEVELOPMENTS PROBABILITY	RE-EVALUATION INPUT-OUTPUT MODEL
FLOW ESTIMATES AND MODEL CHANGES	RE-ESTIMATION	ESTIMATES

Figure 3: Schematic of flow of information in DELPHI rounds

© 2013 SRESA All rights reserved

he then fills in the questionnaire again, this time providing explanations for any views they hold that were significantly divergent from the viewpoints of the other participants. The explanations serve as useful intelligence for others. The idea is that the entire group can thus weigh dissenting views that are based on privileged or rare information. While traditionally conducted via mail, other variations of Delphi can be online or face-to-face. The area of trying to translate scientific knowledge into an informed judgment on evaluating and analyzing decision options is clearly a potential one for the Delphi method. Usually Delphi, whether it be conventional or real-tune, undergoes four distinct phases.

1. The first phase is characterized by exploration of the subject under discussion, wherein each individual contributes additional information he feels is pertinent to the issue.
2. The second phase involves the process of reaching an understanding of how the group views the issue (i.e., where the members agree or disagree and what they mean by relative terms such as importance, desirability, or feasibility).
3. If there is significant disagreement, then that disagreement is explored in the third phase to bring out the underlying reasons for the differences and possibly to evaluate them.
4. The last phase, a final evaluation, occurs when all previously gathered information has been initially analyzed and the evaluations have been fed back for consideration.

4. Case Studies

As mentioned earlier, expert elicitation is widely applied for finding quantitative estimates or forecasting, etc,. In this section, case studies attempting to arrive at expert decisions are presented. Though several methods have been presented in Section 3 for expert elicitation, in the following only those appropriate for a give case are used.

4.1 Example 1: Quantitative estimate

This is a typical example of finding failure probability of a component while applying Risk based inspection. For those who are not familiar with Risk based inspection, it can be briefly explained as a "live" process for developing an inspection programme considering all critical components by evaluating their contribution towards risk. The backbone of Risk based inspection is finding the failure probability and consequence of failure of all components involved and hence evaluates their criticality. In doing so, all credible failure scenarios should be considered along with all possible degradation mechanisms acting on components, which can lead to such scenarios. Since evaluation of failure probability is a critical phase, but for some scenarios, hampered by lack of data, expert judgment is considered as a practical tool for conducting risk based inspection.

A simple example is considered, for illustrating how expert elicitation in risk based inspection is practiced. As discussed earlier, after identifying the suitability of problem for expert judgment, next

Table 1 : Realization of seed questions based on prior knowledge

Category	Prior knowledge on consequential actions	5%	50%	95%
Very high	Bearing replacement required/ repair of bearing due to consequential damage	0.1	0.2	0.3
High	Bearing replacement required, even though no damage is observed	0.03	0.09	0.3
Medium	Some observed wear, not yet at critical limits	0.003	0.01	0.03
Low	No deviation from specified dimension	0.0001	0.001	0.003

Table 2: Expert elicitation for seed variables

Seed variables	Expert 1			Expert 2			Expert 3		
	5%	50%	95%	5%	50%	95%	5%	50%	95%
Very high	0.1	0.4	0.9	0.01	0.2	0.3	0.1	0.2	0.3
High	0.009	0.05	0.1	0.001	0.005	0.01	0.01	0.05	0.1
Medium	0.003	0.006	0.009	0.0005	0.008	0.001	0.001	0.005	0.01
Low	0.0001	0.0005	0.003	0.0001	0.0003	0.0005	0.0005	0.0008	0.001

© 2013 SRESA All rights reserved

step is selecting appropriate seed variables. Below is an example of "Generator failure due to heat". The bearing can overheat, if the lubricant runs or dirt penetrates. The friction caused can rise the bearing temperature leading to its failure. So "how to categorize the failures in bearing" has been considered as seed variables, since sufficient data and prior knowledge is available

With this prior knowledge, experts are asked to provide the 5%, 50% and 95% values for categories Very high, high, medium and low, for defining the generator failure due to rise in bearing temperature. Table 2 shows the some sample values suggested by three experts.

As discussed in section 3.2, it is required to find the l, h , q_l and q_h . l and h are computed as given in equation (1). Considering 10% as overshoot, q_l and q_h are computed, as per equation (2). The values for these parameters are given in Table 3.

Table 3: Range calculation for estimating the weight of experts

	l	h	ql	qh
very high	0.01	0.9	-0.079	0.989
high	0.001	0.3	-0.0289	0.3299
medium	0.001	0.03	-0.0019	0.0329
low	0.0001	0.003	-0.00019	0.00329

Assuming uniform distribution, F(x) is computed as given in Equation (3). These F(x) values are required to compute the parameters r1, r2, r3, r4 for each experts, as per equation (6). Using equation 5 & 7, the informativeness of the three experts are computed. The results are shown in Table 4.

Table 4. Computation of informativeness of experts

I(e,i)	Expert1	Expert2	Expert3
m1	-0.07	0.79	1.04
m2	0.80	2.88	0.81
m3	1.12	1.47	0.79
m4	0.17	1.51	1.29
I(e)	0.50	1.66	0.98

After the expert calibration, the target variables are presented for the following case "Generator failure – short circuit fault". The scenario is as follows: Too high temperature of the winding may result in melting of the insulation of the winding. Consequently a short-circuit fault occurs with sudden stop of the generator, possibly catching fire. This is caused by the contamination of insulation winding by dirt and water. For this scenario, experts gave their observation as shown in **Table. 5**.

Using global weighted decision maker methodology (equation 11), the failure probability values for 5%, 50% and 95% has been evaluated as 0.02, 0.06 and 0.17 respectively.

This can be further subjected for Delphi rounds, with experts views invited for the aggregated results. Again, their views are combined, with appropriate justifications, for obtaining result.

Similarly consequence can also be evaluated, which are finally utilized in deciding the components placement in risk matrix.

4.2 Example 2: Forecasting research areas and their importance ranking

To illustrate the procedure of "Delphi", a typical problem has been framed. It is common in any research area for experts to have diversified approach to tackle a particular problem. To be in line with the topic under discussion, authors have framed an expert elicitation problem on approaches and requirements on conducting "Uncertainty analysis". Accordingly, experts are required to comment on following issues related with uncertainty analysis:

Issue 1 All variables appearing in the problem need to be considered uncertain

Issue 2 Aleatory uncertainty can be neglected if the problem is not amenable

Issue 3 Suitable justification should be provided on application of different uncertainty propagation methods such as Monte Carlo Simulation, Demper Shafer method, Fuzzy approach, etc.

Issue 4 Uncertainy importance measures are an integral part of Uncertainty analysis

Issue 5 More time should be dedicated for characterization of variables than investigating different alternative propagation methods while performing uncertainty analysis

Issue 6 Sensitivity analysis can be considered as a complement / replacement of uncertainty analysis as problem demands.

© 2013 SRESA All rights reserved

Table 5: Aggregated results after expert judgement

Target variables	Expert 1			Expert 2			Expert 3		
	5%	50%	95%	5%	50%	95%	5%	50%	95%
PoF for high	0.01	0.04	0.08	0.007	0.02	0.07	0.008	0.03	0.06

Table 6: Summary of first-round ratings from seven experts

Issues in Uncertainty analysis	Rating given by each expert							Rating _ Mean	Rating_ Median	Quartile Deviation
	E1	E2	E3	E4	E5	E6	E7			
Issue 1	5	5	5	5	4	5	5	4.86	5	0
Issue 2	4	3	5	4	4	5	5	4.29	4	0.5
Issue 3	5	4	4	4	5	4	5	4.43	4	0.5
Issue 4	1	2	2	3	3	2	3	2.64	2	0.5
Issue 5	3	4	4	5	4	4	4	4.00	4	0
Issue 6	2	2	3	3	3	2	1	2.29	2	0.5

Table 7: Summary of second-round ratings from seven experts

Issues in Uncertainty analysis	Rating given by each expert							Rating_ Mean	Rating_ Median	Quartile Deviation
	E1	E2	E3	E4	E5	E6	E7			
Issue 1	5	4	5	5	4	5	5	4.71	5	0.5
Issue 2	4	4	5	4	4	5	5	4.43	4	0.5
Issue 3	5	4	4	4	5	4	4	4.29	4	0.5
Issue 4	2	2	3	3	3	2	3	2.57	3	0.5
Issue 5	3	4	4	4	4	4	4	3.86	4	0
Issue 6	2	2	2	3	3	2	1	2.14	2	0.5

A typical rule for analyzing the ratings from multiple experts with Delphi approach is given in Table 8.

Table 8: Typical rules for analyzing the ratings from multiple experts

1st Round	2nd Round	3rd Round
Rating_Mean (i) ≥ 3.5	If Rating_Mean (i) ≥ 3.5 and QD ≤ 0.5 and Rating_Variant(i)< 15%, the issue is accepted and no further discussion is needed	
Rating_Mean (i) < 3.5	Rating_Mean (i) ≥ 3.5 or Rating_Variant(i)> 15%,	If Rating_Mean (i) ≥ 3.5 and QD ≤ 0.5 and Rating_Variant(i)< 15%, the issue is accepted and no further discussion is needed
Rating_Mean (i) < 3.5	If Rating_Mean (i) ≤ 3.5 and QD ≤ 0.5 and Rating_Variant(i) < 15%, the issue is rejected and no further discussion is needed	

© 2013 SRESA All rights reserved

Experts were asked to rate these issues in the scale of {I strongly disagree, I disgree, Neutral, I agree, I strongly agree}. Typically the ranking or ratings is represented by a Likert scale. Here we used a Likert scale of {1, 2, 3, 4, 5} corresponding to the above statements. If an expert failed to respond to certain criteria statement, the data will not be included in the computation of means or standard deviations.

Delphi initially runs into two rounds of expert elicitation. Table 6 and 7 shows the summary of first and second round ratings given by seven experts for the issues in Uncertainty analysis. In table 8, the quartile deviation (QD) is half the difference between the third (upper) and first (lower) quartiles.

The Delphi questionnaire is ended if one of the following situations occurs:

(1) All of the questionnaire items are either accepted or rejected

(2) There still exist some undetermined questionnaire items; nevertheless, over 75% questionnaire items have their rating_variant values being less than 15%

According to the above basis, rounds for Delphi are decided and based on rules for analyzing the rating, it was decided whether to accept or reject a particular issue.

Table 9 summarizes the analysis results of the ratings given by the seven experts for the two rounds of questionnaires.

Table 9: Summary of the analysis results of ratings given by experts

Issues in Uncertainty analysis	Rating given by each expert							Rating_ Mean	Rating_ Median	Quartile Deviation	Rating_ variant (%)
	E1	E2	E3	E4	E5	E6	E7				
Issue 1	5	5	5	5	4	5	5	4.86	5	0	14.29
	5	4	5	5	4	5	5	4.71	5	0.5	
Issue 2	4	3	5	4	4	5	5	4.29	4	0.5	14.29
	4	4	5	4	4	5	5	4.43	4	0.5	
Issue 3	5	4	4	4	5	4	5	4.43	4	0.5	14.29
	5	4	4	4	5	4	4	4.29	4	0.5	
Issue 4	1	2	2	3	3	2	3	2.64	2	0.5	14.29
	2	2	3	3	3	2	3	2.57	3	0.5	
Issue 5	3	4	4	5	4	4	4	4.00	4	0	14.29
	3	4	4	4	4	4	4	3.86	4	0	
Issue 6	2	2	3	3	3	2	1	2.29	2	0.5	14.29
	2	2	2	3	3	2	1	2.14	2	0.5	

From the analysis, issue 4 and issue 6 are rejected since Rating_Mean is ≤ 3.5 and QD ≤ 0.5 and Rating_ Variant < 15%.

Conclusions

Structured expert judgment has emerged as an effective method for bridging the knowledge gap between hard evidence and experts' experience. Since the whole process is carried out a systematic manner, it has succeeded largely to reduce the scatter in experts' opinions. This paper describes the structured expert judgment procedure detailing various tools and techniques involved in conducting each step in the process. Applications of some of the techniques were explained with suitable case studies.

Although empirical evidence indicates that mathematical methods of aggregation generally yield better results than behavioral methods, the latter methods are often perceived appealing, particularly when experts have knowledge in different areas and the synthesis of their expertise is needed. As decision-makers in general tend to use the most

© 2013 SRESA All rights reserved

convenient aggregation methods of their choice (and not necessarily the most appropriate), researchers call for formalizing the elicitation process and using expert opinion by ensuring the basic principles of rational consensus (i.e. satisfying reproducibility, accountability, empirical control, neutrality, and fairness in resulting assessments), which seems truly timely and appropriate.

References

1. Elicitation of expert opinion for uncertainty and risks, B. M. Ayyub, CRC Press, 2001.
2. Otway, H. and Winterfeldt, D. von, 192. Expert judgement in risk analysis and management: Process, context, and pitfalls. Risk Analysis, 12(1): 83–93.
3. R.M.Cooke, L.H.J. Goosens, "Procedures guide for structured expert judgment", EUR 18820, 1999.
4. Clemen, R. T. and Winkler, R. L., 1999. Combining probability distributions from experts in risk analysis. Risk Analysis, 19(2): 187–203.
5. B. Villain & B. Vérité, A Practical Approach to Expert Elicitation for Bayesian Reliability Analysis of Aging, ESREL 99 proceedings.
6. Tim Bedford, Roger Cooke. Probabilistic Risk Analysis. Foundation and Methods. Cambridge University Press, 2001
7. T. L. Saaty, "The Analytic Network Process: Decision Making with Dependence and Feedback", RWS Publications, 1996,

© 2013 SRESA All rights reserved

Life Cycle Reliability and Safety Engineering
Vol.2 Issue 1 (2013) 33-44

Fuzzy Analysis of the Moment of Resistance of a Doubly Reinforced Concrete Beam with Uncertain Structural Parameters

M.V.Rama Rao [1], Andrzej Pownuk [2], Maarten DeMunck [3], David Moens [4]
[1] *Department of Civil Engineering, Vasavi College of Engineering, Ibrahimbagh, Hyderabad India,*
[2]*Department of Mathematical Sciences, University of Texas, El Paso, USA*
[3]*Cel Kunststoffen, KHLim, Diepenbeek, Belgium.*
[4]*Department of Applied Engineering, Lessius Mechelen - campus De Nayer, Sint-Katelijne-Waver, Belgium*
[1] *e-mail: dr.mvrr@gmail.com*

Abstract

This paper focuses on the static stress analysis of doubly reinforced concrete flexural members subject to parametric uncertainty. The uncertainty is located in the properties of the steel reinforcement in the concrete beam, and expressed as a fuzzy set for the corresponding Young's modulus. The fuzzy set is represented by a number of intervals using a - sublevel technique. The internal moment of resistance of the beam is expressed as a function of the stresses induced by the external moment in the concrete and steel. The stress distribution model for the cross section of the beam given by IS 456-2000 (Indian standard code of practice for plain and reinforced concrete) is applied for this purpose. Due to the interval uncertainties, the stresses in concrete and steel are obtained as interval values, resulting correspondingly in an interval moment of resistance. The interval analysis is performed using three different approaches. A direct interval computation tackles the problem using an interval arithmetic translation of the procedure for obtaining the internal moment of resistance. This method is compared to two response surface based approximate approaches, i.e. a method based on a local Taylor series approximation, and one based on Kriging response surface modelling.

Keywords: ***moment of resistance, concrete beam, fuzzy analysis, response surface, interval computation, Kriging approach***

1. Introduction

In the traditional deterministic methods of analysis, all the parameters of the system are taken to be precisely known. In practice, however, there is always some degree of uncertainty associated with the actual values for structural parameters. As a consequence of this, the structural system will always exhibit some degree of uncertainty. This uncertainty of the structural system needs to be rationally taken into account during the analysis and design of structures. This requires the introduction and application of non-deterministic methods of structural analysis and design. Consequently, non- deterministic approaches are gaining momentum in the field of numerical modelling and analysis. The ability to include non-deterministic properties is of great value for a design engineer. It enables realistic reliability assessment that incorporates the uncertain aspects in the design. Furthermore, the design can be optimized for robust behaviour under varying external influences. Recently, criticism has arisen regarding the general application of the probabilistic concept in this context. Especially when objective information on the uncertainties is limited, probabilistic analysis does not always justify its high computational cost[1]. Consequently, alternative non- probabilistic concepts have been introduced for non-deterministic numerical modelling.

In this context, interval and fuzzy approaches are becoming increasingly popular for the analysis of numerical models that incorporate uncertainty in their description. In the interval approach, uncertainties are considered to be contained within a predefined range. For each uncertainty, the analyst has to provide the lower and upper bound. Modelling with intervals provides a link between design and analysis where uncertainty may be represented by bounded sets of parameters. The fuzzy approach extends this methodology by introducing a level of membership that represents to what extent a certain value is member of the range of possible input values. This

© 2013 SRESA All rights reserved

concept provides the analyst with a tool to express a degree of possibility for a certain value. Based on the α-sublevel technique, the fuzzy analysis requires the consecutive solution of a number of related interval problems. For that reason, much attention goes to the actual solution and implementation of interval analysis.

In recent literature, the application of both the interval and the fuzzy concept for the representation of parametric uncertainty during a classical finite element analysis has been studied extensively. While the problem at the core of the analysis, i.e. the solution of a set of interval equations, is easily formulated, the actual solution of this problem was proven to be extremely problematic[1]. Nevertheless, some solution schemes of fundamentally different nature have been developed. The intention of this paper is to present an illustrative example demonstrating the applicability of the non-deterministic methods based on interval- and fuzzy- concepts to the problems of structural mechanics.

In literature, several methods have been proposed for the solution of equations with interval parameters. Neumaier (1990) [2] discussed several interval arithmetic approaches. Systems of linear interval equation with dependent parameters and symmetric matrix were discussed by Jansson (1991)[3]. Köylüoğlu et al, 1995 [3] applied the concept of interval algebra to the solution of FEM equations with uncertain parameters. Rao and Chen (1998)[5] developed a search-based algorithm to solve a system of linear interval equations to account for uncertainties in engineering problems. The algorithm performs search operations with an accelerated step size in order to locate the optimal setting of the hull of the solution. McWilliam (2001) [6] described an anti-optimization approach for the solution of interval equations. Orisamolu et al. (2000) [7] used a response surface method to approximate the solution. Muhanna and Mullen (2001)[8] handled uncertainty in mechanics problems using an interval-based approach. Muhanna's algorithm is modified by Rama Rao (2006)[9] to study the cumulative effect of multiple uncertainties on the structural response. Neumaier and Pownuk (2007)[10] explored properties of positive definite interval matrices. Skalna, Rama Rao and Pownuk (2008)[11] investigated the solution of systems of fuzzy equations in structural mechanics. Also, specific procedures were developed for fuzzy FE analysis in the context of structural dynamic analysis, based on hybrid approaches, as well as sub-structuring and response surface approaches [12,13,14].

In the present work, non-deterministic methods are applied for the analysis of the internal moment of resistance of a doubly-reinforced beam with uncertain structural parameters. Uncertainties are specified as fuzzy numbers for the area of steel reinforcement and Young's modulus. The internal moment of resistance of the beam is expressed as a function of the stresses induced by the external moment in the concrete and steel.

The stress distribution model for the cross section of the beam given by IS 456-2000 (Indian standard code of practice for plain and reinforced concrete) is applied

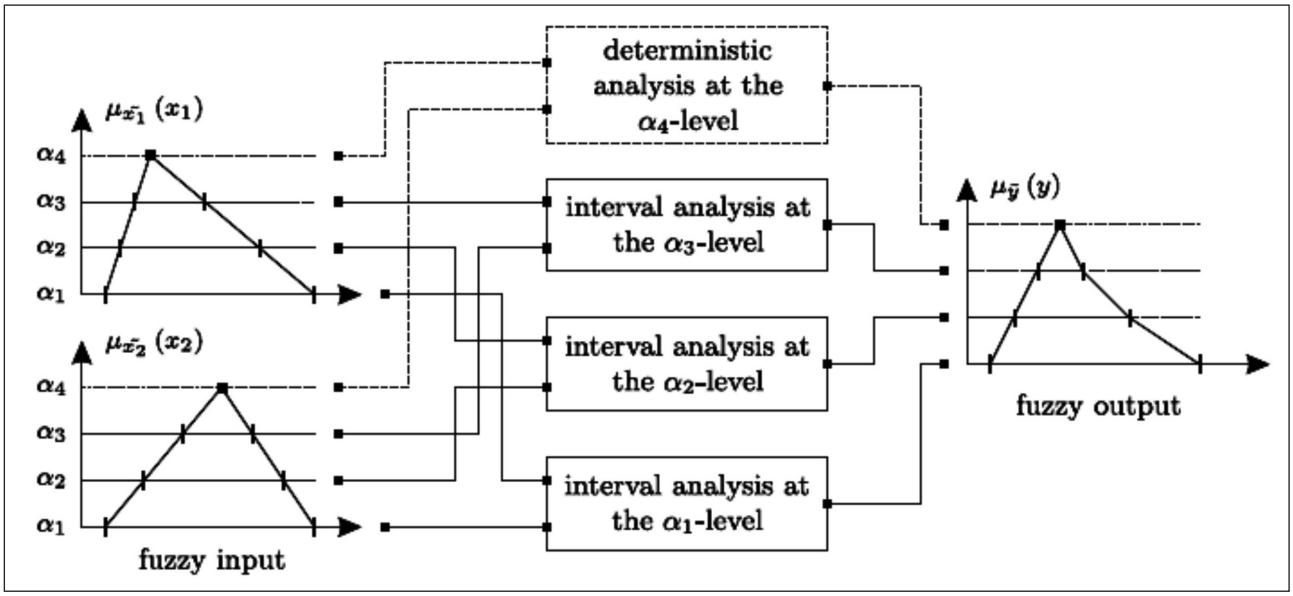

Figure 1 a-level strategy for a function of two triangular fuzzy numbers

© 2013 SRESA All rights reserved

for this purpose. Post cracking behavior up to limit state of serviceability as described by Purushottaman (1986)[15] is considered in the present work. Due to the interval uncertainties, the stresses in concrete and steel are obtained as interval values, resulting correspondingly in an interval moment of resistance. The interval analysis is performed using three different approaches. A direct interval computation tackles the problem using an interval arithmetic translation of the procedure for obtaining the internal moment of resistance. This method is compared to two response surface based approximate approaches, i.e. a method based on Kriging response surface modelling, and one based on local Taylor series expansion.

After a short introduction on implementation approaches for fuzzy analysis in section 2, the paper focuses on the applied response surface based approaches. Section 3 discusses the Taylor as well as Kriging-based response surface approaches. In section 4, the doubly-reinforced beam problem is introduced and an overview of the deterministic procedure for the determination of the internal moment of resistance is presented. Finally, section 5 shows how this problem can be solved when fuzzy uncertainties are present. First, the core problem is translated to an equivalent interval arithmetic counterpart. Secondly, the response surface based approaches are applied and compared.

2. Implementation Strategies for Fuzzy Numerical Analysis

2.1 From fuzzy to interval analysis

Fuzzy sets were introduced by Zadeh (1965)[16]. They are capable of describing linguistic and other incomplete information in a non-probabilistic way. Where classical sets clearly distinguish between members and non-members, fuzzy sets introduce a degree of membership, represented by a *membership function*. The membership function $\mu_{\tilde{x}}(x)$ describes the degree of membership of each element x in the domain X to the fuzzy set $\tilde{x}$:

$$\tilde{x} = \{(x, \mu_{\tilde{x}}(x)) \,|\, (x \in X)(\mu_{\tilde{x}} \in [0,1]\} \quad (1)$$

If $\mu_{\tilde{x}}(x) = 1$, x is definitely a member of $\tilde{x}$. If $\mu\tilde{x}$ $(x) = 0$, x is definitely not a member of $\tilde{x}$. In between, the membership is uncertain.

The most used membership function shape is the triangular shape. Such a fuzzy number with support $[a, b]$ – the interval for which $\mu_{\tilde{x}}(x) > 0$ – and core c – the point for which $\mu_{\tilde{x}}(x) = 1$ – is denoted $(a/c/b)$.

A possible implementation of fuzzy functions is the α *-level strategy*. The intersection of the membership function of each input parameter with a discrete number of α -levels results in an interval $\mathbf{x}_{i,\alpha} = [\underline{x}_i, \bar{x}_i]_\alpha$ for each input parameter and α -level. Using this technique, all possible fuzzy sets can be approximated by a number of intervals. With these input intervals, an interval analysis is done at each α -level. Finally, the fuzzy solution is assembled from the output intervals at each α -level. Figure 1 shows this procedure for a function of two triangular parameters. Using this procedure, the fuzzy analysis can be implemented as a sequence of interval analyses.

In literature, different approaches have been proposed for the solution of the interval problem at the core of the fuzzy analysis. Basically, two approaches can be distinguished. On the one hand, the interval arithmetic approach consists of a step-by-step translation of a deterministic procedure to a sequence of interval operations. This approach in general can lead to a very high amount of conservatism in the result due to the dependency problem [12] and it is only applicable when the core procedure is exactly known. In this work, this approach was applied on the interval calculation of the internal moment of resistance of the reinforced beam (see section 5.1). For other types of problems, e.g., problems where the source code is not accessible, optimisation approaches have been developed in order to solve the interval problem. In this approach, the interval problem is converted into a two-fold optimisation problem, where the bounds on the interval result are found as solutions of the minimisation and maximisation of the analysis outcome, considering the space covered by the interval uncertainties as search domain. The next section gives a general overview of the application of these approaches for fuzzy analysis.

2.2. Global optimisation

The global optimisation procedures perform the search for the exact bounds on the analysis outcome by considering the result as the objective function of an optimisation problem. As one of the pioneers of fuzzy finite element modelling, Rao *et al.* apply a directional search based algorithm to tackle the optimisation [5, 17]. Other global optimisation techniques often encountered in the framework of interval finite element analysis are linear programming Köylüoğlu and Elishakoff, (1998)[18] and genetic algorithms.

© 2013 SRESA All rights reserved

Recently, the innovative Gα D algorithm was introduced by Degrauwe (2007)[19] in this context.

While the optimisation approaches are becoming more and more a standard approach for interval analysis in an engineering context, the global optimisation on the exact goal function can become computationally prohibitive whenever the core analysis is very costly. For this reason, surrogate models of the exact goal function could greatly enhance the performance of the global optimisation part in the fuzzy procedure. Therefore, response surface approaches are becoming more and more popular in this context. In this approach, the goal function of the optimisation problem is approximated by an appropriate surrogate response function, and the optimisation is performed on this response function. The response surface methodology was first applied in the context of interval finite element analysis by Orisamolu *et al.* (2007)[7]. The main advantage of the approach consists of the avoidance of an exact goal function evaluation at each iteration point of the search algorithm, which can be very costly. On the other hand, it is clear that the accuracy of the approach relies completely on the exactness of the approximation of the response function. The next section will discuss the application of the response surface methodology for fuzzy analysis in more detail.

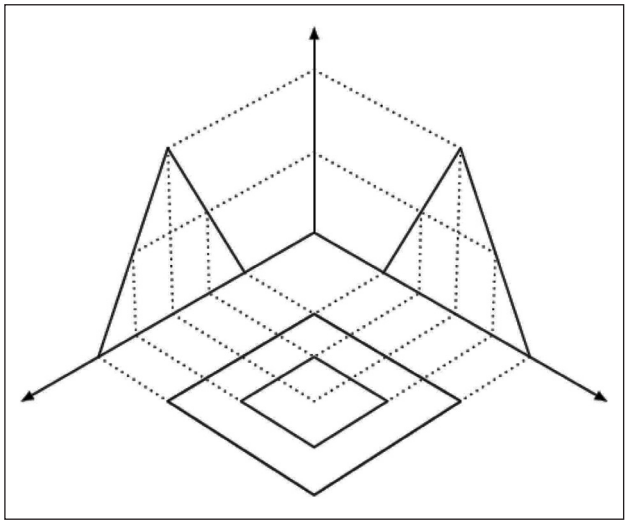

Figure 2 Illustration of property of fuzzy numbers that the feasible region at a higher membership level is a subset of the feasible region at a lower membership level

3. Fuzzy Analysis Based on Response Surface Methodology

Response surface based optimisation techniques prove to be extremely useful in the context of fuzzy analysis. As discussed in the previous section, they enable the analysis of large deterministic problems with high computational cost in a fuzzy context. Furthermore, they also benefit from the high degree of similarity between the optimisation problems that need to be solved when the α -level technique is applied. Indeed, a fuzzy analysis requires the same objective functions to be minimised and maximised on different α -levels or, in optimisation terms, with different bound constraints. Figure 2 shows this for two fuzzy uncertain parameters. The shaded rectangle shows the bound constraints for the optimisation at α -level 0.0. Response surfaces valid at this α -level should approximate the objective functions inside these bounds. The rectangles inside this shaded rectangle show the bound constraints for the optimisations at higher α -levels. It is clear that the same response surfaces approximate the objective functions at these α -levels too. Since the construction of the response surfaces is by far the computationally most expensive part of the algorithm, the computational cost of a fuzzy analysis is only slightly higher than the computational cost of an interval analysis when using a response surface based optimisation technique.

The main question now is how to efficiently build this response surface model. Two approaches, i.e. the Taylor expansion approach and the Kriging approach, both developed by the authors, are now briefly reviewed.

3.1. Local expansion method: Taylor expansion

From mathematical point of view the problem of finding extreme values of stress and strain in concrete beam model can be described as a constrain optimization

$$\begin{cases} \min \psi(p, u(p)) \\ F(p, u(p)) = 0 \\ p_i \in [\underline{p}_i, \overline{p}_i] \end{cases} \tag{2}$$

where $\psi = \psi(p, u(p))$ is some objective function (e.g. stress in steel, strain in concrete etc.), $F(p, u(p)) = 0$ is a system of equilibrium equations, p_i are the uncertain parameters which belong to the ranges $p_i \in [\underline{p}_i, \overline{p}_i]$. In order to find upper and lower bound of the objective function ψ it is possible to apply gradient methods [20]. Gradient of the objective function ψ can be calculated by using methods which are known in the sensitivity analysis

$$\frac{d\psi}{dp_i} = \frac{\partial \psi}{\partial p_i} + \sum_j \frac{\partial \psi}{\partial u_j} \frac{\partial u_j}{\partial p_i} \tag{3}$$

© 2013 SRESA All rights reserved

where $\frac{\partial u_j}{\partial p_i}$ can be calculated from the equation of constraints. (4)

Sensitivity can be calculated also by using adjoint variable method. In this approach it is possible to calculate sensitivity as an derivative form the Lagrange function *L*

$$\frac{d\psi}{dp_i} = \frac{\partial}{\partial p_i} L \tag{5}$$

$$L = \psi + \sum_k \lambda_k F_k, \tag{6}$$

$$\sum_k \frac{\partial F_k}{\partial u_j} \lambda_k = -\frac{\partial \psi}{\partial p_j} \tag{7}$$

The numbers λ_j are so called are Lagrange multipliers. The gradient

$$\nabla\varphi = \left[\frac{d\psi}{dp_1}, ..., \frac{d\psi}{dp_m}\right] \tag{8}$$

can be used in the optimization method. If the function $\psi = \psi(p_1, ..., p_m)$ is uniformly monotone then extreme values can be calculated by using the sign of the component of the gradient.

$$If\ \frac{d\psi}{dp_i} \geq 0\ then\ p_i^{\min} = \underline{p}_i, p_i^{\max} = \overline{p}_i$$

$$If\ \frac{d\psi}{dp_i} < 0\ then\ p_i^{\min} = \overline{p}_i, p_i^{\max} = \underline{p}_i$$

$$\underline{\psi} = \psi(p^{\min}), \overline{\psi} = \psi(p^{\max})$$

The points $[p^{\min}, p^{\max}]$ correspond to the extreme values of the objective function $[\underline{\psi}, \overline{\psi}]$. Each extreme value $[\underline{\psi}_k, \overline{\psi}_k]$ of the objective function correspond with certain point $[p_k^{\min}, p_k^{\max}] \in [\underline{p}_1, \overline{p}_1] \times ... \times [\underline{p}_m, \overline{p}_m]$. In the case of *N* objective functions ψ_k it is necessary to consider 2*N* points $p^{\min,1}, p^{\max,1}, ..., p^{\min,N}, p^{\max,N}$. Fortunately very often the same point p^i correspond with many different extreme values of the function Ψ. In that case it is necessary to evaluate functions Ψ_k only for unique points $p^{(1)}, p^{(2)}, ..., p^{(Nu)}$. Now extreme values can be calculated by using vectors S^{min}, S^{max}

$$\underline{\psi}_k = \psi_k(p^{(s_k^{\min})}), \overline{\psi}_k = \psi_k(p^{(s_k^{\max})}) \tag{9}$$

$S_{\min}^k$ is an index of the point $p^{(i)}$ *w*hich minimize objective function $\underline{\Psi}_k$. $S_{\max}^k$ is an index of the point $p(i)$ which maximizes objective function $\overline{\Psi}_k$.

If the problem is symmetric then it is necessary to evaluate the objective functions ψ_k only in two points. In the worst case, in which there is no symmetry at all it is necessary to evaluate the functions ψ_k in 2*N* points [21].

Presented method is exact if the relations $\psi_k = \psi_k(p)$ are uniformly monotone. According to many numerical experiments [11, 21, 22, 23, 24, 25] even though the function is not monotone then presented method is giving good approximation of the exact solution set. Using presented approach it is possible to create general FEM program with the interval parameters ((Pownuk, 2007))[26]. The program was implemented as a web application and can be run on-line on the author's web page (http://www.pownuk.com)

3.2 Global optimisation using Kriging Response Surface Method

The authors developed a simple but efficient adaptive procedure to select the response points. The authors use the procedure in combination with Kriging response surfaces [27, 28], but the procedure can be used in combination with any response surface method which supports error estimations.

In the first step of the procedure, illustrated in the left contour plots in Figure 3, a small space filling

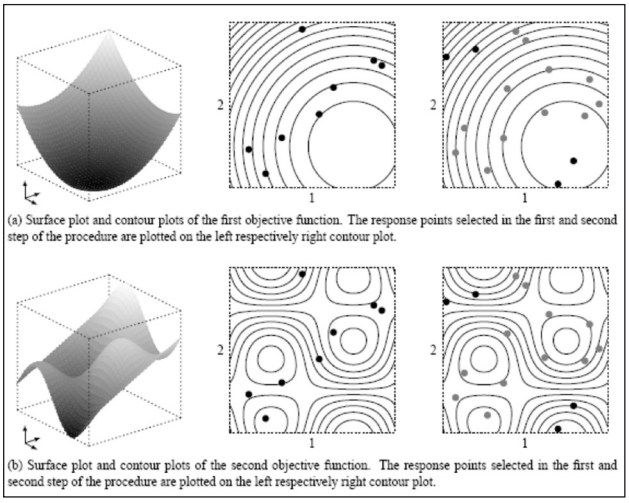

(a) Surface plot and contour plots of the first objective function. The response points selected in the first and second step of the procedure are plotted on the left respectively right contour plot.

(b) Surface plot and contour plots of the second objective function. The response points selected in the first and second step of the procedure are plotted on the left respectively right contour plot.

Figure 3 Illustration of the response point selection process on an example with two objective functions and two uncertain parameters

design (for example a Latin hypercube design) is generated and all objective functions are calculated at these response points by the FE solver. Using this information, initial response surfaces are created. Since these response surfaces will be improved in the second step, one should not use too many response points. The

© 2013 SRESA All rights reserved

authors achieved good results with three to four times the number of uncertain parameters. Additional points are best selected by the adaptive procedure in step two instead of being randomly selected in this step.

In the second step, illustrated in the right contour plots in Figure 3, a large space filling design is calculated. These points are not yet response points; only the few most promising points from this set will become real response points for which an FE analysis will be performed at the end of this step. For each of these points, the function value and the expected error on the function value are estimated using the calculated response surfaces. For each of these candidate response points, the *average maximum improvement* or *AMI* is calculated as

$$AMI = \sum_{\alpha} \sum_{k} (\max(\frac{\min(\tilde{f}_k(x)) - (\tilde{f}_k(x_{new}) - \Delta\tilde{f}_k(x_{new}))}{\min(\tilde{f}_k(x))}, 0)^2) \quad (10)$$

In this formula, $\tilde{f}_k$ is an approximation of a finite element output parameter. $\min(\tilde{f}_k(x))$ is the current minimum value of the approximation, $\tilde{f}_k(x_{new})$ is the value of the approximation in the candidate response point and $\Delta \tilde{f}k$ ($x$new) is the error range on the approximation in this point.

Thus, $\min(\tilde{f}_k(x)) - (\tilde{f}_k(x_{new}) - \Delta\tilde{f}_k(x_{new}))$ tells how much the current minimum can be improved in this candidate response point. If the current minimum cannot be improved in this point, this value will be negative, and will be set to 0 by the max(x, 0) operation. The sum of squares selects the average maximum improvement over all output parameters of interest. The candidate response points with the highest AMI are then selected and added to the response point set. Only in these points (the black points in Figure 3) an FE analysis is performed. For all other points (the grey points in Figure 3), only simple response surface evaluations are necessary. Finally, all response surfaces are recalculated or updated with the new information.

This second step of generating a large set of candidate response points and selecting the most promising points is repeated until a stopping criterion is met. One should continue the procedure until no more improvement can be made, that is, until one does not find any more points with an AMI > 0.

4. Doubly-Reinforced Beam Problem

4.1. General overview

In the present work, the stress distribution on the cross section of a doubly-reinforced concrete beam is considered. As shown in Figure 4, the beam is provided with tension steel reinforcement on the bottom face and compression steel reinforcement on the top face. The beam is subjected to a gravity loading. As a result of this loading, concrete in the zone above the neutral axis will be subjected to compression while the tensile force below the neutral axis will be borne by the steel reinforcement. As a result of this, compressive and tensile strains and stresses are induced in concrete and steel reinforcement respectively. The beam develops a moment of resistance as a result of these stresses and strains such that it equals the bending moment due to the external loads.

Several models were proposed to describe the stress distribution in the cross section of a concrete beam subjected to pure flexure. Initially, the parabolic model was proposed by Hognestad et. Al. (1955) [30]. This was followed by an exponential model proposed by Smith and Young (1955)[31] and the Desai and Krishnan model (1964)[32]. These models are applicable to concretes with strength below 40 MPa. The Indian standard code of practice for plain and reinforced concrete IS 456-2000 [29] allows the assumption of any suitable relationship between the compressive stress distribution and strain in concrete, i.e., rectangular, trapezoidal, parabolic or any other shape, which results in prediction of strength in agreement with material tests, can be used.

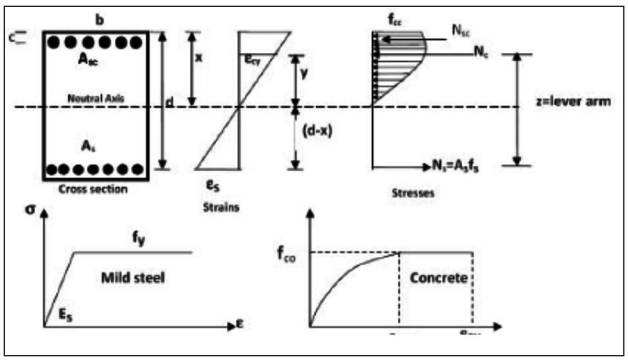

Figure 4 Stress distribution across the cross-section of a doubly-reinforced beam

The stress distribution model suggested by the Indian code IS 456-2000 is followed in the present study (Figure 4).

4.2 Moment of resistance of a doubly-reinforced beam

The moment of resistance of the doubly reinforced concrete section shown in Figure 4 is derived based on the analysis of the stresses and strains in concrete and steel. The beam has a width *b* and an effective

© 2013 SRESA All rights reserved

depth *d*. The effective cover to the reinforcement provided on the top and bottom faces is *c*. The areas of reinforcement in tension and compression are *As* and *Asc*. The strain-distribution is assumed to be linear and ε_{cc} is the strain in concrete at the extreme compression fiber and εs the strain in steel. Let *x* be the neutral axis depth from the extreme compression fiber. In order to calculate the moment of resistance, the neutral axis depth has to be determined, and the stresses both in concrete and in steel have to be computed. The compression stress-distribution in concrete is parabolic. Stresses in concrete in tension are neglected.

The strain ε_{cy} at any level *y* below the neutral axis ($y \le x$) is:

$$\varepsilon_{cy} = \left(\frac{y}{x}\right)\varepsilon_{cc} \tag{11}$$

The resultant compressive force *Nc* and its distance from the neutral axis *y* are given by (Purushottaman, 1986)[15]

$$N_c = \int_{y=0}^{y=x} f_{cy} b dy = \left[C_1\varepsilon_{cc} - C_2\varepsilon_{cc}^2\right]x \tag{12}$$

$$\overline{y} = \frac{\int_{y=0}^{y=X} b f_{cy} y dy}{\int_{y=0}^{y=X} b f_{cy} dy} = \frac{\left[\left(\frac{2C_1}{3}\right) - \left(\frac{3C_2}{4}\right)\right]}{\left[C_1 - C_2\varepsilon_{cc}\right]} \tag{13}$$

with:

$$C_1 = \frac{b.f_{co}}{\varepsilon_{co}}, C_2 = \frac{b.f_{co}}{3.\varepsilon_{co}^2} \tag{14}$$

Strain ε_s and stress f_s in the tensile steel reinforcement A_s are given by:

$$\varepsilon_s = \left(\frac{d-x}{x}\right)\varepsilon_{cc} \tag{15}$$

$$f_s = E_s\varepsilon_s = E_s\left(\frac{d-x}{x}\right)\varepsilon_{cc} \tag{16}$$

Similarly, strain ε_{sc} and stress f_{sc} in the compressive steel reinforcement *Asc* are given by:

$$\varepsilon_{sc} = \left(\frac{x-c}{x}\right)\varepsilon_{cc} \tag{17}$$

$$f_{sc} = E_s\varepsilon_{sc} = E_s\left(\frac{x-c}{x}\right)\varepsilon_{cc} \tag{18}$$

Finally, forces N_s in tensile steel and N_{sc} in compressive steel are obtained from:

$$N_s = A_s F_s \tag{19}$$

$$N_{sc} = A_{sc} F_{sc} \tag{20}$$

If there are no external loads, the equation of longitudinal equilibrium $N_s = N_c + N_{sc}$ leads to:

$$\left[C_1\varepsilon_{cc} - C_2\varepsilon_{cc}^2\right]x + A_{sc}E_s\left(\frac{x-c}{x}\right)\varepsilon_{cc} = A_sE_s\left(\frac{d-x}{x}\right)\varepsilon_{cc} \tag{21}$$

After simplification, the above equation leads to the quadratic equation:

$$\left[C_1 - C_2\varepsilon_{cc}\right]x^2 + (A_{sc} + A_s)E_s x - (cA_{sc} + dA_s)E_s = 0 \tag{22}$$

Applying the lever arm *z* given by

$$z = (y + d - x) \tag{23}$$

the internal resisting moment M_R is given by

$$M_R = N_c z + N_{sc}(d - c) \tag{24}$$

The neutral axis depth *x* can be determined by solving equation (22). This requires ε_{cc} to be known. An iterative procedure is adopted where ε_{cc} is gradually increased, and the corresponding values of N_c, *y* and the internal resisting moment M_R are obtained by using the above procedure. In order to calculate the allowable external bending moment for the cross section, this procedure is repeated until a failure mode is encountered. All possible modes of failure have to be considered:

1. stress in tension reinforcement f_s exceeds the allowable stress in tension 0.87 f_y (equation (16))
2. stress in compression reinforcement f_{sc} exceeds the allowable stress in compression 0.87 f_y (equation (18))
3. strain at the extreme concrete fiber in compression ε_{cc} exceeds the allowable strain ε_{co} = 0.002

The first failure mode that is encountered during the procedure determines the actual failure. Therefore, the moment of resistance at this final iteration represents the allowable external bending moment.

5. Fuzzy Analysis with Uncertain Structural Parameters

The effect of multiple uncertainties on the stress distribution across the cross section as described in the previous section is now analysed. Rama Rao and Pownuk (2007)[33] made the initial efforts to introduce

© 2013 SRESA All rights reserved

uncertainty in the stress analysis of reinforced concrete flexural members by analysing a singly reinforced concrete beam subjected to an interval load. In the current case, uncertainties are introduced on material and geometrical properties.

Consider the case of a doubly reinforced concrete beam with interval values of area of compression reinforcement $A_{sc} = \left[\underline{A}_{sc}, \overline{A}_{sc}\right]$ and tension reinforcement $A_s = \left[\underline{A}_s, \overline{A}_s\right]$ with corresponding interval Young's modulus **Es** . Correspondingly the resulting stresses and strains in concrete and steel are also uncertain and are modeled using interval numbers. The objective of the present study is to determine the resulting interval moment of resistance offered by the beam. This part of the paper first presents the interval translation of the procedure described in section 4.2. The same analysis will be performed using the response surface methods described in section 3.

5.1 Interval arithmetic approach

All the equations developed in section 4 are now extended and made applicable to the interval case. The neutral axis depth **x**, compressive force in concrete **Nc** , force in tensile reinforcement **Ns** and force in compression reinforcement **Nsc** are all expressed as interval quantities. Accordingly, the equation of horizontal equilibrium given by the quadratic equation (22) gets the interval form

$$\left[C_1 - C_2\varepsilon_{cc}\right]x^2 + (A_{sc} + A_s)E_s x - (cA_{sc} + dA_s)E_s = 0 \tag{25}$$

The above equation (25) is a linear quadratic equation with interval coefficients and can be solved for the interval value of the neutral axis depth **x** using the approach outlined by Hansen (1992)[34], Hansen and Walster (2002)[35], provided the value of ε_{cc} is known. The interval compressive force in concrete **Nc** is expressed as

$$\mathbf{N_c} = [C_1\varepsilon_{cc} - C_2\,\varepsilon^{\,2}_{cc}]x \tag{26}$$

The interval compressive force N_{sc} in steel reinforcement is expressed as

$$N_{sc} = A_{sc}E_s\varepsilon_{sc} = A_{sc}E_s\left(\frac{x-c}{x}\right)\varepsilon_{cc} \tag{27}$$

The interval value of lever arm **z** is given by

$$\mathbf{z} = \mathbf{y} + d - \mathbf{x} \tag{28}$$

The interval moment of resistance M_R is now expressed as

$$M_R = N_c \times z + N_{sc} \times (d - c) \tag{29}$$

The iterative analysis as discussed in the previous section is now repeated on this interval procedure, with values of ε_{cc} gradually increased from 0 to ε_{co} (= 0.002). At each iteration point, the linear interval quadratic equation (25) is solved to obtain the interval value of neutral axis depth x. Using this value of x , the interval moment of resistance M_R is computed. The analysis is stopped whenever one of the failure conditions is encountered. Thus, it is subject to the conditions,

$$f_s \le 0.87 f_y \text{ and } f_{sc} \le 0.87 f_y \tag{30}$$

5.2 Taylor expansion using sensitivity analysis

Sensitivity analysis method is described in the papers Pownuk (2000)[24] and Rama Rao and Pownuk[33]. This is specially optimized gradient method which is designed for solution of equations with the interval parameters. Equilibrium equations of the double reinforced beam can be written in the following general form

$$\begin{cases} F_1(x, \varepsilon_{cc,} M, A_s, A_{sc}, ...) = 0 \\ F_2(x, \varepsilon_{cc,} M, A_s, A_{sc}, ...) = 0 \end{cases} \Leftrightarrow F(x, \varepsilon_{cc}) = 0 \tag{31}$$

Explicit form of the functions F_1 , F_2 is given in the following equations (32). Equilibrium of the axial forces $F_1 = N_s - N_c - N_{sc}$=0.

$$-\frac{A_s\varepsilon_{cc}E_s(d-x)}{x} + \frac{A_{sc}\varepsilon_{cc}E_{sc}(c-d+x)}{x} - \frac{b\varepsilon_{cc}^2 f_{co}x}{3\varepsilon_{co}^2} + \frac{b\varepsilon_{cc}f_{co}x}{\varepsilon_{co}} = 0 \tag{32}$$

Equilibrium of the bending moments is given by $F_2 = M_R - N_c z - N_{sc}(d - c) = 0$.

$$\frac{12A_{sc}\varepsilon_{cc}\varepsilon_{co}^2E_{sc}(c-d)(c-d+x) + x(b\varepsilon_{cc}^2 f_{co}x(4d-x) + 4b\varepsilon_{cc}\varepsilon_{co}f_{co}x(x-3d) + 12\varepsilon_{co}^2M)}{12\varepsilon_{co}^2x} = 0 \tag{33}$$

In order to find the solution of the system of equation $F(x, \varepsilon_{cc}) = 0$ the Newton method can be applied

$$\begin{bmatrix} x_{i+1} \\ \varepsilon_{cc,i+1} \end{bmatrix} = \begin{bmatrix} x_i \\ \varepsilon_{cc,i} \end{bmatrix} - (\nabla F(x_{i,}\varepsilon_{cc,i}))^{-1} F(x_{i,}\varepsilon_{cc,i}) \tag{34}$$

where

$$\nabla F = \begin{bmatrix} \frac{\partial F_1}{\partial x} & \frac{\partial F_1}{\partial \varepsilon_{cc}} \\ \frac{\partial F_2}{\partial x} & \frac{\partial F_2}{\partial \varepsilon_{cc}} \end{bmatrix} \tag{35}$$

© 2013 SRESA All rights reserved

Formulas for the partial derivatives $\frac{\partial F_1}{\partial x}, \frac{\partial F_1}{\partial \varepsilon_{cc}}, \frac{\partial F_2}{\partial x}, \frac{\partial F_2}{\partial \varepsilon_{cc}}$ are given in the equations (41, 42, 44 and 45). Let us denote uncertain parameter p (i.e. M,As ,Asc etc.) as pi . Vector of uncertain parameters can be written as p = ($p1$, $p2$, ..., pm) where m is a number of uncertain parameters. Derivative of x and ε_{cc} can be calculated from implicit function theorem

$$\frac{\partial F_1}{\partial p_i}+\frac{\partial F_1}{\partial x}\frac{\partial x}{\partial p_i}+\frac{\partial F_1}{\partial \varepsilon_{cc}}\frac{\partial \varepsilon_{cc}}{\partial p_i}=0 \tag{36}$$

$$\frac{\partial F_2}{\partial p_i}+\frac{\partial F_2}{\partial x}\frac{\partial x}{\partial p_i}+\frac{\partial F_2}{\partial \varepsilon_{cc}}\frac{\partial \varepsilon_{cc}}{\partial p_i}=0 \tag{37}$$

In particular, sensitivity with the respect to the Young modulus of steel $pi = Es$ can be calculated from the following system of equations

$$\frac{\partial F_1}{\partial E_s}+\frac{\partial F_1}{\partial x}\frac{\partial x}{\partial E_s}+\frac{\partial F_1}{\partial \varepsilon_{cc}}\frac{\partial \varepsilon_{cc}}{\partial E_s}=0 \tag{38}$$

$$\frac{\partial F_2}{\partial E_s}+\frac{\partial F_2}{\partial x}\frac{\partial x}{\partial E_s}+\frac{\partial F_2}{\partial \varepsilon_{cc}}\frac{\partial \varepsilon_{cc}}{\partial E_s}=0 \tag{39}$$

where

$$\frac{\partial F_1}{\partial E_s}=\frac{A_S\varepsilon_{cc}(x-d)}{x} \tag{40}$$

$$\frac{\partial F_1}{\partial x}=\frac{\varepsilon_{cc}\left(3A_s d\varepsilon_{co}^2E_s+3A_{sc}\varepsilon_{co}^2E_{sc}(d-c)-bf_{co}x^2(\varepsilon_{cc}-3\varepsilon_{co})\right)}{3\varepsilon_{co}^2x^2} \tag{41}$$

$$\frac{\partial F_1}{\partial \varepsilon_{cc}}=\frac{A_sE_s(X-d)}{X}+\frac{A_{sc}E_{sc}(C-d-X)}{X}-\frac{2b\varepsilon_{cc}f_{co}X}{3\varepsilon_{co}^2}+\frac{bf_{co}X}{\varepsilon_{co}}=0 \tag{42}$$

$$\frac{\partial F_2}{\partial E_s}=0 \tag{43}$$

$$\frac{\partial F_2}{\partial x}=\frac{\varepsilon_{cc}(bf_{co}x^2(2d\varepsilon_{cc}-6d\varepsilon_{co}-\varepsilon_{cc}x+4\varepsilon_{co}x)-6A_{sc}\varepsilon_{co}^2E_{sc}(c-d)^2)}{6\varepsilon_{co}^2x} \tag{44}$$

$$\frac{\partial F_2}{\partial \varepsilon_{cc}}=\frac{6A_{sc}\varepsilon_{co}^2E_{sc}(c-d)(c-d+x)+bf_{co}x^2(4d\varepsilon_{cc}-6d\varepsilon_{co}-\varepsilon_{cc}x+2\varepsilon_{co}x)}{6\varepsilon_{co}^2x} \tag{45}$$

Using the solutions of the system of equations (36) and (37) it is possible to get the gradients

$$\nabla x=\left[\frac{\partial x}{\partial p_1},\frac{\partial x}{\partial p_2},,...,\frac{\partial x}{\partial p_m}\right] \tag{46}$$

$$\nabla \varepsilon_{cc}=\left[\frac{\partial \varepsilon_{cc}}{\partial p_1},\frac{\partial \varepsilon_{cc}}{\partial p_2},,...,\frac{\partial \varepsilon_{cc}}{\partial p_m}\right] \tag{47}$$

Using the sign of the gradient ∇x and $\nabla\varepsilon_{cc}$ it is possible to get extreme combination of the uncertain parameters $p_i \in [\underline{p}_i, \overline{p}^i]$.

If $\frac{\partial x}{\partial p_i} \geq 0$ then $p_i^{\min}=\underline{p}_i, p_i^{\max}=\overline{p}_i$; *If* $\frac{\partial x}{\partial p_i}<0$ then $p_i^{\min}=\overline{p}_i, p_i^{\max}=\underline{p}_i$. A Similar relation can be created for ε_{cc}. Finally extreme values of x and ε_{cc} can be calculated by using specific combinations of endpoints.

$$\underline{x}=x(p^{min}), \overline{x}=x(p^{max}),\ \underline{\varepsilon}_{cc}=x(p^{min}), \overline{\varepsilon}_{cc}=x(p^{max}) \tag{48}$$

where $x = x(p)$, $\varepsilon_{cc} = \varepsilon_{cc}(p)$ are implicit functions which are defined by the equation (31). In order to calculate extreme stress in steel f_s or extreme concrete fiber f_{cc} it is necessary to calculate appropriate gradients ∇f_s, ∇f_{cc} and repeat the whole procedure. Interval moment of resistance can be calculated by using sensitivity analysis. In order to do that it is necessary to calculate the gradient ∇M_R. From the equation (29) and chain rule we have

$$\frac{d}{dp_i}M_R=\frac{\partial M_R}{\partial p_i}+\frac{\partial M_R}{\partial x}\frac{\partial x}{\partial p_i}+\frac{\partial M_R}{\partial \varepsilon_{cc}}\frac{\partial \varepsilon_{cc}}{\partial p_i} \tag{49}$$

where p_i is the uncertain parameter, $\frac{\partial x}{\partial p_i}, \frac{\partial \varepsilon_{cc}}{\partial p_i}$ can be calculate from the system of equation (36) & (37).

If $p_i = E_s$ then from the equations (24) and (49) it is possible to derive

$$\frac{dM_R}{dE_s}=\frac{\partial M_R}{\partial E_s}+\frac{\partial M_R}{\partial x}\frac{\partial x}{\partial E_s}+\frac{\partial M_R}{\partial \varepsilon_{cc}}\frac{\partial \varepsilon_{cc}}{\partial E_s} \tag{50}$$

where

$$\frac{\partial M_R}{\partial E_s}=0 \tag{51}$$

$$\frac{\partial M_R}{\partial x}=\frac{\varepsilon_{cc}(6A_{sc}\varepsilon_{co}^2E_{sc}(c-d)^2+bf_{co}x^2(-2d\varepsilon_{cc}+6d\varepsilon_{co}+\varepsilon_{cc}x-4\varepsilon_{co}x))}{6\varepsilon_{co}^2x^2} \tag{52}$$

$$\frac{\partial M_R}{\partial \varepsilon_{CC}}=\frac{bf_{co}x^2(-4d\varepsilon_{cc}+6d\varepsilon_{co}+\varepsilon_{cc}x-2\varepsilon_{co}x)-6A_{sc}\varepsilon_{co}^2E_{sc}(c-d)(c-d+x)}{6\varepsilon_{co}^2x} \tag{53}$$

$\frac{\partial x}{\partial E_s}, \frac{\partial \varepsilon_{cc}}{\partial E_s}$ are the solution of the system of equations (38) and (39).

If $\frac{\partial}{\partial p_i}(M_R)\geq 0$ *then* $p_i^{\min}=\underline{p}_i, p_i^{\max}=\overline{p}_i$.

If $\frac{\partial}{\partial p_i}(M_R)<0$ *then* $p_i^{\min}=\overline{p}_i, p_i^{\max}=\underline{p}_i$.

Extreme values of the moment of resistance can be calculated as $\underline{M}_R = M_R(p^{min})$, $\overline{M}_R = M_R(p^{max})$. In order to improve reliability of the method monotonicity tests can be applied [25].

© 2013 SRESA All rights reserved

In order to calculate extreme values of any function ψ which depend on x and ε_{cc} (e.g. moment resistance M_R, f_{cc} etc.) the following method can be applied.

Algorithm of the gradient method

1. Calculate midpoint of all interval parameters $pi = mid(\mathbf{p}i)$ (e.g. $E0 = mid(\mathbf{E})$).
2. Find x_c, ε_{cc} at the midpoint by using Newton method [34](or any other method for the solution of the system of nonlinear equations).
3. From the system of equation (38) find $\frac{\partial x}{\partial E_s}, \frac{\partial \varepsilon_{cc}}{\partial E_s}$ (it is necessary to solve this system for all interval parameter p_i in order to calculate $\frac{\partial x}{\partial p_i}, \frac{\partial \varepsilon_{cc}}{\partial p_j}$
4. Calculate sensitivity of the each interval function ψ_j and each interval parameter p_i (e.g. M_R, stress in Extreme concrete fiber f_{cc} , stress in steel reinforcement f_s etc.) from the formula (49)

$$\frac{d\psi_j}{dp_i} = \frac{\partial \psi_j}{\partial p_i} + \frac{\partial \psi_j}{\partial x}\frac{\partial x}{\partial p_i} + \frac{\partial \psi_j}{\partial \varepsilon_{cc}}\frac{\partial \varepsilon_{cc}}{\partial p_i} \tag{54}$$

5. For each objective function find appropriate combination of endpoints, which help us to calculate extreme values of the objective function ψi .

$$If\ \frac{d\psi_i}{dp_j} \geq 0 \quad then \quad p_{j,i}^{\min} = \underline{p}_i,\ p_{j,i}^{\max} = \overline{p}_i.$$

$$If\ \frac{d\psi_i}{dp_j} < 0 \quad then \quad p_{j,i}^{\min} = \overline{p}_i,\ p_{j,i}^{\max} = \underline{p}_i$$

6. Using appropriate endpoints combinations evaluate the value of the functions ψ_i

$$\underline{\psi}_i = \psi(p_i^{\min}), \overline{\psi}_i = \psi(p_i^{\max}) \tag{55}$$

In order to evaluate the function ψi it is necessary to solve system of equations (31) for each combinations of endpoints $p* = (p_1^*, p_2^*, .., p_{2n}^*)$

$$F(x_c, \varepsilon_{cc}, p_1^*, p_2^*, ..., p_m^*) = 0 \tag{56}$$

and then find the value

$$\psi_i(p^*) = \psi_i(p_1^*, p_2^*, ..., p_m^*, x_c(x_c, \varepsilon_{cc}, p_1^*, p_2^*, ..., p_m^*), \varepsilon_{cc}(x_c, \varepsilon_{cc}, p_1^*, p_2^*, ..., p_m^*)) \tag{57}$$

5.3. Kriging response surface based optimisation method

The Kriging response surface based optimisation method described in section 3.2, considers the deterministic procedure described in section 4.2 as a black box function with three inputs (the area of compression reinforcement A_{sc} and the area of tension reinforcement A_s with the corresponding Young's modulus E_s and three outputs (the moment of resistance M_R , the resultant compressive force N_c and its distance from the neutral axis y).

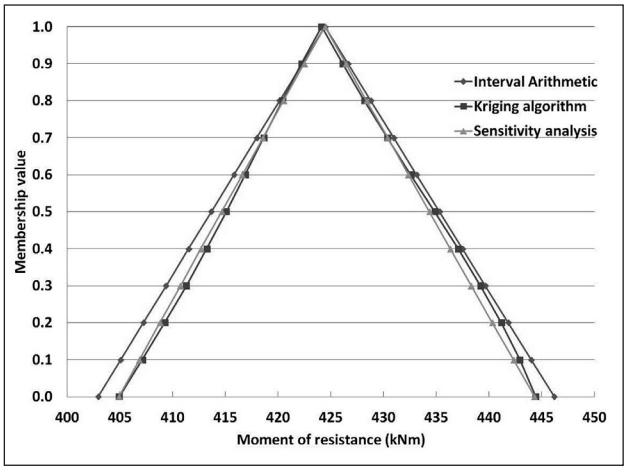

Figure 5 Comparison of fuzzy M_R obtained using the three approaches

In the first step of the procedure, 10 response points are selected using a Latin hypercube design. The second step of the procedure is repeated 5 times, each time adding the two most promising response points from a set of candidate response points consisting of 20 Latin hypercube points and all vertex points. In the third step of the procedure, the minimum and maximum of the response surfaces are located using MCS [37], a global optimisation algorithm. This step does not need any objective function evaluations.

In total, 20 response points (20 objective function evaluations) are required to model the three outputs of the black-box function with three inputs.

5.4. Results and discussion

The results of the different approaches are now compared for a specific case, where the beam has the dimensions $b = 300mm$, $d = 500mm$ and the effective cover to reinforcement $c = 50mm$. The beam is reinforced with 8 steel bars of 25 mm diameter in the tension zone ($As = 3929mm^2$) and 4 Tor50 bars of 20 mm diameter ($Asc = 1257mm^2$). Allowable compressive stress in concrete is $13.4\times10^8\ N/mm^2$ and the corresponding allowable strain in concrete is 0.002. The Young's modulus of steel is 2.0×10^9

© 2013 SRESA All rights reserved

N/mm^2. The stress-strain curve for concrete and steel as detailed in IS 456-2000 is adopted (see figure 4).

Fuzzy uncertainty is introduced on the area and Young's modulus of steel reinforcement using triangular fuzzy membership functions. These are constructed such that the core is the reference value, and the support yields intervals of ±5 percent of the nominal value. The analysis is performed using the α -level strategy applied on 11 levels. The corresponding interval values of neutral axis depth, strain and stress in concrete and stress in steel reinforcement as well as moment of resistance are computed at various levels of uncertainty and membership functions are plotted using the procedures outlined in the previous sections.

Figure 5 shows the plot of interval moment of resistance M_R obtained using the three methods outlined in the previous section. It is observed that there is an excellent agreement among the results obtained using the three methods. However, it is also observed that the direct interval approach makes a slight overestimation of the value of M_R. This is owing to the problem of dependency of parameters. Also, it is observed that both response surface based approaches perform very well. The Kriging approach is able to capture the non-linear higher order behaviour in the membership function. From a designer's point of view, it can be concluded that under the considered uncertainty, an external bending moment of up to 405 *kNm* is allowable, yielding safe conditions in the worst case.

6. Conclusions

This paper compares the performance of three different approaches for the fuzzy analysis of a doubly reinforced concrete beam with uncertain structural parameters. The approaches all focus on the solution of the equations which describe stress and strain in a doubly reinforced concrete beam in the presence of fuzzy model parameters. At the core of the fuzzy solution, the interval problem is solved using either optimization algorithms applied on an approximate surrogate response surface model, or by interval arithmetic translation of the problem.

Both the optimization approaches based on the sensitivity method and the Kriging approach perform well on this problem. Due to the monotonic behaviour of the output quantities of the problem with respect to the interval parameters, the sensitivity based approach returns the exact results in a very efficient way. The Kriging results show that a very close approximation of the exact results is obtained. This approach has the advantage that it does not require monotonicity. Finally, the interval arithmetic approach yields only minor conservatism, as in this case, the dependency problem did not have a major impact on the applied algorithms.

Acknowledgement

This research was supported by the project 'Fuzzy Finite Element Method", IWT/SBO 60043 granted by the Institute for the Promotion of innovation by Science and Technology in Flanders, Belgium. The first author gratefully acknowledges the help and support received from Prof. Stefan Vandewalle, Department of Computer Science, Katholieke Universiteit Leuven, Belgium.

References

1. D. Moens and D. Vandepitte. A survey of non-probabilistic uncertainty treatment in finite element analysis. *Computer Methods in Applied Mechanics and Engineering*, 194(14-16):1527–1555, 2005. ISI Impact Factor 2005: 1.553; times cited: 22.
2. A. Neumaier. *Interval Methods for Systems of Equations*. Cambridge University Press, Cambridge, 1990.
3. C. Jansson. Interval linear systems with symmetric matrices, skew-symmetric matrices and dependencies in the right hand side. *Computing*, 46(3):265–274, 1991.
4. U. K¨oyl¨uo˘glu, A.S. C. akmak, and S.R.K. Nielsen. Interval algebra to deal with pattern loading and structural uncertainties. *Journal of Engineering Mehanics*, 121(11):1149–1157, 1995.
5. S.S. Rao and L. Chen. Numerical solution of fuzzy linear equations in engineering analysis. *International Journal for Numerical Methods in Engineering*, 43:391–408, 1998.
6. S. McWilliam. Anti-optimization of uncertain structures using interval analysis. *Computers &Structures*, 79:421–430, 2001.
7. I.R. Orisamolu, B.K. Gallant, U.O. Akpan, and T.S. Koko. Practical fuzzy finite element analysis of structures. *Finite Elements in Analysis and Design*, 38:93–111, 2000.
8. R.L. Muhanna and R.L. Mullen. Uncertainty in mechanics problems interval-based approach. *Journal of Engineering Mechanics*, 127(6):557–566, 2001.
9. M.V. Rama Rao. Fuzzy finite element analysis of structures with uncertainty in load and material properties. *SERC Journal of Structural Engineering*, 33(2):129–137, 2006.
10. A. Neumaier and A. Pownuk. Linear systems with large uncertainties with applications to truss structures. *Reliable Computing*, 13(1):149–172, 2007.
11. I. Skalna, M.V. Rama Rao, and A. Pownuk. Systems of fuzzy equations in structural mechanics.*Journal of Computational and Applied Mathematics*, 218(1):149–156, 2008.
12. D. Moens and D. Vandepitte. A fuzzy finite element procedure for the calculation of uncertain frequency response functions of damped structures: Part 1 - procedure. *Journal of Sound andVibration*, 288(3):431–462, 2005. ISI Impact Factor 2005: 0.898; times cited: 7.

© 2013 SRESA All rights reserved

13. D. Moens, M. De Munck, and D. Vandepitte. Envelope frequency response function analysis of mechanical structures with uncertain modal damping characteristics. *Computer Modelling inEngineering & Sciences*, 22(2):129–149, 2007. ISI impact factor 2007: 1.653.
14. M. De Munck, D. Moens, W. Desmet, and D. Vandepitte. A response surface based optimisation algorithm for the calculation of fuzzy envelope FRFs of models with uncertain properties. *Computers & Structures, Special Issue on Uncertainties in Structural Analysis - Their Effect on Robustness, Sensitivity, and Design*, 86(10):1080–1092, 2008. ISI Impact Factor 2007: 0.934.
15. P. Purushottaman. *Reinforced Concrete Structural Elements-Behaviour, Analysis and Design*. Tata McGraw-Hill Publishing Company Limited, New Delhi, India, 1986.
16. L.A. Zadeh. Fuzzy sets. *Information and Control*, 8:338–353, 1965.
17. S.S. Rao and J.P. Sawyer. Fuzzy finite element approach for the analysis of imprecisely defined systems. *AIAA Journal*, 33(12):2364–2370, 1995.
18. U. K¨oyl¨uo˘glu and I. Elishakoff. A comparison of stochastic and interval finite elements applied to shear frames with uncertain stiffness properties. *Computers & Structures*, 67:91–98, 1998.
19. D. Degrauwe. *Uncertainty propagation in structural analysis by fuzzy numbers*. PhD thesis, K.U.Leuven, 2007.
20. J. Nocedal and S.J. Wright. *Numerical optimization*. Springer, 1999.
21. A. Pownuk. Numerical solutions of fuzzy partial differential equation and its application in computational mechanics. In M. Nikravesh, L.A. Zadeh, and V. Korotkikh, editors, *Fuzzy Partial Differential Equations and Relational Equations: Reservoir Characterization and Modeling*, pages 308–347. Physica-Verlag, 2004.
22. A Pownuk. *Application of Fuzzy Sets Theory to Assessment of Reliability of Civil Engineering Structures*. Ph.D. dissertation, Silesian Technical University in Gliwice, Gliwice, Poland, 2001.
23. A. Pownuk. Applications of sensitivity analysis for modelling of structures with uncertain parameters. In *International Conference on Interval Methods in Science and Engineering Interval'2000*, pages 116–117, Karlsruhe, Germany, 2000.
24. A. Pownuk. Calculation of displacement in elastic and elastic-plastic structures with interval parameters. In *33 rd SOLID MECHANICS CONFERENCE (SolMech2000)*, pages 160–161, Zakopane, Poland, September 5-9 2000.
25. A. Pownuk. Efficient method of solution of large scale engineering problems with interval parameters based on sensitivity analysis. In *Proceeding of NSF workshop on Reliable EngineeringComputing*, pages 305–316, Savannah, Georgia, USA, September 15-17 2004.
26. A. Pownuk. General interval fem program based on sensitivity analysis. *The University of Texas at El Paso, Department of Mathematical Sciences Research Reports Series Texas ResearchReport*, (2007-06), 2007.
27. Jerome Sacks, William J. Welch, Toby J. Mitchell, and Henry P. Wynn. Design and analysis of computer experiments. *Statistical Science*, 4(4):409–435, 1989.
28. Wim C. M. van Beers and Jack P. C. Kleijnen. Kriging interpolation in simulation: a review. In R. G. Ingalls, M. D. Rossetti, J. S. Smith, and B. A. Peters, editors, *Proceedings of the 2004Winter Simulation Conference*, pages 113–121, 2004.
29. Bureau of Indian standards. Indian standard code for plain and reinforced concrete (is 456-2000), fourth revision, 2000.
30. E. Hognestad, N.W. Hanson, and D. McHendry. Concrete stress distribution in ultimate strength design. *ACI Journal*, 52(6):455–479, 1955.
31. G.M. Smith and L.E. Young. Ultimate flexural analysis based on stress strain curves of cylinders. *ACI Journal*, 53(6):597–609, 1955.
32. P. Desai and S. Krishnan. Equation for stress strain curves of concrete. *ACI Journal*, 61(3):345–356, 1964.
33. M.V. Rama Rao and A. Pownuk. Stress distribution in a reinforced concrete flexural member with uncertain structural parameters. Technical Report 2007-05, The University of Texas at El Paso, Department of Mathematical Sciences, El Paso, TX, 2007.
34. E.R. Hansen. *Global Optimization Using Interval Analysis*. Dekker, New York, 1992.
35. E.R. Hansen and W. Wallster. Sharp bounds on interval polynomial roots. *Reliable Computing*, 8:115–122, 2002.
36. A. Pownuk. Applications of sensitivity analysis for modelling of structures with uncertain parameters. In *Proceeding of International Conference on Interval Methods in Science and Engineering Interval'2000*, pages 116–117, Karlsruhe, Germany, 2000.
37. A.Neumaier. MCS: Global optimization by multilevel coordinate search. http://www.mat.univie.ac.at/_neum/software/mcs/

© 2013 SRESA All rights reserved

Life Cycle Reliability and Safety Engineering
Vol.2 Issue 1 (2013) 45-51

Sensitivity Studies on Fatigue Crack Growth Parameters in Concrete

Pervaiz Fathima K.M. and J.M. Chandra Kishen*

Research Scholar, *Professor Department of Civil Engineering Indian Institute of Science, Bangalore 560012, India
*email: chandrak@civil.iisc.ernet.in

Abstract:

The phenomenon of fatigue is one of the major causes of failure in concrete structures. The rate of fatigue crack propagation in concrete depends on a number of parameters, such as load, tensile strength, crack length, fracture toughness and the size of specimen. In this work, a fatigue crack propagation law is derived from the dissipation potential within a thermodynamic framework using the concepts of dimensional analysis and self-similarity. A deterministic as well as a probabilistic sensitivity study is carried out to determine which parameter affects fatigue crack propagation the most. This study also helps to identify the parameters that can be considered as deterministic or random.

Keywords: ***Fatigue, crack, sensitivity, concrete, dissipation potential***

1. Introduction

Understanding the mechanism of fatigue in concrete and its modeling is still an ongoing research field. Fatigue crack growth in concrete is a complex phenomenon starting from micro-cracking to formation of macro-crack and its propagation leading to failure; all this occurring simultaneously at micro, meso and macro levels. The energy approach is the most viable method to handle complex phenomena and is used in this work with thermodynamics as the framework. Thermodynamics assumes the existence of two kinds of potentials, a thermodynamic potential and a dissipation potential [1]. Given a thermodynamic system, the state laws are derived from the thermodynamic potential. The free energy is usually taken as the thermodynamic potential. In mechanics terminology, the laws of elasticity can be derived from this. In an irreversible process, where energy of the system is degraded, the complementary laws of evolution are defined by a dissipation potential. This potential helps to arrive at an evolution equation depending on the internal variable of the phenomenon [1]. The available expressions in literature for dissipation potential are empirical, mostly applicable to metals and are derived using the theory of continuum damage mechanics [2-6]. Analytical expressions for dissipation potential in the context of fatigue crack propagation in concrete within a fracture mechanics framework are not available in literature. In this work, an analytical expression for the dual of dissipation potential is derived from which a fatigue crack propagation law is obtained. This is done using the concepts of dimensional analysis and self-similarity. Different parameters that possibly affect fatigue crack propagation such as load, tensile strength, crack length and fracture toughness are chosen. The possibility of each of these parameters being either random or deterministic is discussed. A deterministic as well as probabilistic sensitivity study is conducted to understand the effect of uncertainty in each of the input parameters on the fatigue life and also the hierarchy of importance of the input parameters. This also helps to decide whether a given input parameter is to be considered random or deterministic.

2. Fatigue Crack Propagation Law

In this section, a fatigue crack propagation law is derived from the dual of dissipation potential using dimensional analysis and self-similarity concepts. A thermodynamic system is defined by its state variables which include observable variables and internal variables. Observable variables include temperature and total strain and these are sufficient to define a reversible (elastic) process. Internal variables describe the internal microstructure of the material and the past history is captured in these variables. They are necessary to describe an irreversible or a dissipative process. The choice of the internal variables is dictated by the phenomenon under study and its application.

© 2013 SRESA All rights reserved

The plastic strain ε_p, the damage variable D or the crack length a are few internal variables depending on whether the phenomenon under study is plasticity, damage or fracture respectively. Associated with the set of independent state variables is a set of dependent state variables called the thermodynamic properties or associated variables or dual variables. The thermodynamic potential allows one to write relations between observable variables and its associated variables. However, for internal variables it allows only the definition of their associated variables. On the other hand, a dissipation potential allows one to get the relationship between the internal variables and its associated variables. In order to describe the dissipation process or the evolution of the internal variables, a dissipation potential is needed [1]. Let V_k be the internal variables and A_k, their corresponding associated variables, where k=1,2,.., depending on the number of internal variables involved. Dissipation is defined as the sum of product of the thermodynamic force (associated variable) A_k and the respective flux variable ($\dot{V}_k$). Dissipation potential Φ is a function of the flux variables, the gradient of which gives the thermodynamic force causing it.

$$A_k = \frac{\partial \Phi}{\partial \dot{V}_k} \tag{1}$$

The Legendre-Fenchel transform enables us to define the corresponding potential, $\Phi^*(A_k)$, the dual of Φ with respect to the variables $\dot{V}_k$, such that

$$\dot{V}_k = \frac{\partial \Phi^*}{\partial A_k} \tag{2}$$

This equation is called the normality property. The dissipation potential and its dual must essentially be a positive, convex scalar valued function possessing a value zero at the origin to ensure automatic satisfaction of second law of thermodynamics [1]. Here, an expression for the dual of dissipation potential is derived using dimensional analysis, the theory of intermediate asymptotics and self similarity. The system is a cracked concrete beam under three-point bending; the thermodynamic process is the propagation of crack with increasing number of load cycles. This process being irreversible, energy is dissipated. Crack length is the internal variable, the evolution of the flux of this variable, i.e. the rate of crack propagation is the quantity of interest. The conjugate of this variable, that is, the thermodynamic force causing it is the strain energy release rate G. Since the loading alternates between a maximum and minimum amplitude, the strain energy release rate range ΔG is considered. The dissipation potential is in terms of the rate of crack propagation $\dot{a}$; when differentiated with respect crack rate, it gives the energy release rate range ΔG. But it is easier to calculate ΔG rather than rate of crack propagation $\dot{a}$. Hence, we make use of the Legendre-Fenchel transformation and are thus interested in deriving the expression for the dual of dissipation potential, the differentiation of which with respect to ΔG will give the rate of crack propagation $\dot{a}$. To begin with, a preliminary relationship between the various parameters involved in the phenomenon is obtained using dimensional analysis. To do so, the variables on which the dual of dissipation potential depends are selected. The variables on which the dissipation potential depends should include a loading parameter, material parameters and the state variable in whose evolution we are interested in, that is, the crack length. First, consider the strain energy release rate range ΔG, it is the energy required for unit crack propagation. It depends on the loading, crack length, specimen geometry and the type of material. During fatigue loading, for each cycle, part of the strain energy is used for crack propagation and the remaining is dissipated. Also, it is the thermodynamic force causing crack propagation. Hence, this is one of the most important parameters that will affect dissipation potential. Sometimes, the variable in the evolution of which we are interested can itself become a parameter [1]. So, in this problem, the crack length, a is also considered as a parameter on which the dissipation potential depends. The material parameters included are the tensile strength f_t and the fracture energy G_F. Tensile strength is an important parameter to be considered because cracking occurs in concrete only when the major principal stress exceeds this value. Fracture energy is another very important material parameter which must be included since it is related to the toughness of the material. Concrete exhibits strong size effect which is reflected in the value of G_F. Considering all the above parameters, the dual of the dissipation potential Φ^* can be written as

$$\Phi^* = f(\Delta G, a, G_F, f_t) \tag{3}$$

Table 1 gives the dimensions of each of these quantities. Applying Buckingham's Π theorem; choosing G_F and f_t as having independent dimensions and using them to non-dimensionalize the remaining quantities, we obtain,

$$\frac{\Phi^*}{f_t} = \phi\left(\frac{\Delta G}{G_F}, \frac{f_t}{G_F} a\right) \tag{4}$$

© 2013 SRESA All rights reserved

Φ^* is thus a function of two dimensionless products given by,

$$\Phi^* = f_t\ \phi(\Pi_1, \Pi_2) \tag{5}$$

Where, . $\Pi_1 = \frac{\Delta G}{G_F}$ and $\Pi_2 = \frac{f_t}{G_F} a$

Dimensional analysis merely transforms *f* of Equation 3 to ϕ of Equation 5. Finding ϕ does not belong to the frame of dimensional analysis; this must be done by experimental or numerical means. Although dimensional analysis is considered as a universal tool, however, there are physical problems that cannot be solved by dimensional analysis in principle. For example, the problem that involves information about the initial and boundary conditions, the system behavior in the initial times, the details of process generation, its behavior near the system boundaries, decay via equilibration, energy dispersion or dissipation during the process evolution. The present problem belongs to this category as it deals with energy dissipated during fatigue crack propagation. Consequently, more sophisticated tools must be employed to cope successfully with these problems. The theory of intermediate asymptotics, which can be considered as a generic extension of dimensional analysis can be adopted [7]. The intermediate asymptotic is a time-space dependent solution of an evolution equation that has already forgotten its initial conditions, but still does not feel the limitations imposed by the system boundary. It is an approximate solution to a complex problem, valid in a certain range. It can be represented by the self-similar solution, which is the exact solution to a simplified problem, valid in the whole range. The consideration of self-similar solutions as intermediate asymptotics allows us to understand the role of dimensional analysis in establishing self-similarity and determining self-similar variables [8]. Two kinds of self-similar solutions exist, complete self-similarity and incomplete self-similarity. For details on concepts of self-similarity, one may refer to the book by Barenblatt [8]. Complete self-similarity renders a quantity non essential. Therefore, considering incomplete self similarity in both the dimensionless products, we get

$$\Phi^* = f_t\ \Pi_1^{b_1} \Pi_2^{b_2} \tag{6}$$

$$\text{Or}, \quad \Phi^* = f_t \left(\frac{\Delta G}{G_F}\right)^{b_1} \left(\frac{f_t}{G_F} a\right)^{b_2} \tag{7}$$

$$\text{Or}, \quad \Phi^* = \Delta G^{b_1}\ G_F^{-b_1-b_2}\ f_t^{1+b_2}\ a^{b_2} \tag{8}$$

The constants b_1 and b_2 cannot be obtained from dimensional analysis in principle [7]. These constants can be obtained from experiments. The dual of the dissipation potential Φ^* represents the energy dissipated during the process of fatigue and it is very difficult to compute its value over a large number of cycles. However, the flux variables and the dual variables are quite easy to measure and it is on their values that modeling and identification are based. The evolution laws are therefore directly identified but the dissipation potential is used as guideline for writing their analytical expression. It is clear that although Φ^* is difficult to measure, the flux variable, i.e., the rate of crack propagation $\dot{a}$ and the dual variable, i.e., the energy release rate range ΔG are easy to measure from experiments. Hence, on the basis of these values the unknown constants are obtained. If the function Φ^* is differentiable, the normality property is preserved and the complementary laws of evolution can be written as [1]

$$\dot{a} = \frac{da}{dN} = \frac{\partial \Phi^*}{\partial \Delta G} \tag{9}$$

where, *a* is the crack length and *N* is the number of cycles. The fatigue crack propagation law is thus written as

$$\frac{da}{dN} = b_1 \Delta G^{b_1 - 1}\ G_F^{-b_1-b_2}\ f_t^{1+b_2}\ a^{b_2} \tag{10}$$

The unknown constants are determined through a calibration process using experimental results. In this study, the experimental results of Bazant and Xu [9] are used. It involves testing concrete beams of three different sizes (namely small, medium and large) with an initial notch equal to 0.2 times the depth of the specimen, subjected to cyclic loads under three point bending. The geometry details and material properties are given in Table 2. The thickness of all three specimens was 38 mm and span to depth ratio was 2.5. The maximum load applied was 80% of the peak load and minimum load was maintained at zero. The tensile strength of concrete used was 2.86 MPa. Knowing the load range, crack length, number cycles and the geometry details, ΔG and $\frac{da}{dN}$ can be computed. All the values on the right hand side of Equation 10 are known except for the constants b_1 and b_2, and also experimental value of $\frac{da}{dN}$ is known. Through an optimization process, the constants are computed such that the error, i.e. difference between the value of $\frac{da}{dN}$ as predicted by the model and the experimental value is minimized. The data of the small specimen is used for

© 2013 SRESA All rights reserved

calibration. The values of the constants b_1 and b_2 for the best fit are found to be 6.7 and -0.7 respectively. Figure 1 shows the variation of log $\frac{da}{dN}$ with log (ΔK_I) for the small specimen that was used for calibration purpose. Here, δK_I is the mode I stress intensity factor range. The model is used to predict $\frac{da}{dN}$ for other specimens. Figure 2 shows the variation of log $\frac{da}{dN}$ with log (ΔK_I) for medium and large specimens. A very good match between the predicted and experimental result is observed, thereby validating the model.

3. Nature of the Parameters Affecting Fatigue

In this section, the nature of each of the parameters that affect fatigue crack growth in concrete is elucidated. That is, whether each parameter can be treated as a deterministic one or as random is discussed here. The parameters that affect fatigue crack growth in concrete are load, geometry, material properties namely elastic modulus and tensile strength, fracture properties namely crack length and fracture toughness. We consider below each of these parameters.

Load: Fatigue occurs due to repeated or cyclic load, therefore, the load considered here is the load range varying between a maximum (P_{max}) and minimum (P_{min}). External loading is highly unpredictable and hence must be considered as a random variable.

Geometry: The span, width and depth of the member are usually deterministic quantities.

Material properties: The elastic modulus and tensile strength for concrete are well known to vary from specimen to specimen of the same mix. Hence these two parameters will be considered as random quantities.

Crack length: Crack length in concrete is a quantity that is very difficult to measure. The demarcation between the true crack length and the visible crack length or the indirectly computed value is not clear and all these values differ from each other. Hence it is necessary to consider this variable as random. Crack length in concrete can be measured directly by optical microscopy or high speed photography; or it can be measured indirectly using compliance technique, ultrasonic measurement or acoustic emission technique.

Fracture Energy: The fracture energy or the fracture toughness is usually regarded as a material property and its value is supposed to be a constant. But in concrete, this value is dependent on size and like other material properties, it varies from specimen to specimen and hence, it is appropriate to consider it as a random quantity.

Since, most of these parameters are random in nature, it is important to study the effect of uncertainty in these parameters on fatigue crack growth in concrete. In the next section, a sensitivity study is done to know the effect of each of the input quantities on the fatigue life.

4. Sensitivity Study

Sensitivity refers to the variation in output of a model with respect to changes in the values of the model's inputs. Sensitivity analysis is performed to determine which of the input parameters have a dominant effect on the output or which parameters are the key drivers of a model's results. Alternatively, it can also be used to infer as to which parameters in the model can be considered as random and which as deterministic; the most sensitive variables are to be considered as random whereas the less sensitive ones can be considered as deterministic. Stochastic sensitivity analysis on fatigue behaviour of steel structures was conducted by Kala [10], where Paris law was used to describe fatigue crack growth, In Section 2, an expression for the dual of dissipation potential was obtained in the context of fatigue, from which a fatigue crack propagation law for concrete has been proposed. This law takes into consideration different parameters such as the crack length, loading parameter, fracture energy and the tensile strength. The fatigue life or the number of cycles to failure N_f is obtained from Equation 10 and is given by

$$\int_0^{N_f} dN = \int_{a_o}^{a_c} \frac{da}{b_1 \Delta G^{b_1-1} G_F^{-b_1-b_2} f_t^{1+b_2} a^{b_2}} \tag{11}$$

$$\text{or } N_f = \int_{a_o}^{a_c} \frac{da}{b_1 \Delta G^{b_1-1} G_F^{-b_1-b_2} f_t^{1+b_2} a^{b_2}} \tag{12}$$

Here, a deterministic as well as probabilistic (sampling based) sensitivity study is conducted to determine which parameters are more sensitive and play a dominant role on dissipation potential and fatigue crack propagation. The deterministic as well as the probabilistic methods of sensitivity can be considered as complementary and it is worthwhile to do both [11].

4.1 Deterministic sensitivity study

Deterministic Sensitivity analysis is conducted and presented as a Tornado diagram, which is more commonly used in decision analysis. A tornado

© 2013 SRESA All rights reserved

diagram consists of a set of horizontal bars, referred as swings corresponding to each variable. The length of the bar for a given variable represents the extent to which the output quantity is sensitive to this variable. The swings are displayed in a descending order from top to bottom, such that the swings are in a wide to narrow arrangement resembling a tornado [12]. The most sensitive variable will have the largest swing and is at the top and, the least sensitive variable is at the bottom and has the shortest swing. To obtain this, the following steps are performed.

1. First we obtain the value of N_f for the mean values of all the input variables. This is called the base value.
2. One of the variables takes the extreme (lowest and highest) value possible and all other variables are maintained at their mean values. This gives the corresponding low/high value of N_f for that variable accordingly. The extreme value is obtained based on the coefficient of variation given in Table 3 for each variable. The procedure is repeated for all the variables one after the other.
3. The swing value is computed as

$$\text{Swing} = \text{Max(Low,Base,High)} - \text{Min(Low,Base,High)}$$

The tornado diagram is obtained by constructing the swing for each variable by plotting the corresponding low and high values normalized with the base value. The data from experimental results of medium specimen [9] are taken for this purpose. Tornado diagram is constructed by computing the swing in the number of cycles to failure as shown in Figure 3. From this figure, it is seen that the load range ΔP is the most sensitive parameter followed by the crack length *a*. The material parameter, represented by the fracture energy (G_F) is the next sensitive parameter, followed by the elastic modulus and the structural size. The tensile strength f_t, is the least sensitive one. The conclusion that can be drawn from this study is that it is the load range that affects fatigue crack propagation the most and hence in fatigue analysis it must be considered as a random variable. The material parameters namely tensile strength and elastic modulus are comparatively less sensitive and can be treated as deterministic. The crack length is the second most sensitive parameter and hence care should be taken to get this value of crack length as accurately as possible.

4.2 Probabilistic sensitivity study

In this section, a probabilistic sensitivity analysis is done by computing the sensitivity coefficients. From this, the influence in the variation of the number of cycles to failure, on the variability of input random quantities is studied. Since the number of parameters that affect fatigue crack growth which are random is high, Monte-Carlo simulation technique is used here to generate random samples. By knowing the distribution and statistical parameters of the random variables, random samples are generated using the Latin Hypercube Sampling (LHS) method. The LHS method is used to reduce the sample size. The technique involves stratified sampling on each of the input variables. The range of each input variable is exhaustively divided into *m* disjoint intervals of equal probability. For each input variable, one observation is randomly drawn from each interval. The *m* values of the first variable generated by this process are paired at random without replacement with the *m* values of the second variable. The process continues with each successive input variable. The advantage of using LHS rather than simple sampling is that the statistical estimates of the output values from the simulation will always have more precision than the latter one [13]. Hence with fewer samples one can achieve the desired accuracy. Using these randomly obtained samples the coefficient of variation is computed. The sensitivity coefficient, P_i is computed by knowing the coefficient of variation using

$$p_i = 100\frac{v_{yi}^2}{v_y^2} \tag{13}$$

Where, v_{yi} is the coefficient of variation of the output quantity keeping the i^{th} input parameter as random and all other parameters as deterministic and, $i = 1,2,\ldots,n$, where n is the number of input quantities examined in the sensitivity analysis. v_y is the coefficient of variation of the output quantity, considering all the input quantities as random ones. The concept is based on the assumption that a higher value of sensitivity coeffcient p_i indicates a higher degree of correlation and therefore higher influence of input variable on the output [10]. The sensitivity study is performed on the medium sized beam specimen [9]. The statistical parameters used in the sensitivity analysis for all the variables considered are shown in Table 3, along with the computed sensitivity coefficients. The mean values for each variable are the values reported from experimental observations. All the parameters are assumed to be normally distributed. A higher coefficient of sensitivity value of a given input variable indicates a higher influence on the output parameter.

© 2013 SRESA All rights reserved

Table 1: Variables considered and their dimensions

Variable	Definition	Dimension
Φ^*	Dual of the dissipation potential	FL^{-2}
ΔG	Energy release rate range	FL^{-1}
a	Crack length	L
G_F	Fracture energy	FL^{-1}
f_t	Tensile strength	FL^{-2}

Table 2: Geometry and load details [8]

Specimen	Depth mm	G_F N/mm	Peak Load N
Small	38	0.049	1815
Medium	76	0.083	2986
Large	152	0.134	5184

Table 3: Sensitivity coefficients of various parameters

Variable	Coefficient of variation	Sensitivity Coefficient p_i %
ΔP	0.25	92.73
a	0.2	2.53
D	0.05	0.89
G_F	0.2	0.16
E	0.15	0.07
f_t	0.2	0.0004

From Table 3, it is evident that the load range is the most sensitive parameter followed by the crack length and specimen size. This is followed by the fracture energy. The elastic modulus and the tensile strength are least sensitive to fatigue crack growth rate in concrete.

4.3 Probability distribution function

The probability distribution function is another way to check the sensitivity of different parameters. In this, the ultimate fatigue life N_c is plotted against the probability that the computed life N_f is less than a particular N_c value. The number cycles to failure are computed through a Monte Carlo simulation considering one variable random at a time and all others deterministic. If the probability distribution function depicts a steeper curve for a parameter, it implies that this parameter is less sensitive [14]. A cumulative distribution function is obtained and shown in Figure 4. From this it is seen that the curves for tensile strength and elastic modulus are almost vertical and hence can be deemed as the least sensitive. The fracture energy is the next least sensitive parameter. The curves for load range, crack length and specimen size are flatter and hence more sensitive in affecting fatigue life.

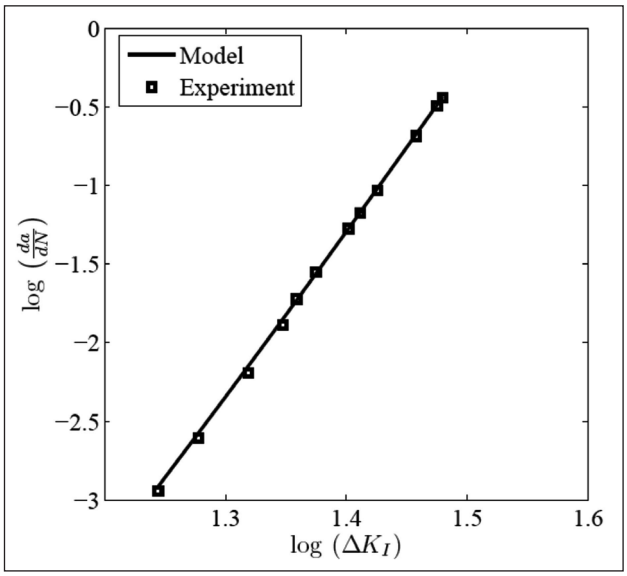

Figure 1: Calibration of the model using data of small specimen [8].

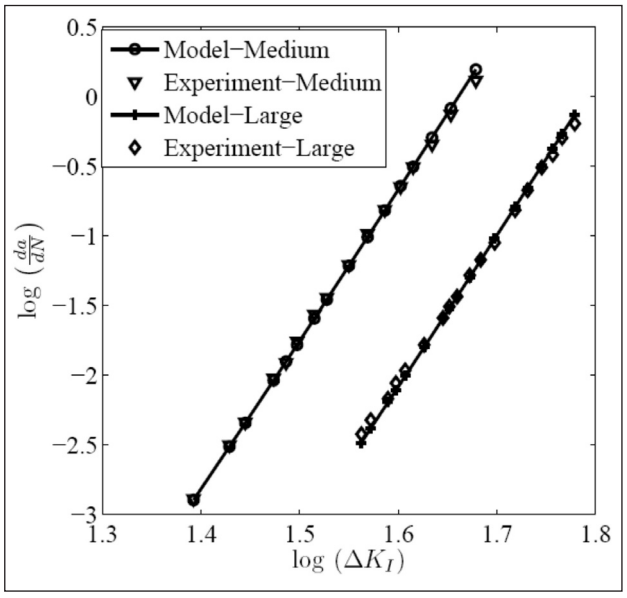

Figure 2: Comparison of the fatigue crack propagation rate using the proposed model with experimental results [8].

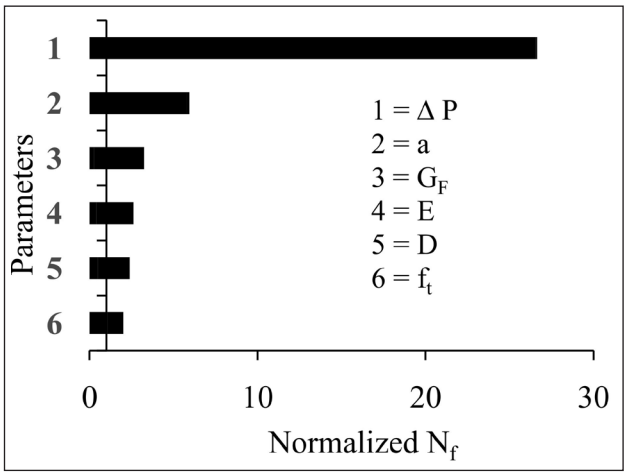

Figure 3: Tornado diagram

© 2013 SRESA All rights reserved

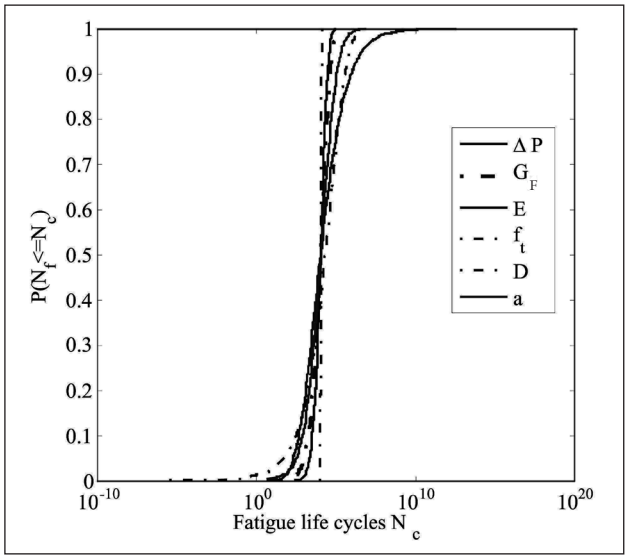

Figure 4: Cumulative distribution curves of fatigue life N_f for different random variables.

4.4 Hybrid uncertainty modeling

Uncertainty in a parameter may be classified into two types, namely; randomness and vagueness. The probability theory is suitable to deal with randomness type of uncertainty, whereas the theory of fuzzy sets is more appropriate for vagueness type of uncertainty. Uncertainty assessment using only one of the approaches may sometimes be incomplete [15]. The term fuzziness is generally used to describe processes that cannot be given precise definition or precisely measured. In the previous subsections, it is seen that the crack length is one of the most sensitive parameters after the loading parameter. It is difficult to precisely define or measure crack length in concrete because of the tortuosity of cracks and presence of microcracking at the tip of the macrocrack and hence the crack length can also be considered as fuzzy. Further work needs to be done using a hybrid approach in order to understand the effect of uncertainties in fatigue crack growth parameters on the fatigue life.

5. Conclusions

In this work, a fatigue crack propagation law is derived from the dual of dissipation potential using the concepts of dimensional analysis and self-similarity. The random nature of various parameters affecting fatigue crack growth in concrete is discussed. Both deterministic as well as probabilistic sensitivity studies are conducted and presented in the form of Tornado diagram, sensitivity coefficients and cumulative distribution curves. All these studies together suggest that loading is the most sensitive parameter affecting the fatigue crack propagation in concrete and therefore must be considered as a random quantity in fatigue studies. This observation is obvious because it is the parameter that mainly influences the thermodynamic force causing crack growth during fatigue. The second most sensitive parameter is the crack length. The accurate determination of crack length is not straightforward hence more focus is required to obtain the actual crack length in concrete. This observation also signifies the importance of early detection of cracks in existing structures as fatigue life is significantly affected by this parameter. The fracture energy considered in the present study is dependent on size and is the next most sensitive parameter. Structural size though not explicitly considered in the present study to be a parameter affecting crack growth, its importance is highlighted albeit indirectly. The material properties like elastic modulus and tensile strength are the least sensitive and can be assumed to be deterministic in fatigue crack growth studies.

References

1. Lemaitre J. and Chaboche J., "Mechanics of solid materials", Cambridge University Press, Cambridge, 1990.
2. Lemaitre J., "A continuum damage mechanics model for ductile fracture", Journal of engineering materials and technology, Vol 107, pp. 83–89, 1985.
3. Tai W., "Plastic damage and ductile fracture in mild steels", Engineering Fracture Mechanics, Vol 37, pp. 853–880, 1990.
4. Chandrakanth S. and Pandey P., "An isotropic damage model for ductile material", Engineering Fracture Mechanics, Vol 50, pp. 457–465, 1995.
5. Wang T., "Unified CDM model and local criterion for ductile fracture – I", Engineering Fracture Mechanics, Vol 42, No. 1, pp. 177 – 183, 1992.
6. Bonora N., "A nonlinear CDM model for ductile failure", Engineering Fracture Mechanics, Vol 58, pp. 11–28, 1997.
7. Ruzicka M.C., "On dimensionless numbers", Chemical Engineering and design, Vol 86, pp. 835 – 868, 2008.
8. Barenblatt G., "Scaling", Cambridge University Press, New York, 2004.
9. Bazant Z. P. and Xu K., "Size effect in fatigue fracture of concrete", ACI Materials Journal, Vol 88, No. 4, pp. 390–399, 1991.
10. Kala Z., "Sensitivity analysis on fatigue behaviour of steel structure under in-plane bending", Nonlinear Analysis: Modelling and Control, Vol 11, No. 1, pp. 33-45, 2006.
11. Marchand J. R. E., Clement F., and Peping., "Deterministic sensitivity analysis for a model for flow in porous media", Advances in Water Resources, Vol 31, No. 8, pp. 1025-1037, 2008.
12. Binici B. and Mosalam K., "Analysis of reinforced concrete columns retrofitted with fiber reinforced polymer lamina", Composites Part B, Vol 38, pp. 265–276, 2008.
13. Hora S. and Helton J.C., "A distribution-free test for the relationship between model input and output when using latin hypercube sampling", Reliability engineering and system safety, Vol 79, No. 3, pp. 333-339, 2003.
14. Sain T. and Chandra Kishen J.M., "Probabilistic assessment of fatigue crack growth in concrete", International Journal of Fatigue, Vol 30, No. 12, pp. 2156-2164, 2008.
15. Anoop M.B. and Balaji Rao K., "Determination of bounds on failure probability in the presence of hybrid uncertainties", Sadhana, Vol 33, No. 6, pp.753-765, 2008.

© 2013 SRESA All rights reserved

Life Cycle Reliability and Safety Engineering
Vol.2 Issue 1 (2013) 52-68

Bounds on Reliability of Structures with Multiple Design Points using MHDMR

A. S. Balu & B. N. Rao*
Structural Engineering Division, Department of Civil Engineering,
Indian Institute of Technology Madras, Chennai, INDIA
e-mail: ***bnrao@iitm.ac.in***

Abstract

To assess the reliability of structures involving both aleatory and epistemic uncertainties, in conjunction with multiple design points, every configuration of the interval variables needs to be explored. To reduce the computational cost involved, this paper presents a novel uncertainty analysis method for estimating the reliability of structural systems involving multiple design points in the presence of mixed uncertain variables. The proposed method involves Multicut-High Dimensional Model Representation technique for the limit state function approximation, transformation technique to obtain the contribution of the fuzzy variables to the convolution integral and fast Fourier transform for solving the convolution integral. In the proposed method, efforts are required in evaluating conditional responses at a selected input determined by sample points, as compared to full scale simulation methods. Therefore, the proposed technique estimates the failure probability accurately with significantly less computational effort compared to the direct Monte Carlo simulation.

Keywords : ***Structural reliability, Multiple design points, High Dimensional Model Representation, Random variables, Fuzzy variables.***

1. Introduction

Reliability analysis taking into account the uncertainties involved in a structural system plays an important role in the analysis and design of structures. Due to the complexity of structural systems the information about the functioning of various structural components has different sources and the failure of systems is usually governed by various uncertainties, all of which are to be taken into consideration for reliability estimation. Uncertainties present in a structural system can be classified as aleatory uncertainty and epistemic uncertainty. Aleatory uncertainty information can be obtained as a result of statistical experiments and has a probabilistic or random character. Epistemic uncertainty information can be obtained by the estimation of the experts and in most cases has an interval or fuzzy character. Therefore, the development of rigorous mathematical methods of combining the existing information for obtaining general estimates of the reliability of the entire structural system represents an actual problem.

When aleatory uncertainty is only present in a structural system, then the reliability estimation involves determination of the probability that a structural response exceeds a threshold limit, defined by a limit state function influenced by several random parameters. Structural reliability can be computed adopting probabilistic method involving the evaluation of multidimensional integral [1, 2]. Broadly two classes of approaches are commonly available for the reliability estimation, which can be labeled as gradient-based and simulation-based methods. In the first case, there is a need of estimating the gradient of the limit state function in a relevant point around which the largest concentration of the probability mass in the failure region can be found. These methods are popularly known as first- or second-order reliability method (FORM/SORM) [1−3]. A crucial point in their application is the need of knowing the limit state function explicitly. But, in reality, the limit state functions are of implicit nature and highly nonlinear. Therefore, a detailed finite element (FE) modeling of the structure is necessary in combination with reliability analysis tools. FE methods for linear and nonlinear structures in conjunction with FORM/SORM have been successfully applied for structural reliability computations [4]. But, such methods are effective in evaluating very small probabilities of failure

© 2013 SRESA All rights reserved

for small-scale problems. In regard to the large-scale problems, merging of FORM/SORM, with commercial FE programs is not straight forward especially when the nonlinear problems are addressed [5].

In addition, the main contribution to the reliability integral comes from the neighbourhood of design points. When multiple design points exist, available optimization algorithms may converge to a local design point and thus erroneously neglect the main contribution to the value of the reliability integral from the global design point(s). Moreover, even if a global design point is obtained, there are cases for which the contribution from other local or global design points may be significant [6]. In that case, multipoint FORM/SORM is required for improving the reliability analysis [7].

In contrast to the gradient-based methods, simulation-based methods [8−10] hinge upon the creation of generating synthetic set of basic random variables samples and simulating the actual limit state function repeated times. The major disadvantages of the Monte Carlo simulation (MCS) are that the results are of a statistical value and the random sampling error will produce inaccuracy within the results. The importance sampling technique [9, 10], a commonly used variance reduction technique, requires an appropriate importance sampling function in order to take full advantage of this method. Sakamoto et al. [11] demonstrated the use of FFT in the probabilistic analysis. In order to use FFT, the limit state function must be separable; hence response surface concept was adopted to get separable and closed form expression of the implicit limit state function [11]. Penmetsa and Grandhi [12], implemented two-point adaptive nonlinear approximation [13] to construct the approximate limit state function and used FFT technique to estimate the failure probability. The High Dimensional Model Representation (HDMR) is used to approximate the limit state function at the MPP and FFT techniques are adopted to evaluate the convolution integral in probabilistic analysis [14]. The first-order HDMR component functions are approximated using linear and quadratic least-squares technique. In this method, efforts are required in evaluating conditional responses at a selected input determined by sample points, as compared to full scale simulation methods.

In the presence of only epistemic uncertainty in a structural system, possibilistic approaches to evaluate the minimum and maximum values of the response are available [15−17]. All the reliability models discussed above are based on only one kind of uncertain information; either random variables or fuzzy input, but do not accommodate a combination of both types of variables. However, in reality, for some engineering problems in which some uncertain parameters are random variables, others are interval or fuzzy variables, using one kind of reliability model cannot obtain the best results. To determine the bounds of reliability of a structural system involving both random and interval or fuzzy variables, every configuration of the interval variables needs to be explored. Hence, the computational effort involved in estimating the bounds of the failure probability increases tremendously in the presence of multiple design points and mixed uncertain variables. Hence there is considerable interest in developing efficient methods for dealing with problems comprising of mixed uncertain variables. Moller et al. [18] presented a methodology for estimating the membership function of the safety index by considering fuzzy randomness using Fuzzy First Order Reliability Method. However the calculation of the failure probability from the safety index values is prone to errors. Adduri and Penmetsa [19] adopted two-point adaptive nonlinear approximation to construct the approximate limit state function using a second order response surface model, and used FFT technique to estimate the bounds on structural reliability in the presence of both random and fuzzy variables. In addition other techniques of combining the probabilistic and non-probabilistic approaches to calculate the structural responses and their bounds can also be found in the literature [20−23].

This paper explores the potential of coupled Multicut-HDMR (MHDMR)-FFT technique in evaluating the reliability of a structural system with multiple design points, for which some uncertainties can be quantified using fuzzy membership functions while some are random in nature. The paper is organized as follows. Section 2 presents a brief overview of HDMR and its applicability to reliability analysis. Section 3 describes the concepts of MHDMR. Section 4 presents the mathematical formulation for obtaining the membership function of failure probability. Section 5 presents three numerical examples to illustrate the performance of the present method. Comparisons have been made with direct MCS method to evaluate the

© 2013 SRESA All rights reserved

accuracy and computational efficiency of the present method.

2. Concept of HDMR and its Application to Reliability Analysis

The fundamental principle underlying the HDMR [24−27] is that, from the perspective of the output/ response, the order of cooperative effects between the independent variables will die off rapidly. The HDMR is generated by expressing system response as a hierarchical, correlated function expansion of a mathematical structure and evaluating each term of the expansion independently. One may show that the system response, which is a function of N input variables, $g(\boldsymbol{x}) = g(x_1, x_2, \ldots, x_N)$, can be expressed as summands of different dimensions:

$$g(\boldsymbol{x}) = g_0 + \sum_{i=1}^{N} g_i(x_i) + \sum_{1 \le i_1 < i_2 \le N} g_{i_1 i_2}(x_{i_1}, x_{i_2}) + \ldots + \sum_{1 \le i_1 < \ldots < i_l \le N} g_{i_1 i_2 \ldots i_l}(x_{i_1}, x_{i_2}, \ldots, x_{i_l}) + \ldots + g_{12\ldots N}(x_1, x_2, \ldots, x_N) \quad (1)$$

where g_0 is a constant term representing the mean response of $g(\boldsymbol{x})$. The function $g_i(x_i)$ describes the independent effect of variable x_i acting alone, although generally nonlinearly, upon the output $g(\boldsymbol{x})$. The function $g_{i_1 i_2}(x_{i_1}, x_{i_2})$ gives pair correlated effect of the variables x_{i_1} and x_{i_2} upon the output $g(\boldsymbol{x})$. The last term $g_{12\ldots N}(x_1, x_2, \ldots, x_N)$ contains any residual correlated behavior over all of the system variables. The expansion functions are determined by evaluating the input-output responses of the system relative to the defined reference point $\boldsymbol{c} = \{c_1, c_2, \ldots, c_N\}$ along associated lines, surfaces, subvolumes, etc. (i.e. cuts) in the input variable space. This process reduces to the following relationship for the component functions in Equation 1.

$$g_0 = g(\boldsymbol{c}) \quad (2)$$

$$g_i(x_i) = g(x_i, \boldsymbol{c}^i) - g_0 \quad (3)$$

$$g_{i_1 i_2}(x_{i_1}, x_{i_2}) = g_{i_1 i_2}(x_{i_1}, x_{i_2}, \boldsymbol{c}^{i_1 i_2}) - g_{i_1}(x_{i_1}) - g_{i_2}(x_{i_2}) - g_0 \quad (4)$$

where the notation $g(x_i, \boldsymbol{c}^i) = g(c_1, c_2, \ldots, c_{i-1}, x_i, c_{i+1}, \ldots, c_N)$ denotes that all the input variables are at their reference point values except x_i. The g_0 term is the output response of the system evaluated at the reference point $\boldsymbol{c}$. The higher order terms are evaluated as cuts in the input variable space through the reference point. Therefore, each first-order term $g_i(x_i)$ is evaluated along its variable axis through the reference point. Each second-order term $g_{i_1 i_2}(x_{i_1}, x_{i_2})$ is evaluated in a plane defined by the binary set of input variables x_{i_1}, x_{i_2} through the reference point, etc. The process of subtracting off the lower order expansion functions removes their dependence to assure a unique contribution from the new expansion function.

Considering terms up to first- and second-order in Equation 1 yields first-order and second-order HDMR approximations of $g(\boldsymbol{x})$ as

$$\tilde{g}(\boldsymbol{x}) = \sum_{i=1}^{N} g(c_1, \ldots, c_{i-1}, x_i, c_{i+1}, \ldots, c_N) - (N-1) g(\boldsymbol{c}) \quad (5)$$

and

$$\tilde{g}(\boldsymbol{x}) = \sum_{\substack{i_1=1, i_2=1 \\ i_1<i_2}}^{N} g(c_1, \ldots, c_{i_1-1}, x_{i_1}, c_{i_1+1}, \ldots, c_{i_2-1}, x_{i_2}, c_{i_2+1}, \ldots, c_N) - (N-2) \sum_{i=1}^{N} g(c_1, \ldots, c_{i-1}, x_i, c_{i+1}, \ldots, c_N) + \frac{(N-1)(N-2)}{2} g(\boldsymbol{c}) \quad (6)$$

respectively. It can also be noted that, compared with FORM (which retains only linear terms) and SORM (which retains only quadratic terms), first- and second-order HDMR respectively, provide more accurate approximation $\tilde{g}(\boldsymbol{x})$ of the original implicit limit state function $g(\boldsymbol{x})$. If first-order HDMR approximation is not sufficient second-order HDMR approximation may be adopted at the expense of additional computational cost.

3. Multicut-HDMR

The main limitation of truncated cut-HDMR expansion is that depending on the order chosen sometimes it is unable to accurately approximate $g(\boldsymbol{x})$, when multiple design points exist on the limit state function or when the problem domain is large. In this section, a new technique based on MHDMR is presented for approximation of the original implicit

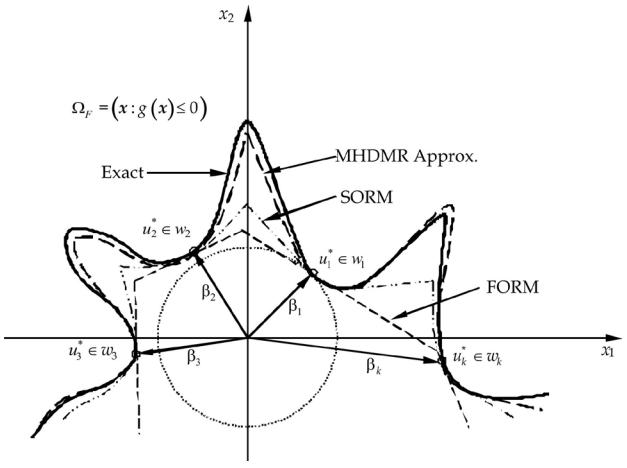

Figure 1: Concept of MHDMR approximation of original limit state/ performance function in conjunction with the weight function

© 2013 SRESA All rights reserved

limit state function, when multiple design points exist. The basic principles of cut-HDMR may be extended to more general cases. MHDMR is one extension where several cut-HDMR expansions at different reference points are constructed, and the original implicit limit state function $g(\boldsymbol{x})$ is approximately represented not by one, but by all cut-HDMR expansions. In the present work, weight function is adopted for identification of multiple reference points closer to the limit surface. The theme of MHDMR approximation of the original implicit limit state function is schematically explained through Figure 1.

Let $\boldsymbol{d}^1, \boldsymbol{d}^2, \ldots, \boldsymbol{d}^{m_d}$ be the m_d identified reference points closer to the limit state function based on the weight function presented later in Section 3.1. The MHDMR approximation of the original implicit limit state function is based on the principles of cut-HDMR expansion, where individual cut-HDMR expansions are constructed at different reference points $\boldsymbol{d}^1, \boldsymbol{d}^2, \ldots, \boldsymbol{d}^{m_d}$ by taking one at a time as follows:

$$g^k(\boldsymbol{x}) = g_0^k + \sum_{i=1}^{N} g_i^k(x_i) + \sum_{1 \le i_1 < i_2 \le N} g_{i_1 i_2}^k(x_{i_1}, x_{i_2}) + \ldots + \sum_{1 \le i_1 < \ldots < i_l \le N} g_{i_1 i_2 \ldots i_l}^k(x_{i_1}, x_{i_2}, \ldots, x_{i_l}) + \ldots + g_{12\ldots N}^k(x_1, x_2, \ldots, x_N); \quad k = 1, 2, \ldots, m_d \tag{7}$$

The original implicit limit state function $g(\boldsymbol{x})$ is approximately represented by blending all locally constructed m_d individual cut-HDMR expansions as follows:

$$g(\boldsymbol{x}) \cong \sum_{k=1}^{m_d} \lambda_k(\boldsymbol{x}) \left[g_0^k + \sum_{i=1}^{N} g_i^k(x_i) + \ldots + g_{12\ldots N}^k(x_1, x_2, \ldots, x_N) \right] \tag{8}$$

The coefficients $\lambda_k(\boldsymbol{x})$ possess the properties:

$$\lambda_k(\boldsymbol{x}) = \begin{cases} 1 & \text{if } \boldsymbol{x} \text{ is in any cut subvolume of the } k\text{-th reference point expansions} \\ 0 & \text{if } \boldsymbol{x} \text{ is in any cut subvolume of other reference point expansions} \end{cases} \tag{9}$$

and

$$\sum_{k=1}^{m_d} \lambda_k(\boldsymbol{x}) = 1 \tag{10}$$

There are a variety of choices to define $\lambda_k(\boldsymbol{x})$ In the present study, the metric distance $\alpha_k(\boldsymbol{x})$ from any sample point to the reference point $\boldsymbol{d}^k; \quad k = 1, 2, \ldots, m_d$

$$\alpha_k(\boldsymbol{x}) = \left[\sum_{i=1}^{N} \left(x_i - d_i^k \right)^2 \right]^{\frac{1}{2}}; \quad d_i^k \equiv k - \text{th reference point} \tag{11}$$

is used to define

$$\lambda_k(\boldsymbol{x}) = \frac{\bar{\lambda}_k(\boldsymbol{x})}{\sum_{s=1}^{m_d} \bar{\lambda}_s(\boldsymbol{x})} \tag{12}$$

where

$$\bar{\lambda}_k(\boldsymbol{x}) = \prod_{s=1;\, s \ne k}^{m_d} \alpha_s(\boldsymbol{x}) \tag{13}$$

The coefficients $\lambda_k(\boldsymbol{x})$ determine the contribution of each locally approximated function to the global function. The properties of the coefficients $\lambda_k(\boldsymbol{x})$ imply that the contribution of all other cut-HDMR expansions vanish except one when $\boldsymbol{x}$ is located on any cut line, plane, or higher dimensional ($\le l$) sub-volumes through that reference point, and then the MHDMR expansion reduces to single point cut-HDMR expansion. As mentioned above, the l-th order cut-HDMR approximation does not have error when $\boldsymbol{x}$ is located on these sub-volumes. When m_d cut-HDMR expansions are used to construct a MHDMR expansion, the error free region in input $\boldsymbol{x}$ space is m_d times that for a single reference point cut-HDMR expansion. Therefore, the accuracy will be improved.

Therefore, the first-order MHDMR approximations of the original implicit limit state function with m_d reference points can be respectively expressed as

$$\tilde{g}(\boldsymbol{x}) \cong \sum_{k=1}^{m_d} \lambda_k(\boldsymbol{x}) \left[\sum_{i=1}^{N} g^k\left(d_1^k, \ldots, d_{i-1}^k, x_i, d_{i+1}^k, \ldots, d_N^k\right) - (N-1)\, g^k\left(\boldsymbol{d}^k\right) \right] \tag{14}$$

and

$$\tilde{g}(\boldsymbol{x}) \cong \sum_{k=1}^{m_d} \lambda_k(\boldsymbol{x}) \left[\begin{array}{l} \sum_{i_1=1, i_2=1; i_1<i_2}^{N} g^k\left(d_1^k, \ldots, d_{i_1-1}^k, x_{i_1}, d_{i_1+1}^k, \ldots, d_{i_2-1}^k, x_{i_2}, d_{i_2+1}^k, \ldots, d_N^k\right) \\ -(N-2) \sum_{i=1}^{N} g^k\left(d_1^k, \ldots, d_{i-1}^k, x_i, d_{i+1}^k, \ldots, d_N^k\right) \\ + \frac{(N-1)(N-2)}{2}\, g^k\left(\boldsymbol{d}^k\right) \end{array} \right] \tag{15}$$

3.1 Weight Function for identification of multiple reference points

The most important part of MHDMR approximation of the original implicit limit state function is identification of multiple reference points closer to the limit state function. The proposed weight function is similar to that used by Kaymaz and McMahon [28] for weighted regression analysis. Among the limit state function responses at all sample points, the most likelihood point is selected based on

© 2013 SRESA All rights reserved

closeness to zero value, which indicates that particular sample point is close to the limit state function.

In this study two types of procedures are adopted for identification of reference points closer to the limit state function, namely: (1) first-order method, and (2) second-order method. The procedure for identification of reference points closer to the limit state function using first-order method proceeds as follows: (a) n $(=3,5,7 \text{ or } 9)$ equally spaced sample points $\mu_i-(n-1)\sigma_i/2$, $\mu_i-(n-3)\sigma_i/2$, …, μ_i, …, $\mu_i+(n-3)\sigma_i/2$ $\mu_i+(n-1)\sigma_i/2$ are deployed along each of the random variable axis x_i with mean μ_i and standard deviation σ_i, through an initial reference point. Initial reference point is taken as mean value of the random variables; (b) The limit state function is evaluated at each sample point; (c) Using the limit state function responses at all sample points, the weight corresponding to each sample point is evaluated using the following weight function,

$$w^I = \exp\left(-\frac{g(c_1,\ldots,c_{i-1},x_i,c_{i+1},\ldots,c_N)-g(\boldsymbol{x})\big|_{\min}}{\left|g(\boldsymbol{x})\big|_{\min}\right|}\right) \quad (16)$$

Second-order method of identification of reference points closer to the limit state function, proceeds as follows: (a) A regular grid is formed by taking n $(=3,5,7 \text{ or } 9)$ equally spaced sample points $\mu_{i_1}-(n-1)\sigma_{i_1}/2$, $\mu_{i_1}-(n-3)\sigma_{i_1}/2$, …, μ_{i_1}, …, $\mu_{i_1}+(n-3)\sigma_{i_1}/2$, $\mu_{i_1}+(n-1)\sigma_{i_1}/2$ along the random variable x_{i_1} axis with mean μ_{i_1} and standard deviation σ_{i_1}, and n $(=3,5,7 \text{ or } 9)$ equally spaced sample points $\mu_{i_2}-(n-1)\sigma_{i_2}/2$, $\mu_{i_2}-(n-3)\sigma_{i_2}/2$, …, μ_{i_2}, …, $\mu_{i_2}+(n-3)\sigma_{i_2}/2$, $\mu_{i_2}+(n-1)\sigma_{i_2}/2$ along the random variable x_{i_2} axis with mean μ_{i_2} and standard deviation σ_{i_2}, through an initial reference point. Initial reference point is taken as mean value of the random variables; (b) The limit state function is evaluated at each sample point; (c) Using the limit state function responses at all sample points, the weight corresponding to each sample point is evaluated using the following weight function,

$$w^{II} = \exp\left(-\frac{g(c_1,\ldots,c_{i_1-1},x_{i_1},c_{i_1+1},\ldots,c_{i_2-1},x_{i_2},c_{i_2+1},\ldots,c_N)-g(\mathbf{x})\big|_{\min}}{\left|g(\mathbf{x})\big|_{\min}\right|}\right) \quad (17)$$

Sample points $\boldsymbol{d}^1,\boldsymbol{d}^2,\ldots,\boldsymbol{d}^{m_d}$ with maximum weight are selected as reference points closer to the limit state function, for construction of m_d individual cut-HDMR approximations of the original implicit limit state function locally.

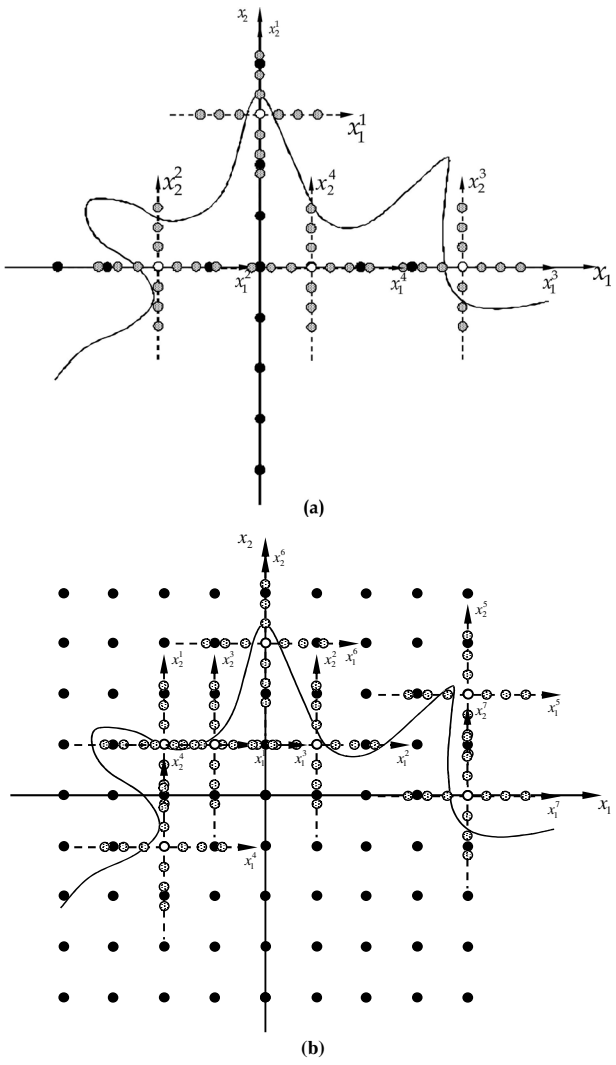

Figure 2: MHDMR approximation of original limit state/ performance function; with (a) FF sampling scheme; and (b) SF sampling scheme

3.2 Sampling schemes

In this study, two types of sampling schemes, namely FF and SF are adopted, which are schematically illustrated in Figures 2(a) and 2(b).

Figure 2(a) shows FF sampling scheme involving first-order method of identification of reference points closer to the limit state function and blending of locally constructed individual first-order HDMR approximations of the original implicit limit state function at different identified reference points $\boldsymbol{d}^1,\boldsymbol{d}^2,\ldots,\boldsymbol{d}^{m_d}$ using the coefficients $\lambda_k(\boldsymbol{x})$ to form MHDMR approximation $\tilde{g}(\boldsymbol{x})$ of $g(\boldsymbol{x})$ using Equation 14. Figure 2(b) shows SF sampling scheme involving second-order method of identification of reference points closer to the limit state function

© 2013 SRESA All rights reserved

and blending of locally constructed individual first-order HDMR approximations of the original implicit limit state function at different identified reference points $\boldsymbol{d}^1, \boldsymbol{d}^2, \ldots, \boldsymbol{d}^{m_d}$ using the coefficients $\lambda_k(\boldsymbol{x})$ to form MHDMR approximation $\tilde{g}(\boldsymbol{x})$ of $g(\boldsymbol{x})$ using Equation 14.

4. Estimation of Failure Probability Bounds in Presence of Mixed Uncertain Variables

Let $\boldsymbol{x} = \{x_1, x_2, \ldots, x_N\}$ be the N −dimensional input variables vector, which comprises of r number of random variables and f number of fuzzy variables with $N = r + f$. The first-order HDMR approximation of $g(\boldsymbol{x})$ can be divided into three parts, the first part with only the random variables, the second part with only the fuzzy variables and the third part is a constant which is the output response of the system evaluated at the reference point, as follows

$$\tilde{g}(\boldsymbol{x}) \cong \sum_{i=1}^{r} g(x_i, \boldsymbol{c}^i) + \sum_{i=r+1}^{N} g(x_i, \boldsymbol{c}^i) - (N-1) g(\boldsymbol{c}) \quad (18)$$

The joint membership function of the fuzzy variables part is obtained using suitable transformation of the variables and interval arithmetic algorithm. Using this approach, the minimum and maximum values of the fuzzy variables part are obtained at each α -cut.

To obtain the approximation of the first-order HDMR component functions of fuzzy variables part of the nonlinear limit state function in Equation 18, n sample points x_{iL}, $x_{iM} - (n-3)(x_{iM} - x_{iL})/(n-1)$ $x_{iM} - (n-5)(x_{iM} - x_{iL})/(n-1)$, … , x_{iM} , … , $x_{iM} + (n-5)(x_{iU} - x_{iM})/(n-1)$, $x_{iM} + (n-3)(x_{iU} - x_{iM})/(n-1)$, x_{iU} are deployed along axis of each of the fuzzy variable x_i having triangular membership function with the triplet number $[x_{iL}, x_{iM}, x_{iU}]$. Similarly, n sample points $\mu_i - (n-1)\sigma_i/2$, $\mu_i - (n-3)\sigma_i/2$, …, μ_i, …, $\mu_i + (n-3)\sigma_i/2$, $\mu_i + (n-1)\sigma_i/2$ are deployed along axis of each of the random variable x_i with mean μ_i and standard deviation σ_i.

Using the bounds of the fuzzy variables part at each α -cut along with the constant part and the random variables part (which now depends on $\{x_1, x_2, \ldots, x_r\} \in \Re^r$ alone), the joint density functions are obtained by (i) identifying the reference points $\boldsymbol{d}^1, \boldsymbol{d}^2, \ldots, \boldsymbol{d}^{m_d} \in \Re^r$ closer to the limit state function and (ii) blending of locally constructed individual first-order HDMR approximations in the rotated Gaussian space at different identified reference points using the coefficients $\lambda_k(x_1, x_2, \ldots, x_r)$ to form global approximation, and (iii) performing the convolution using FFT, which upon integration yields the bounds of the failure probability. As an alternative the bounds of the failure probability can also be obtained by performing MCS on the global approximation in the original $\{x_1, x_2, \ldots, x_r\} \in \Re^r$ space, obtained by blending of locally constructed individual first-order HDMR approximations of the original limit state function at different identified reference points.

4.1 Transformation of interval variables

Optimization techniques are required to obtain the minimum and maximum values of a nonlinear response within the bounds of the interval variables. This procedure is computationally expensive for problems with implicit limit state functions, as optimization requires the function value and gradient information at several points in the iterative process. But, if the function is expressed as a linear combination of interval variables, then the bounds of the response can be expressed as the summation of the bounds of the individual variables. Therefore, fuzzy variables part of the nonlinear limit state function in Equation 18 is expressed as a linear combination of intervening variables by the use of first-order HDMR approximation in order to apply an interval arithmetic algorithm, as follows

$$\sum_{i=r+1}^{N} g(x_i, \boldsymbol{c}^i) = z_1 + z_2 + \ldots + z_f \quad (19)$$

where $z_i = (\beta_i x_i + \gamma_i)^{\kappa}$ is the relation between the intervening and the original variables with κ being order of approximation taking values $\kappa = 1$ for linear approximation, $\kappa = 2$ for quadratic approximation, $\kappa = 3$ for cubic approximation, and so on. The bounds of the intervening variables can be determined using transformations. If the membership functions of the intervening variables are available, then at each α -cut, interval arithmetic techniques can be used to estimate the response bounds at that level.

4.2 Estimation of failure probability bounds using FFT

The concept of FFT can be applied to the problem if the limit state function is in the form of a linear combination of independent variables and when either the marginal density or the characteristic function of each basic random variable is known. To achieve this linear function, HDMR concepts are used to express the random variables part of the nonlinear limit state function along with the values of the constant

© 2013 SRESA All rights reserved

part and the fuzzy variables part at each α-cut, which depends on $\{x_1, x_2, \ldots, x_r\} \in \Re^r$, as a linear combination of lower order component functions. The steps involved in the proposed method for failure probability estimation are as follows:

(i) If $\boldsymbol{u} = \{u_1, u_2, \ldots, u_r\}^T \in \Re^r$ is the standard Gaussian variable, let $\boldsymbol{u}^{k*} = \{u_1^{k*}, u_2^{k*}, \ldots, u_r^{k*}\}^T$ be the MPP or design point, determined by a standard nonlinear constrained optimization. The MPP has a distance β_{HL}, which is commonly referred to as the Hasofer–Lind reliability index. Construct an orthogonal matrix $\boldsymbol{R} \in \Re^{r \times r}$ whose r–th column is $\boldsymbol{\alpha}^{k*} = \boldsymbol{u}^{k*}/\beta_{HL}$, i.e., $\mathbf{R} = [\mathbf{R}_1 \,|\, \boldsymbol{\alpha}^{k*}]$ where $\boldsymbol{R}_1 \in \Re^{r \times r-1}$ satisfies $\boldsymbol{\alpha}^{k*T} \boldsymbol{R}_1 = 0 \in \Re^{1 \times r-1}$. The matrix $\boldsymbol{R}$ can be obtained, for example, by Gram–Schmidt orthogonalization. For an orthogonal transformation $\boldsymbol{u} = \boldsymbol{R}\boldsymbol{v}$. Let $\boldsymbol{v} = \{v_1, v_2, \ldots, v_r\}^T \in \Re^r$ be the rotated Gaussian space with the associated MPP $\boldsymbol{v}^{k*} = \{v_1^{k*}, v_2^{k*}, \ldots, v_r^{k*}\}^T$. The transformed limit state function $g(\boldsymbol{v})$ therefore maps the random variables part along with the values of the constant part and the fuzzy variables part at each α-cut, into rotated Gaussian space $\boldsymbol{v}$.

(ii) The first-order HDMR approximation of $g(\boldsymbol{v})$ in the rotated Gaussian space $\boldsymbol{v}$ with $\boldsymbol{v}^{k*} = \{v_1^{k*}, v_2^{k*}, \ldots, v_r^{k*}\}^T$ as reference point can be represented as follows:

$$\tilde{g}^k(\boldsymbol{v}) \equiv g^k(v_1, v_2, \ldots, v_r) = \sum_{i=1}^{r} g^k\left(v_1^{k*}, \ldots, v_{i-1}^{k*}, v_i, v_{i+1}^{k*}, \ldots, v_r^{k*}\right) - (r-1)\, g\left(\boldsymbol{v}^{k*}\right) \quad (20)$$

(iii) In addition to the MPP as the chosen reference point, the accuracy of first-order HDMR approximation in Equation 20 may depend on the orientation of the first $r-1$ axes. In the present work, the orientation is defined by the matrix $\boldsymbol{R}$. The terms $g^k\left(v_1^{k*}, \ldots, v_{i-1}^{k*}, v_i, v_{i+1}^{k*}, \ldots, v_r^{k*}\right)$ are the individual component functions and are independent of each other. Equation 20 can be rewritten as,

$$\tilde{g}^k(\boldsymbol{v}) = a^k + \sum_{i=1}^{r} g^k\left(v_i, \boldsymbol{v}^{k*^i}\right) \quad (21)$$

where $a^k = -(r-1)\, g(\boldsymbol{v}^{k*})$.

(iv) New intermediate variables are defined as

$$y_i^k = g^k\left(v_i, \boldsymbol{v}^{k*^i}\right) \quad (22)$$

The purpose of these new variables is to transform the approximate function into the following form

$$\tilde{g}^k(\boldsymbol{v}) = a^k + y_1^k + y_2^k + \cdots + y_r^k \quad (23)$$

(v) Due to the rotational transformation in v-space, the component functions y_i^k in Equation 23 are expected to be linear or weakly nonlinear function of random variables v_i. In this work both linear and quadratic approximations of y_i^k are considered.

(vi) The linear and quadratic approximations are considered as $y_i^k = b_i + c_i v_i$ and $y_i^k = b_i + c_i v_i + e_i v_i^2$ respectively. The coefficients $b_i \in \Re$, $c_i \in \Re$ and $e_i \in \Re$ (non-zero) are obtained by least-squares approximation from exact or numerically simulated conditional responses $\left\{g^k(v_i^1, \boldsymbol{v}^{k*^i}), g^k(v_i^2, \boldsymbol{v}^{k*^i}), \ldots, g^k(v_i^n, \boldsymbol{v}^{k*^i})\right\}^T$ at n sample points along the variable axis v_i. Then Equation 20 results in

$$\tilde{g}^k(\boldsymbol{v}) \equiv a^k + y_1^k + y_2^k + \cdots + y_r^k = a^k + \sum_{i=1}^{r} (b_i + c_i v_i) \quad (24)$$

and,

$$\tilde{g}^k(\boldsymbol{v}) \equiv a^k + y_1^k + y_2^k + \cdots + y_r^k = a^k + \sum_{i=1}^{r} (b_i + c_i v_i + e_i v_i^2) \quad (25)$$

(vii) The global approximation is formed by blending of locally constructed individual first-order HDMR approximations in the rotated Gaussian space at different identified reference points using the coefficients λ_k.

$$\tilde{g}(\boldsymbol{v}) = \sum_{k=1}^{m_d} \lambda_k \tilde{g}^k(\boldsymbol{v}) \quad (26)$$

(viii) Since v_i follows standard Gaussian distribution, marginal density of the intermediate variables y_i can be easily obtained by simple transformation (using chain rule).

$$p_{Y_i}(y_i) = p_{V_i}(v_i) \left| dv_i / dy_i \right| \quad (27)$$

(ix) Now the approximation is a linear combination of the intermediate variables y_i. Therefore, the joint density of $\tilde{g}(\boldsymbol{v})$, which is the convolution of the individual marginal density of the intervening variables y_i, can be expressed as follows:

$$p_{\tilde{G}}(\tilde{g}) = p_{Y_1}(y_1) * p_{Y_2}(y_2) * \ldots * p_{Y_r}(y_r) \quad (28)$$

where $p_{\tilde{G}}(\tilde{g})$ represents the joint density of the transformed limit state function $\tilde{g}(\boldsymbol{v})$.

(x) Applying FFT on both sides of Equation 28, leads to

© 2013 SRESA All rights reserved

$$FFT\left[p_{\tilde{G}}(\tilde{g})\right] = FFT\left[p_{Y_1}(y_1)\right] \cdot FFT\left[p_{Y_2}(y_2)\right] \ldots FFT\left[p_{Y_r}(y_r)\right] \quad (29)$$

(xi) By applying inverse FFT on both side of Equation 29, the joint density of the limit state function $\tilde{g}(\boldsymbol{v})$ is obtained.

(xii) The probability of failure is given by the following equation

$$P_F = \int_{-\infty}^{0} p_{\tilde{G}}(\tilde{g}) d\tilde{g} \quad (30)$$

(xiii) The membership function of failure probability can be obtained by repeating the above procedure at all confidence levels of the fuzzy variables part.

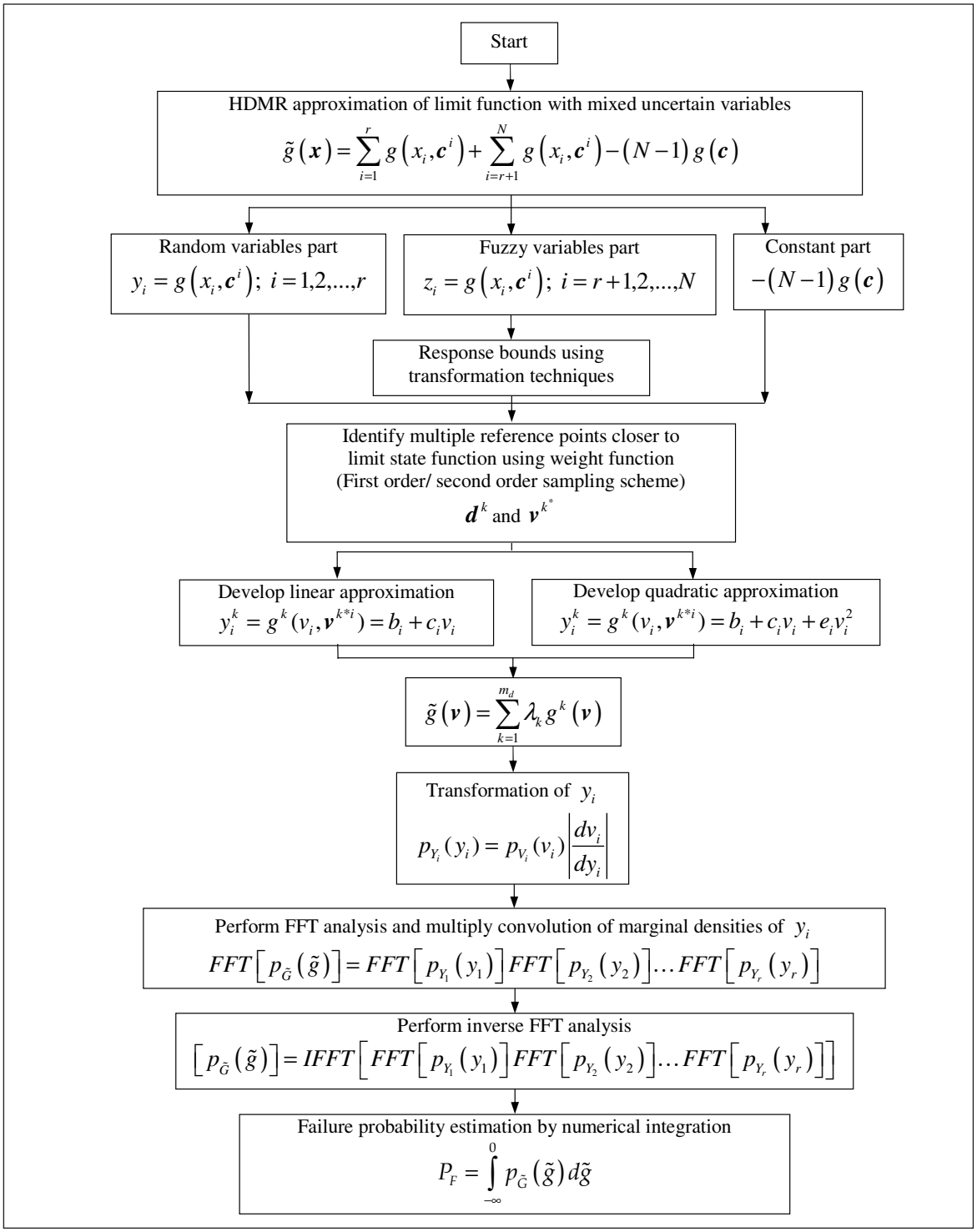

Figure 3: Flowchart of Coupled MHDMR−FFT based reliability analysis

© 2013 SRESA All rights reserved

A flow diagram for MHDMR approximation with multiple reference points closer to the limit state function, and estimation of membership function of failure probability P_F by performing the convolution using FFT in conjunction with linear and quadratic approximations is shown in Figure 3.

4.3. Estimation of failure probability bounds using MCS

The failure probability can be easily estimated by performing MCS on the MHDMR approximation $\tilde{g}(\boldsymbol{x})$ of the original implicit limit state function $g(\boldsymbol{x})$ and is given by

$$P_F = \frac{1}{N_S}\sum_{i=1}^{N_S} \mathcal{I}\left[\tilde{g}\left(\boldsymbol{x}^i\right) < 0\right] \tag{31}$$

where $\boldsymbol{x}^i$ is i^{th} realization of X, N_S is the sampling size, $\mathcal{I}[.]$ is a deciding function of fail or safe state such that $\mathcal{I} = 1$, if $\tilde{g}(\boldsymbol{x}^i) < 0$ otherwise zero. A flow diagram for the MHDMR approximation with multiple reference points closer to the limit state/performance function, and estimation of membership function of failure

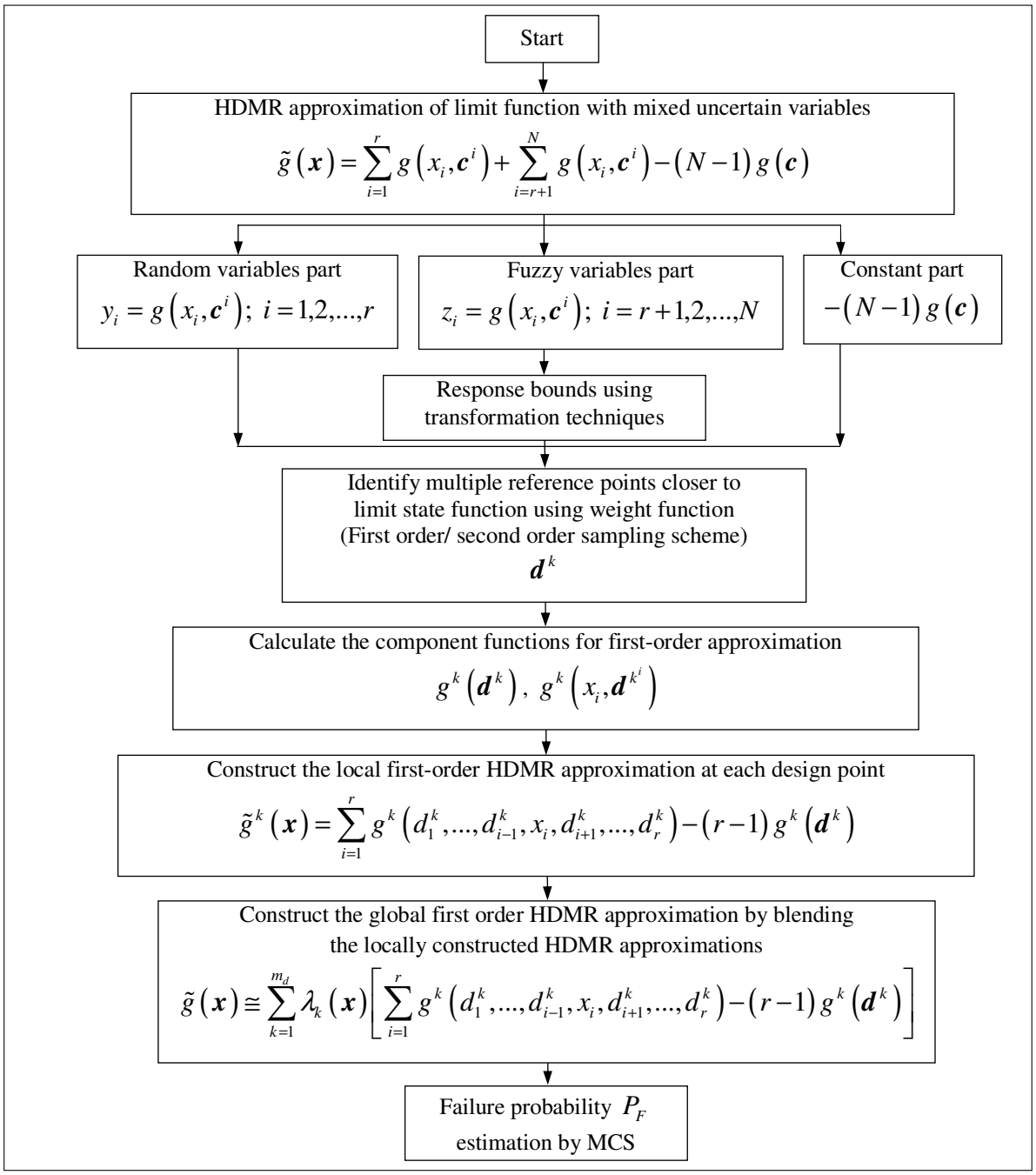

Figure 4: Flowchart of Coupled MHDMR−MCS based reliability analysis

© 2013 SRESA All rights reserved

probability P_F by performing MCS on the global approximation is shown in Figure 4.

4.4 Computational effort

If N, f, n, m, m_d and N_S respectively denote the number of uncertain variables, the number of fuzzy variables, the number of sample points taken along each of the variable axis, the number of α-cuts, the number of identified design points and the sampling size required for MCS, then using the first-order HDMR approximation the total cost of original function evaluation entails a maximum of $m_d\left(N\times(n-1)+1\right)$ by the proposed method. It can be easily verified that the total computational cost of the proposed method is far less than $(m\cdot 2^f+1)N_S$ number of function evaluations required for the crude method involving the MCS, especially for large finite element models. As a few low order component functions of HDMR are used, the sample savings due to HDMR are significant compared to traditional sampling. Hence the reliability analysis using HDMR relies on an accurate reduced model being generated with a small number of full model simulations. This clearly demonstrates the computational efficiency of the proposed formulations. The efficiency and robustness of the proposed method is expected to increase with increase in the complexity of the structure, number of fuzzy variables and number of α-cuts.

5. Numerical Examples

Three numerical examples involving explicit hypothetical mathematical functions and implicit functions from structural mechanics problems are presented to illustrate the performance of the present method. To evaluate the accuracy and the efficiency of the present method, comparisons of the estimated membership function of the failure probability P_F, both by performing the convolution using FFT and MCS on the global approximation, have been made with that obtained using direct MCS. The coefficient of variation (COV) δ of the estimated failure probability P_F by direct MCS for the sampling size N_S considered, is computed using

$$\delta=\sqrt{\frac{\left(1-P_F\right)}{N_S P_F}} \tag{32}$$

When comparing computational efforts by various methods in evaluating the failure probability P_F, the number of original limit state function evaluations is chosen as the primary comparison tool in this paper. This is because of the fact that, number of function evaluations indirectly indicates the CPU time usage. For direct MCS, number of original function evaluations is same as the sampling size. While evaluating the failure probability P_F through direct MCS, CPU time is more because it involves number of repeated actual finite-element analysis.

5.1 Parabolic performance function

The limit state function considered is a parabola of the form:

$$g\left(\boldsymbol{x}\right)=-x_1^2-x_2+x_3 \tag{33}$$

where x_1 and x_2 are assumed to be independent standard normal variables. The variable x_3 is assumed to be fuzzy with triangular membership function having the triplet [5.0, 7.0, 9.0].

The initial reference point $\boldsymbol{c}$ is taken as respectively the mean values and nominal values of the random and fuzzy variables. The first-order HDMR approximation, which is constructed over the initial reference point, is divided into two parts, one with only the random variables, and the other with the fuzzy variables. The joint membership function of the fuzzy part of limit state function is obtained using suitable transformation of the fuzzy variables. In this example, the joint membership function is same as the membership function of the fuzzy variable x_3. As shown in Figure 5, the limit state function given by Equation 33 is symmetric about x_2 for given value of x_3 (say the nominal value of $x_3=7$ at $\alpha=1$), and has two design points. The two actual design points of the limit state function shown in Figure 5, obtained using recursive quadratic programming (RQP) algorithm [29] are (2.54, 0.49) and (−2.54, 0.49) with reliability indices $\beta_1=\beta_2=2.588$.

Table 1 illustrates computational details and identification of reference points $\boldsymbol{d}^1,\boldsymbol{d}^2$ using FF sampling scheme with five equally spaced sample points ($n=5$) along each of the variable axis. In Table 1 the values corresponding to $\alpha=0^{(L)}$ and $\alpha=0^{(R)}$ respectively indicate the extreme left and right values of the limit state function $g(\boldsymbol{x})$ at zero confidence level (ie $\alpha=0$). Table 1 shows two reference points $\boldsymbol{d}^1=(2,0)$ and $\boldsymbol{d}^2=(-2,0)$ closer to the function (obtained using the bounds of the fuzzy variables part at each α-cut and the random variables part in Equation 18) producing maximum weight (obtained using Equation 16). After identification of the two reference points (2, 0) and (−2, 0), local individual first-order HDMR approximations of the original limit

© 2013 SRESA All rights reserved

Table1: Identification of multiple design points with FF sampling

Sample points		$g(\boldsymbol{x})$			$g(\boldsymbol{x})\|_{\min}$			w^I		
x_1	x_2	$\alpha=0^{(L)}$	$\alpha=1$	$\alpha=0^{(R)}$	$\alpha=0^{(L)}$	$\alpha=1$	$\alpha=0^{(R)}$	$\alpha=0^{(L)}$	$\alpha=1$	$\alpha=0^{(R)}$
−2.0	0.0	1.00	3.00	5.00				1.000	1.000	1.000
−1.0	0.0	4.00	6.00	8.00				0.050	0.368	0.549
0.0	0.0	5.00	7.00	9.00				0.018	0.264	0.449
1.0	0.0	4.00	6.00	8.00				0.050	0.368	0.549
2.0	0.0	1.00	3.00	5.00	1.0	3.0	5.0	1.000	1.000	1.000
0.0	−2.0	7.00	9.00	11.00				0.002	0.135	0.301
0.0	−1.0	6.00	8.00	10.00				0.001	0.189	0.368
0.0	0.0	5.00	7.00	9.00				0.018	0.264	0.449
0.0	1.0	4.00	6.00	8.00				0.050	0.368	0.549
0.0	2.0	3.00	5.00	7.00				0.135	0.513	0.670

Table 2: Identification of multiple design points with SF sampling

Sample points		$g(\boldsymbol{x})$			$g(\boldsymbol{x})\|_{\min}$			w^{II}		
x_1	x_2	$\alpha=0^{(L)}$	$\alpha=1$	$\alpha=0^{(R)}$	$\alpha=0^{(L)}$	$\alpha=1$	$\alpha=0^{(R)}$	$\alpha=0^{(L)}$	$\alpha=1$	$\alpha=0^{(R)}$
−2.0	−2.0	3.00	5.00	7.00				0.018	0.018	0.264
−1.0	−2.0	6.00	8.00	10.00				0.001	0.001	0.097
0.0	−2.0	7.00	9.00	11.00				0.000	0.000	0.069
1.0	−2.0	6.00	8.00	10.00				0.001	0.001	0.097
2.0	−2.0	3.00	5.00	7.00				0.018	0.018	0.264
−2.0	−1.0	2.00	4.00	6.00				0.050	0.050	0.368
−1.0	−1.0	5.00	7.00	9.00				0.002	0.002	0.135
0.0	−1.0	6.00	8.00	10.00				0.001	0.001	0.097
1.0	−1.0	5.00	7.00	9.00				0.002	0.002	0.135
2.0	−1.0	2.00	4.00	6.00				0.050	0.050	0.368
−2.0	0.0	1.00	3.00	5.00				0.135	0.135	0.513
−1.0	0.0	4.00	6.00	8.00				0.007	0.007	0.189
0.0	0.0	5.00	7.00	9.00	−1.0	1.0	3.0	0.002	0.002	0.135
1.0	0.0	4.00	6.00	8.00				0.007	0.007	0.189
2.0	0.0	1.00	3.00	5.00				0.135	0.135	0.513
−2.0	1.0	0.00	2.00	4.00				0.368	0.368	0.717
−1.0	1.0	3.00	5.00	7.00				0.018	0.018	0.264
0.0	1.0	4.00	6.00	8.00				0.007	0.007	0.189
1.0	1.0	3.00	5.00	7.00				0.018	0.018	0.264
2.0	1.0	0.00	2.00	4.00				0.368	0.368	0.717
−2.0	2.0	−1.00	1.00	3.00				1.000	1.000	1.000
−1.0	2.0	2.00	4.00	6.00				0.050	0.050	0.368
0.0	2.0	3.00	5.00	7.00				0.018	0.018	0.264
1.0	2.0	2.00	4.00	6.00				0.050	0.050	0.368
2.0	2.0	−1.00	1.00	3.00				1.000	1.000	1.000

© 2013 SRESA All rights reserved

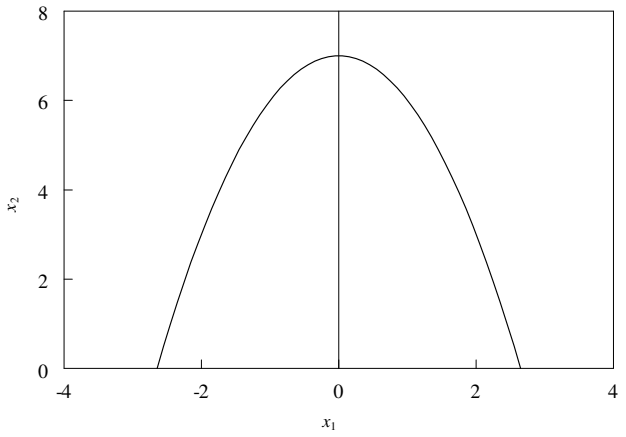

Figure 5: Limit state function of parabolic performance function

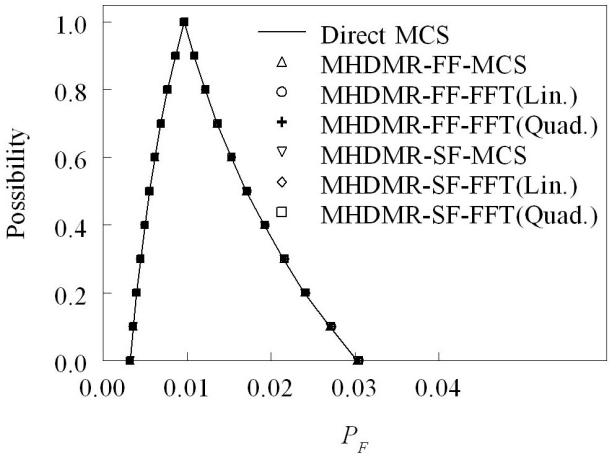

Figure 6: Membership function of failure probability for parabolic limit state function

state function are constructed at the two reference points by deploying $n = 5$ sample points along each of the variable axis. Local approximations of the original limit state function are blended together to form global approximation. The bounds of the failure probability are obtained both by performing the convolution using FFT in conjunction with linear and quadratic approximations, and MCS on the global approximation.

Figure 6 shows the membership function of the failure probability P_F estimated both by performing the convolution using FFT in conjunction with linear and quadratic approximations, and MCS on the global approximation, as well as that obtained using direct MCS. The COV (computed using Equation 32) of the lower and upper bounds of the failure probability P_F obtained using direct MCS, corresponding to $N_S = 10^6$ at zero confidence (α-cut) level are 0.01761 and 0.00566.

In addition, effect of SF sampling scheme on the estimated membership function of the failure probability P_F is studied, and Table 2 presents computational details and identification of reference points closer to the limit state function using SF sampling scheme. Table 2 shows two reference points $\boldsymbol{d}^1 = (-2, 2)$ and $\boldsymbol{d}^2 = (2, 2)$ closer to the function (obtained using the bounds of the fuzzy variables part at each α-cut and the random variables part in Equation 18) producing maximum weight (obtained using Equation 17). The bounds of the failure probability are obtained. Figure 6 also shows the membership function of the failure probability estimate obtained by the proposed method based on SF sampling scheme.

The effect of number of sample points is studied by varying n from 3 to 9. When compared with direct MCS, maximum absolute error in the membership function of failure probability estimated both by performing the convolution using FFT in conjunction with linear and quadratic approximations, and MCS on the global approximation is tabulated in Table 3. The computational effort in terms of number of function evaluations for various methods is tabulated in Table 4.

Tables 3 and 4 clearly demonstrate the computational efficiency of the proposed methodology. It is observed that $n = 7$ provides the optimum number of function calls with acceptable accuracy in evaluating the failure probability with the present method.

5.2 Cantilever steel beam

A cantilever steel beam of 1.0 m with cross-sectional dimensions of (0.1 × 0.01) m is considered as shown in Figure 7, to examine the accuracy and efficiency of the proposed method for the membership function of failure probability estimation. The beam is subjected to an in-plane moment at the free end and a concentrated load at 0.4 m from the free end. The structure is assumed to have failed if the square of the von Mises stress at the support (at A in Figure 7) exceeds specified threshold $V_{\max}$. Therefore, the limit state function is defined as

$$g(\boldsymbol{x}) = V_{\max} - V(\boldsymbol{x}) \tag{34}$$

where $V(\boldsymbol{x})$ is the square of the von Mises stress, expressed as a quadratic operator on the stress vector.

In this example, loads x_1 and x_2, modulus of elasticity of the beam E and threshold quantity $V_{\max}$ are taken as uncertain variables. The variations of

© 2013 SRESA All rights reserved

Table 3: Maximum absolute error (%) (Parabolic function)

Method	$n=3$	$n=5$	$n=7$	$n=9$
MHDMR-FF-MCS	0	0	0	0
MHDMR-FF-FFT-Lin.	1.1047	1.1047	1.1047	1.1047
MHDMR-FF-FFT-Quad.	0.6683	0.6683	0.6683	0.6683
MHDMR-SF-MCS	0	0	0	0
MHDMR-SF-FFT-Lin.	1.1047	1.1047	1.1047	1.1047
MHDMR-SF-FFT-Quad.	0.6683	0.6683	0.6683	0.6683

Table 4: No. of function evaluations (Parabolic function)

Method	$n=3$	$n=5$	$n=7$	$n=9$
Direct MCS	21×10^6	21×10^6	21×10^6	21×10^6
MHDMR-FF-MCS	15	27	39	51
MHDMR-FF-FFT-Lin.	19	43	75	115
MHDMR-FF-FFT-Quad.	15	27	39	51
MHDMR-SF-MCS	15	27	39	51
MHDMR-SF-FFT-Lin.	19	43	75	115
MHDMR-SF-FFT-Quad.	19	43	75	115

E and $V_{\max}$ are expressed as $E = E_0\left(1+\varepsilon\, x_3\right)$ and $V_{\max} = V_{\max 0}\left(1+\varepsilon\, x_4\right)$. Here, ε is small deterministic quantity representing the coefficient of variation of the random variables and are taken to equal to 0.05, $E_0 = 2\times10^5$ N/m^2 denotes the deterministic component of modulus of elasticity and $V_{\max 0} = 6.15\times10^9$ N/m^2 denotes the deterministic component of threshold quantity. All variables are assumed to be independent. The properties of the mixed uncertain variables are defined in Table 5.

Table 5: Properties of the uncertain variables (Cantilever beam)

Uncertain variable	Type of variable			
	Random			Fuzzy
	Mean	Std. Dev.	Distribution type	
x_1	1	1	Normal	
x_2	0	1	Normal	
x_3				[0.0 2.0 4.0]
x_4				[0.0, 0.1, 0.2]

The limit state function given in Equation 34 is approximated using first-order HDMR by deploying $n=5$ sample points along each of the variable axis and taking respectively the mean values and nominal values of the random and fuzzy variables as initial reference point (1.0, 0.0, 2.0, 0.1). The approximated limit state function is divided into two parts, one with only the random variables along with the value of the constant part, and the other with the fuzzy variables. The joint membership function of the fuzzy part of approximated limit state function is obtained using suitable transformation of the fuzzy variables.

Using FF sampling scheme the sample point $\boldsymbol{d} = (1,-2)$ is identified as reference point closer to the limit state function producing maximum weight. In this case since only one reference point is identified, local approximation is same as the global approximation. The bounds of the failure probability are obtained both by performing the convolution using FFT in conjunction with linear and quadratic approximations, and MCS on the global approximation.

Figure 8 shows the membership function of the failure probability estimated both by performing the convolution using FFT in conjunction with linear and quadratic approximations, and MCS on the global approximation, as well as that obtained using direct MCS. The COV of the lower and upper bounds of the failure probability obtained using direct MCS, corresponding to $N_S = 10^6$ at zero confidence level are 0.31623 and 0.00361.

In addition the membership function of the failure probability obtained by the proposed method based on SF sampling scheme is also shown in Figure 8. The effect of number of sample points is studied by varying *n* from 3 to 9. When compared with direct MCS, maximum absolute

© 2013 SRESA All rights reserved

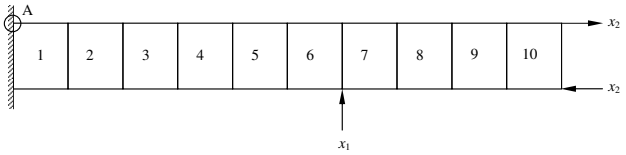

Figure 7: Cantilever steel beam

error in the membership function of the failure probability estimated both by performing the convolution using FFT in conjunction with linear and quadratic approximations, and MCS on the global approximation is tabulated in Table 6. The computational effort is tabulated in Table 7.

Table 6: Maximum absolute error (%) (Cantilever beam)

Method	$n=3$	$n=5$	$n=7$	$n=9$
MHDMR-FF-MCS	8.3333	1.0909	1.0909	1.0909
MHDMR-FF-FFT-Lin.	6.1174	1.0068	1.0068	1.0068
MHDMR-FF-FFT-Quad.	3.7651	0.8680	0.8680	0.8680
MHDMR-SF-MCS	5.000	0.9091	0.9091	0.9091
MHDMR-SF-FFT-Lin.	2.1744	0.6785	0.6785	0.6785
MHDMR-SF-FFT-Quad.	1.8639	0.4993	0.4993	0.4993

Table 7: No. of function evaluations (Cantilever beam)

Method	$n=3$	$n=5$	$n=7$	$n=9$
Direct MCS	21×10^6	21×10^6	21×10^6	21×10^6
MHDMR-FF-MCS	10	18	26	34
MHDMR-FF-FFT-Lin.	14	34	62	98
MHDMR-FF-FFT-Quad.	10	18	26	34
MHDMR-SF-MCS	10	18	26	34
MHDMR-SF-FFT-Lin.	14	34	62	98
MHDMR-SF-FFT-Quad.	14	34	62	98

Tables 6 and 7 clearly demonstrate the computational efficiency of the proposed methodology. It is observed that $n=7$ provides the optimum number of function calls with acceptable accuracy in evaluating the failure probability with the present method.

5.3. 80-bar 3D-truss structure

A 3D-truss, shown in Figure 9, is considered in this example to examine the accuracy and efficiency of the proposed method for the membership function of failure probability estimation. The loads at various levels are considered to be random while the cross-sectional areas of the angle sections at various levels are assumed to be fuzzy as given in Table 8. The maximum horizontal displacement at the top of the tower is considered to be the failure criterion, as given below.

$$g(\boldsymbol{x}) = \Delta_{\text{lim}} - \Delta(\boldsymbol{x}), \tag{35}$$

The limiting deflection Δ_{lim} is assumed to be 0.15 m. The limit state function given in Equation 35 is approximated using first-order HDMR by deploying $n=5$ sample points along each of the variable axis and taking respectively the mean values and nominal values of the random and fuzzy variables as initial reference point. The approximated limit state function is divided into two parts, one with only the random variables along with the value of the constant part, and the other with the fuzzy variables. The joint membership function of the fuzzy part of approximated limit state function is obtained using suitable transformation of the fuzzy variables.

The two reference points closer to the function producing maximum weights, 1.0 and 0.977 are identified. After identification of the two reference points, local first-order HDMR approximations are constructed at the reference point by deploying $n=5$ sample points along each of the variable axis. The bounds of the failure probability are obtained both by performing the convolution using FFT in conjunction with linear and quadratic approximations and MCS on the global approximation.

Figure 10 shows the membership function of the failure probability estimated both by performing the convolution using FFT and MCS on the global approximation, as well as that obtained using direct MCS. The COV of the lower and upper bounds of the failure probability obtained using direct MCS, corresponding to $N_S = 10^6$ at zero confidence level are 0.31622 and 0.01274.

In addition, effects of SF sampling scheme and the number of sample points on the estimated membership function of the failure probability are studied. Figure 10 also shows the membership function of the failure probability estimate obtained by the proposed method based on SF sampling

© 2013 SRESA All rights reserved

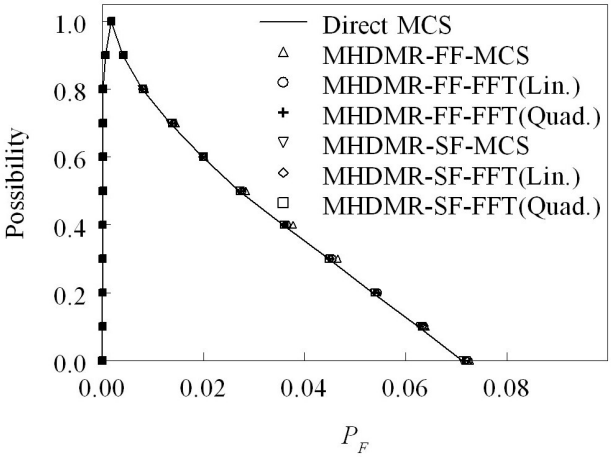

Figure 8: Membership function of failure probability for cantilever steel beam

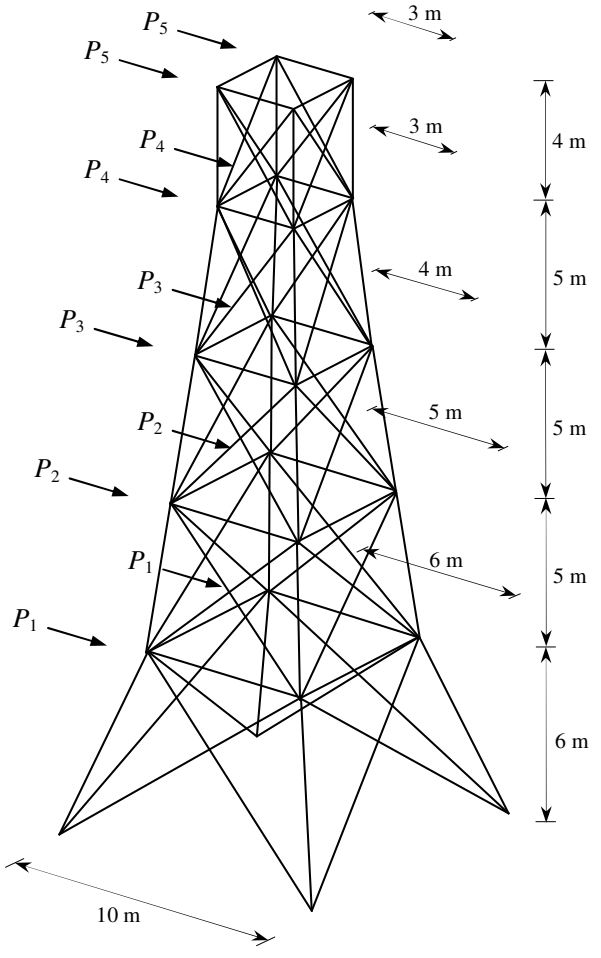

Figure 9: 80-bar 3D-truss structure

scheme. When compared with direct MCS, maximum absolute error in the membership function of the failure probability estimated both by performing the convolution using FFT in conjunction with linear

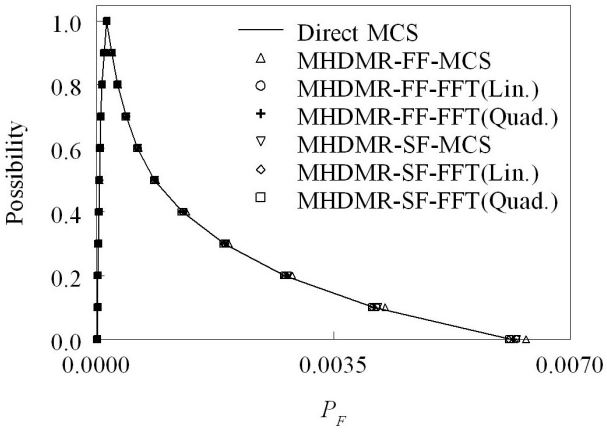

Figure 10: Membership function of failure probability for 80-bar 3D-truss structure

Table 8: Properties of the uncertain variables (3-D truss)

Uncertain variable	Type of variable			
	Random			Fuzzy
	Mean	COV	Distribution type	
P_1 (N)	1000	0.1	Normal	
P_2 (N)	2000	0.1	Normal	
P_3 (N)	3000	0.1	Normal	
P_4 (N)	4000	0.1	Normal	
P_5 (N)	5000	0.1	Normal	
A_1 (mm^2)				[6867 7630 8393]
A_2 (mm^2)				[5571 6190 6809]
A_3 (mm^2)				[3870 4300 4730]
A_4 (mm^2)				[2088 2320 2552]
A_5 (mm^2)				[1539 1710 1881]

and quadratic approximations, and MCS on the global approximation is tabulated in Table 9. The computational effort in terms of number of function evaluations for various methods is tabulated in Table 10. Tables 9 and 10 clearly demonstrate the computational efficiency of the proposed methodology. It is observed that $n = 7$ provides the optimum number of function calls with acceptable

© 2013 SRESA All rights reserved

Table 9: Maximum absolute error (%) (3-D truss)

Method	$n=3$	$n=5$	$n=7$	$n=9$
MHDMR-FF-MCS	7.1307	6.2745	4.5777	4.5777
MHDMR-FF-FFT-Lin.	6.0013	4.462	1.7241	1.7241
MHDMR-FF-FFT-Quad.	4.8920	2.7653	0.9818	0.9818
MHDMR-SF-MCS	4.2763	3.0140	1.8182	1.8182
MHDMR-SF-FFT-Lin.	2.7133	1.1785	0.9740	0.9740
MHDMR-SF-FFT-Quad.	2.4553	1.1021	0.7103	0.7103

Table 10: No. of function evaluations (3-D truss)

Method	$n=3$	$n=5$	$n=7$	$n=9$
Direct MCS	21×10^6	21×10^6	21×10^6	21×10^6
MHDMR-FF-MCS	33	63	93	123
MHDMR-FF-FFT-Lin.	73	223	453	763
MHDMR-FF-FFT-Quad.	33	63	93	123
MHDMR-SF-MCS	33	63	93	123
MHDMR-SF-FFT-Lin.	73	223	453	763
MHDMR-SF-FFT-Quad.	73	223	453	763

accuracy in evaluating the failure probability with the present method.

6. Summary and Conclusions

This paper presented a novel uncertain analysis method for estimating the membership function of the reliability of structural systems involving multiple design points in the presence of mixed uncertain (both random and fuzzy) variables. The method involves MHDMR technique for the limit state function approximation, transformation technique to obtain the contribution of the fuzzy variables to the convolution integral and fast Fourier transform for solving the convolution integral at all confidence levels of the fuzzy variables. Weight function is adopted for identification of multiple reference points closer to the limit surface. Using the bounds of the fuzzy variables part at each confidence level along with the constant part and the random variables part, the joint density functions are obtained by (i) identifying the reference points closer to the limit state function and (ii) blending of locally constructed individual first-order HDMR approximations in the rotated Gaussian space at different identified reference points to form global approximation, and (iii) performing the convolution using FFT, which upon integration yields the bounds of the failure probability. As an alternative the bounds of the failure probability are estimated by performing MCS on the global approximation in the original space, obtained by blending of locally constructed individual first-order HDMR approximations of the original limit state function at different identified reference points.

The results of three numerical examples involving explicit hypothetical mathematical function and structural mechanics problems indicate that the proposed method provides accurate and computationally efficient estimates of the membership function of the failure probability. The results obtained from the proposed method are compared with those obtained by direct MCS. The numerical results show that the present method is efficient for structural reliability estimation involving any number of fuzzy and random variables with any kind of distribution.

Two types of sampling schemes, namely FF, and SF, are adopted in this study for MHDMR approximation of the original limit state function construction. MHDMR approximation using FF sampling scheme provides desired accuracy to the predicted failure probability with least number of function evaluations. In order to reduce the approximation error further, SF sampling based MHDMR approximation of the original limit state function could be used in reliability analysis, but the number of function evaluations increases significantly compared to FF sampling. A parametric study is conducted with respect to the number of sample points n used in FF and SF sampling based MHDMR approximation and its effect on the estimated failure probability is investigated. An optimum number of sample points n must be chosen in approximation of the original limit state function. It can be observed from the reported results that $n=5$ or 7 works very well for all problems in this paper.

References

1. Madsen, H.O., Krenk, S., and Lind, N.C., Methods of Structural Safety, Prentice-Hall, New Jersey, 1986.
2. Rackwitz, R., "Reliability analysis−a review and some perspectives", Structural Safety, Vol. 23, No. 4, pp.365–395, 2001.

© 2013 SRESA All rights reserved

3. Breitung, K., "Asymptotic approximations for multinormal integrals" ASCE Journal of Engineering Mechanics, Vol. 110, No. 3, pp.357–366, 1984
4. Liu, P.L., and Der Kiureghian, A., "Finite element reliability of geometrically nonlinear uncertain structures", ASCE Journal of Engineering Mechanics, Vol. 117, No. 8, pp.1806–1825, 1991.
5. Impollonia, N., and Sofi, A., "A response surface approach for the static analysis of stochastic structures with geometrical nonlinearities", Computer Methods in Applied Mechanics and Engineering, Vol. 192, No. 37−38, pp.4109−4129, 2003.
6. Au, S.K., Papadimitriou, C., and Beck, J.L., "Reliability of uncertain dynamical systems with multiple design points", Structural Safety, Vol. 21, pp.113−133, 1999.
7. Der Kiureghian, A., and Dakessian, T., "Multiple design points in first and second order reliability", Structural Safety, Vol. 20, No. 1, pp.37–49, 1998.
8. Rubinstein, R.Y., Simulation and the Monte Carlo method, Wiley, New York, 1981.
9. Melchers, R.E., "Importance sampling in structural systems", Structural Safety, Vol. 6, No. 1, pp.3–10, 1989.
10. Au, S.K., and Beck, J.L., "Estimation of small failure probabilities in high dimensions by subset simulation", Probabilistic Engineering Mechanics, Vol. 16, No. 4, pp.263–277, 2001.
11. Sakamoto, J., Mori, Y., and Sekioka, T., "Probability analysis method using fast Fourier transform and its application", Structural Safety, Vol. 19, No. 1, pp.21–36, 1997.
12. Penmetsa, R.C., and Grandhi, R.V., "Adaptation of fast Fourier transformations to estimate structural failure probability", Finite Elements in Analysis and Design, Vol. 39, No.5−6, pp.473–485, 2003.
13. Wang, L.P., and Grandhi, R.V., "Safety index calculation using intervening variables for structural reliability analysis", Computers and Structures, Vol. 59, No. 6, pp.1139–1148, 1996.
14. Rao, B.N., and Chowdhury, R., "Probabilistic analysis using high dimensional model representation and fast Fourier transform", *International Journal for Computational Methods in Engineering Science and Mechanics, Vol.* 9, No. 6, pp.342−357, *2008.*
15. Briabant, V., Oudshoorn, A., Boyer, C., and Delcroix, F., "Nondeterministic possibilistic approaches for structural analysis and optimal design", AIAA Journal, Vol. 37, No. 10, pp.1298–1303, 1999.
16. Dong, W.M., and Wong, F.S., "Fuzzy weighted averages and implementation of the extension principle", Fuzzy Sets and Systems, Vol. 21, No. 2, pp.183–199, 1987.
17. Penmetsa, R.C., and Grandhi, R.V., "Uncertainty propagation using possibility theory and function approximations", Mechanics Based Design of Structures and Machines, Vol. 81, No. 15, pp.1567–1582, 2003.
18. Moller, B., Graf, W., and Beer, M., "Safety assessment of structures in view of fuzzy randomness", Computers and Structures, Vol. 81, No. 15, pp.1567–1582, 2003.
19. Adduri, P.R., and Penmetsa, R.C., "Confidence bounds on component reliability in the presence of mixed uncertain variables", International Journal of Mechanical Sciences, Vol. 50, No. 3, pp.481–489, 2008.
20. Guo, S.X., and Lv, Z.Z., "Hybrid probabilistic and non-probabilistic model of structural reliability", Journal of Mechanical Strength, Vol. 24, pp.524–526, 2002.
21. Qiu, Z.P., Yang, D., and Elishakoff, I., "Probabilistic interval reliability of structural systems", International Journal of Solids and Structures, Vol. 45, pp.2850–2860, 2008.
22. Qiu, Z.P., and Wang, J., "The interval estimation of reliability for probabilistic and non-probabilistic hybrid structural system", Engineering Failure Analysis, Vol. 17, pp.1142–1154, 2010.
23. Wang, J., and Qiu, Z.P., "The reliability analysis of probabilistic and interval hybrid structural system", *Applied Mathematical Modelling,* Vol. 34, pp.3648–3658, 2010.
24. Rabitz, H., and Alis, O.F., "General foundations of high dimensional model representations", Journal of Mathematical Chemistry, Vol. 25, No. 2−3, pp.197–233, 1999.
25. Alis, O.F., and Rabitz, H., "Efficient implementation of high dimensional model representations", Journal of Mathematical Chemistry, Vol. 29, No. 2, pp.127–142, 2001.
26. Li, G., Wang, S.W., and Rabitz, H., "High dimensional model representations generated from low dimensional data samples−I. mp−Cut−HDMR", Journal of Mathematical Chemistry, Vol. 30, No. 1, pp.1–30, 2001.
27. Sobol, I.M., "Theorems and examples on high dimensional model representations", Reliability Engineering and System Safety, Vol. 79, No. 2, pp.187–193, 2003.
28. Kaymaz, I., and McMahon, C.A., "A response surface method based on weighted regression for structural reliability analysis", Probabilistic Engineering Mechanics, Vol. 20, No.1, pp.11−17, 2005.
29. Lim, O.K., and Arora, J.S., "An active set RQP algorithm for engineering design optimization", Computer Methods in Applied Mechanics and Engineering, Vol. 57, No. 1, pp.51−65, 1986.

© 2013 SRESA All rights reserved

SRESA JOURNAL SUBSCRIPTION FORM

Subscriber Information (Individual)

Title	First Name	Middle Name	Last Name

Street Address Line 1

Street Address line 2

City	State/Province	Postal Code	Country

Work Phone	Home Phone	E-mail address

Subscriber Information (Institution)

Name of Institution/ Library _____

Name and Designation of Authority for Correspondence _____

Address of the Institution/Library _____

Subscription Rates

	Subscription Quantity	**Rate**	**Total**
Annual Subscription (in India)	_____	Rs. 15, 000	_____
(Abroad)	_____	$ 500	_____
	_____		_____
	_____		_____

Payment mode (please mark)

Cheque ☐ Credit Card ☐ Master Card ☐ Visa ☐ Online Banking ☐ Cash ☐ De mand Draft ☐

Credit card Number _____

Credit Card Holders Name _____

Credit Card Holde _____

Guidelines for Preparing the Manuscript

A softcopy of the complete manuscript should be sent to the Chief-Editors by email at the address: editor@sresa.org.in. The manuscript should be prepared using 'Times New Roman' 12 font size in double spacing, on an A-4 size paper. The illustrations and tables should not be embedded in the text. Only the location of the illustrations and tables should be indicated in the text by giving the illustration / table number and caption.

The broad structure of the paper should be as follows: a) Title of the paper – preferably crisp and such that it can be accommodated in one or maximum two lines with font size of 14 b) Name and affiliation of the author(s), an abstract of the paper in ~ 100 words giving brief overview of the paper and d) Five key words which indicates broad subject category of the paper. The second page of the paper should start with the title followed by the Introduction

A complete postal address should be given for all the authors along with their email addresses. By default the first author will be assumed to be the corresponding author. However, if the first author is not the corresponding author it will be indicated specifically by putting a star superscript at the end of surname of the author.

The authors should note that the final manuscript will be having double column formatting, hence, the size of the illustration, mathematical equations and figures should be prepared accordingly.

All the figures and tables should be supplied in separate files along with the manuscript giving the figure / table captions. The figure and table should be legible and should have minimum formatting. The text used in the figures and tables should be such that after 30% reduction also it should be legible and should not reduced to less than font 9.

Last section of the paper should be on list of references. The reference should be quoted in the text using square bracket like '[1]' in a chronological order. The reference style should be as follow:

1. Pecht M., Das D, and Varde P.V., "Physics-of-Failure Method for Reliability Prediction of Electronic Components", Reliability Engineering and System Safety, Vol 35, No. 2, pp. 232- 234, 2011.

After submitting the manuscript, it is expected that reviews will take about three months; hence, no communication is necessary to check the status of the manuscript during this period. Once, the review work is completed, comments, will be communicated to the author.

After receipt of the revised manuscript the author will be communicated of the final decision regarding final acceptance. For the accepted manuscript the author will be required to fill the copy right form. The copy right form and other support documents can be down loaded from the SRESA website: http://www.sresa.org.in

Authors interested in submitting the manuscript for publication in the journal may send their manuscripts to the following address:

Society for Reliability and Safety
RN 68, Dhruva Complex
Bhabha Atomic Research Centre,
Mumbai – 400 085 (India)
e-mail : editor@sresa.org.in

The Journal is published on quarterly basis, i.e. Four Issues per annum. Annual Institutional Subscription Rate for SAARC countries is Indian Rupees Ten Thousand (Rs. 10,000/-) inclusive of all taxes. Price includes postage and insurance and subject to change without notice. For All other countries the annual subscription rate is US dollar 500 ($500). This includes all taxes, insurance and postage.

Subscription Request can be sent to SRESA Secretariat (please visit the SRESA website for details)

© 2013 SRESA All rights reserved

SRESA's International Journal of

Life Cycle Reliability and Safety Engineering

Contents

Vol.2 **Issue No.1** **Jan - March 2013** **ISSN - 2250 0820**